University of Vermont
ScholarWorks @ UVM

Graduate College Dissertations and Theses | Dissertations and Theses

2018

Characterization Of A Novel Vps26c-Retromer Complex And Its Interaction With An Endosomal Trafficking Pathway Regulated By The Snare Vti13 In Controlling Polarized Growth And Cell Wall Organization In Arabidopsis Thaliana

Suryatapa Ghosh Jha
University of Vermont

Follow this and additional works at: https://scholarworks.uvm.edu/graddis

 Part of the Cell Biology Commons, Genetics and Genomics Commons, and the Plant Sciences Commons

Recommended Citation
Ghosh Jha, Suryatapa, "Characterization Of A Novel Vps26c-Retromer Complex And Its Interaction With An Endosomal Trafficking Pathway Regulated By The Snare Vti13 In Controlling Polarized Growth And Cell Wall Organization In Arabidopsis Thaliana" (2018). *Graduate College Dissertations and Theses*. 948.
https://scholarworks.uvm.edu/graddis/948

This Dissertation is brought to you for free and open access by the Dissertations and Theses at ScholarWorks @ UVM. It has been accepted for inclusion in Graduate College Dissertations and Theses by an authorized administrator of ScholarWorks @ UVM. For more information, please contact donna.omalley@uvm.edu.

CHARACTERIZATION OF A NOVEL VPS26C-RETROMER COMPLEX AND ITS INTERACTION WITH AN ENDOSOMAL TRAFFICKING PATHWAY REGULATED BY THE SNARE VTI13 IN CONTROLLING POLARIZED GROWTH AND CELL WALL ORGANIZATION IN *ARABIDOPSIS THALIANA*

A Dissertation Presented

by

Suryatapa Ghosh Jha

to

The Faculty of the Graduate College

of

The University of Vermont

In Partial Fulfillment of the Requirements
for the Degree of Doctor of Philosophy
Specializing in Plant Biology

October, 2018

Defense Date: July 19, 2018
Dissertation Examination Committee:

Mary L. Tierney, Ph.D., Advisor
Bryan A. Ballif, Ph.D., Chairperson
Stephen Everse, Ph.D.
Jeanne M. Harris, Ph.D.
Jill C. Preston, Ph.D.
Cynthia J. Forehand, Ph.D., Dean of the Graduate College

ABSTRACT

The endosomal trafficking system is a network of highly coordinated cellular pathways that control the growth and function of cells. The coordination of secretion and endocytosis in cells is one of the primary drivers of polarized growth, where new plasma membrane and cell wall components are deposited at the growing apex. In plants, one of the cell types exhibiting polarized growth are the root hairs. Root hairs are regulated extensions of epidermal cells called trichoblasts and are essential for anchorage, absorption of water and nutrients, and plant-microbe interactions. In this thesis, I characterize a previously undescribed protein involved in retromer function and endosomal trafficking pathways that regulate tip growth in root hairs of *Arabidopsis thaliana.*

The large retromer complex functions in recycling receptors in endosomal trafficking pathways essential for diverse developmental programs including cell polarity, programmed cell death, and shoot gravitropism in the model plant, *Arabidopsis thaliana*. I have characterized VPS26C, a novel member of the large retromer complex, that is essential in maintaining root hair growth in Arabidopsis. We used Bimolecular Fluorescence Complementation (BiFC) analysis to demonstrate thatVPS26C interacts with previously characterized core retromer subunits VPS35A and VPS29. Genetic analysis also indicates that *vps26c* suppresses the root hair growth and cell wall organization phenotypes of a null mutant of the SNARE VTI13 that localizes to early endosomes and the vacuole membrane, indicating a crosstalk between the VPS26C-retromer and VTI13-dependent vesicular trafficking pathways. Phylogenetic analysis was used to show that VPS26C genes are present in most angiosperms but appear to be absent in monocot genomes. Moreover, using a genetic complementation assay, we have demonstrated that *VPS26C* shares deep conservation of biochemical function with its human ortholog (DSCR3/VPS26C).

We also used an affinity purification-based proteomic analysis to identify proteins associated with VTI13 in young seedlings. Preliminary results suggest that a number of proteins linked to cell plate organization in plants are associated with the VTI13 proteome, emphasizing the potential role of this pathway in new cell wall biosynthesis/organization. Additionally, we have identified endoplasmic reticulum (ER)-body proteins, involved in plant defense response pathways, suggesting that either the VTI13 endosomal trafficking pathway is functioning in plant defense responses, or the ER-body proteins have additional independent function(s) in Arabidopsis roots that depend on VTI13.

In summary, I have described a novel retromer complex essential for polarized growth in Arabidopsis. *VPS26C* is an ancient gene and shares sequence and functional homology between human and Arabidopsis. *vps26c* is a genetic suppressor of the *vti13*-dependent root hair growth and cell wall organization pathways. Proteomic analysis of VTI13 endosomes in young seedlings suggests that a number of proteins associated with cell plate formation are associated with VTI13 compartments, supporting the genetic analysis described here and serves as a starting point to further describe the role of this pathway in controlling polarized growth in plants.

CITATION

Material from this dissertation has been published in the following form:

Jha, S.G., Larson, E.R., Humble, J., Domozych, D. S., Barrington, D.S., and Tierney, M.L.. (2018). Vacuolar Protein Sorting 26C encodes an evolutionarily conserved large retromer subunit in eukaryotes that is important for root hair growth in Arabidopsis thaliana. Plant J, 94 (4), 595-611

DEDICATION

I dedicate this dissertation to Dadu, my maternal grandfather Sri Santosh Kumar Mitra, for loving me unconditionally, and for teaching me to always work hard to succeed, and then to take a moment to celebrate the success too. I miss you, Dadu.

I also dedicate this work to Sanket, my son, the light of my life. Above all, you will always be my most rewarding accomplishment.

ACKNOWLEDGEMENTS

Words often seem scant when I want to thank so many people for contributing immensely in some ways or the other throughout my graduate career. First of all, I would like to thank my advisor, Mary Tierney, for her mentorship and the care with which she guided me throughout the years. Most of what I have learnt in these years, came from her. I will be eternally grateful and could not have asked for a better mentor for this crucial phase of my career. I owe my growth as a scientific thinker to you.

I am extremely thankful for an extraordinary dissertation committee who had guided me over the years to critically think about my work, and their useful comments and advice have steered me to ask pertinent biological questions and move my work forward.

This achievement is as much mine as it is my mother, Sulekha Ghosh's. She has always taught me to believe in myself, and that there is no alternative to hard work. It is because of her encouragement to pursue my dreams, and her immense belief in me that has led me to be successful. Maa, everything that I am today is because of you. You have taught me to enjoy the process and give my best to whatever I do, and that is the most important lesson I live by, always. I am thankful to my father, Chandan Ghosh, for being ever supportive of me and for teaching me to find joy in little things. I would also like to thank my biggest cheerleader, my sister, Kuntala Bose for teaching me how to be reasonable, to go forward to achieve my dreams, and so many more things. I am thankful to you for your faith in me; you are my best friend, and I love you. My love and gratefulness go out to my son, Sanket. He has understood my commitments far more sensibly than I had

expected of someone his age. Thank you Sanket, also for giving me company in the lab while I worked away the weekend afternoons.

People in the University of Vermont community, thank you so very much for the conversations, for the laughs and for making this place so much fun. I looked forward to work with you every single day these past six years. I would like to especially mention the people I am fortunate enough to know and be friends with: Tom Addison, Sanhita Chakraborty, Laura Hill, Anne Kelsen, Jamie Kostyun, Emily Larson, Connor Lewis, Meghan McKeown, Nikisha Patel, Beck Powers, Jill Preston, Ramya Srinivasan, Brittany Verrico, and Prince Zogli. Each one of you has inspired me in so many ways and continue to do so and have helped me grow and be a better human being.

Finally, I am beyond thankful to the love of my life, my husband, Hira Nand Jha, for being my rock. Your love for me and our family, and your support towards me makes everything possible. Thank you for being 'The wind beneath my wings'. I am excited to embark on the next adventure of our lives, with you by my side.

TABLE OF CONTENTS

LIST OF TABLES

LIST OF FIGURES

CHAPTER 1: MINI-REVIEW

Retromer or Retriever: Role of VPS26C in endosomal trafficking

Introduction

The endomembrane system is a highly coordinated network controlling cellular function and development in living organisms. This system is responsible for the synthesis, sorting, and distribution of proteins within cells in a manner that is often crucial for growth and viability. The endosomal trafficking of cargo to the storage and lytic vacuoles in plants, or the lysosome in animal systems, involves the action of **S**oluble **N**SF **A**ttachment **Re**ceptors (SNAREs) that control the fusion of vesicles carrying cargo with the target membrane. The VTI (**V**acuolar Protein Sorting-**t**en **i**nteracting (Fischer von Mollard, et al., 1997) family of SNAREs in *Arabidopsis thaliana* (Arabidopsis) includes VTI11, VTI12 and VTI13 and functions in trafficking cargo between the *trans*-Golgi network (TGN) or early endosomes and the lytic or storage vacuole (Surpin et al., 2003; Niihama et al., 2005; Sanmartin et al., 2007). Genetic analysis of these proteins has shown that the function of each VTI family member is required for distinct aspects of plant growth. VTI11 traffics cargo to the lytic vacuole and is essential for shoot gravitropism (Yano et al., 2003) and vascular development in leaves (Shirakawa et al., 2009) while VTI12 functions in trafficking proteins to the storage vacuole and is critical for autophagy in Arabidopsis (Surpin et al., 2003; Sanmartin et al, 2007). VTI13 localizes to membranes of the early endosome and lytic vacuole and is important for root hair growth and cell wall organization in Arabidopsis (Larson et al., 2014).

Coordinated with the process of trafficking cargo to the vacuole is a retrograde pathway involving the retromer that is necessary for recycling cargo and endosomal membrane proteins to the *trans*-Golgi network (TGN). The importance of the retromer complex in endosomal trafficking is demonstrated by loss of function mutants that exhibit severe developmental disorders in both plant and animal systems (Zelazny et al., 2013; Munch et al., 2015; Jha et al., 2018; Williams et al., 2017; Tammineni et al., 2017; Appel et al., 2018). The coordination of endosomal trafficking pathways between the TGN and the vacuole is also underscored by recent studies supporting a genetic interaction between specific retromer-dependent endosomal trafficking pathways and a VTI-SNARE dependent pathway to the lytic vacuole required for both shoot gravitropism and root hair growth in Arabidopsis (Hashiguchi et al., 2010; Jha et al., 2018).

The identity of protein complexes involved in retrograde endosomal trafficking in eukaryotes has been recently expanded to include a retromer-like "retriever" complex (McNally et al., 2017) that associates with endosomes using a mechanism distinct from the retromer complex in human cells, and which functions in the recycling of retriever-specific cargo. In this chapter we will summarize our understanding of the retromer complex in plants, focusing on a newly described Vacuolar Protein Sorting (VPS) 26 large retromer protein (VPS26C) required for root hair growth that appears to have a retriever function, in common with the human VPS26C. In addition, we will discuss genetic studies that implicate interactions between trafficking pathways regulated by the retromer in plants and the VTI family of SNAREs in controlling plant development.

The Classic Retromer Complex

The retromer complex was initially characterized in yeast and was shown to function in the endosome-to-Golgi retrieval of Vps10p, the transmembrane receptor of vacuolar carboxypeptidase Y (Seaman et al., 1997). Retromers were subsequently defined to be a heteropentameric complex containing large and small subunits. In yeast, the large retromer subunit consists of three highly conserved proteins, VPS35, VPS29 and VPS26 (Haft et al., 2000; Seaman, 2004) and is responsible for interaction with cargo proteins in a retrograde trafficking pathway from endosomes to the TGN (Seaman et al., 1998; Burda et al., 2002). The small subunit of the retromer in yeast consists of a dimer of two nexin proteins, VPS5p and VPS17p, that function in membrane binding, curvature and tubulation (Horazdovsky et al., 1997; Seaman et al., 1998; Carlton et al., 2004).

In mammalian systems, the large retromer subunit is composed of a single VPS35 and VPS29 protein that can complex with one of two VPS26 paralogs, VPS26A and VPS26B (Seaman et al., 1998). VPS26A and VPS26B in mice do not appear to be functionally redundant (Bugarcic et al., 2011), suggesting that different versions of the large retromer complex may function in distinct endosomal trafficking pathways. The small subunit of the retromer in mammalian systems is composed of a heterodimer of two sorting nexins consisting of either SNX1 or SNX2 and SNX5 or SNX6 and functions in binding membranes and recruiting the large retromer subunit to the endosomal membrane (Bonifacino et al., 2008; Collins et al., 2008). While the large and small retromer subunits form a stable complex in yeast (Seaman et al., 1998), the interaction between these two subunits is much weaker and transient in higher eukaryotes (Harbor and Seaman, 2011;

Swarbrick et al., 2011). In addition to the sorting nexins that form the small retromer subunit, many animal genomes also encode additional sorting nexins that function in retrograde endosomal trafficking pathways involving the retromer complex. For example, SNX3 has been shown to interact with the large retromer subunit and control endosomal trafficking pathways involved in sorting Wnt (Harterink et al., 2011), while SNX27 serves as a cargo adapter for the large retromer subunit on endosomal membranes (Gallon et al., 2014).

The retromer in animal systems has been shown to retrieve transmembrane receptors from endosomal membranes and recycle them to the TGN. The retromer-mediated retrieval of receptors includes Carboxypeptidase Y (Seaman et al., 1997), Bone Morphogenetic Protein (BMP) Type I receptor SMA-6 in *Caenorhabditis elegans* (Gleason et al., 2014), and several G-Protein Coupled Receptors (GPCRs) in a range of organisms (Temkin et al., 2011; Bugarcic et al., 2011), including *Drosophila melanogaster* (Wang et al., 2014). Retromers are also involved in recycling of the phagocytic receptor CED-1 from phagosomes to the plasma membrane in *C. elegans* (Chen et al., 2010), and the neurotransmitter receptor, GLR-1, from dendrites to the cell body (Zhang et al., 2012). In addition, retromer complexes have been implicated in the retrograde recycling of transmembrane proteins from the plasma membrane to the TGN (Bai and Grant, 2015), and transport between peroxisomes and mitochondria (Braschi et al., 2010).

A working model that has been used to characterize retromer-dependent trafficking of cargo proteins in animal systems involves recognition of cargo by the large retromer

subunit bound to the sorting nexin SNX27 on endosomal membranes, recruitment of the WASH complex to these membranes to promote interaction of the retromer with the actin cytoskeleton, and interaction of the small retromer subunit with the large retromer complex to facilitate membrane curvature, tubulation and retrograde transport of cargo. However, two papers (Simonetti et al., 2017; Kvainickas et al., 2017) describing the retrograde transport of CI-MPR receptor from late endosomal membranes to the TGN have recently brought this model into question. Both studies showed that the SNX proteins within the small subunit of the retromer were required for retrograde trafficking of the CI-MPR receptor in humans while down regulation of the VPS35 large retromer subunit had no effect on the recycling of this receptor from late endosomal membranes. These studies support a new model for retromer trafficking in which the small subunit of the retromer is essential for the retrograde trafficking of receptors from late endosomal membranes to the TGN.

Retromer function in plants

The availability of a number of plant genomes and the strong conservation of retromer subunit sequences has been used to identify retromer subunits in a variety of plant species. In Arabidopsis, VPS35 and VPS26 are both encoded by three gene family members while VPS29 is a single copy gene. In contrast, the small retromer subunit is composed of a heterodimer containing SNX1 and either SNX2a or SNX2b, homologs of the yeast VPS5p sorting nexin (Niemes et al., 2010). In plants, genetic studies have shown that the core retromer functions independently of its interaction with the sorting nexins (Pourcher et al., 2010). Analysis of retromer function in Arabidopsis indicates that the large and small

subunit of the retromer are required for endosomal trafficking pathways controlling diverse aspects of plant development. Genetic analysis has shown that single *vps26a* and *vps26b* show no developmental defect in Arabidopsis, but the *vps26a vps26b* double mutant displays severely stunted growth, indicating a redundancy in the function of VPS26 paralogs (Zelazny et al., 2013). A similar analysis of VPS35 family members has shown that a vps35b vps35c double mutant exhibits a dwarf growth phenotype, early senescence and is defective in trafficking proteins to the storage vacuole (Yamazaki et al., 2008). Loss of function mutants for VPS29 exhibit pleotropic growth phenotypes and are defective in the auxin homeostasis and endosomal trafficking of PIN1 in conjunction with the small retromer subunit protein SNX1 during plant development (Jaillais et al., 2007; Kleine-Vehn et al., 2008). Retromer subunit mutants have also been shown to be defective in unique aspects of plant development and delineate a role for VPS35A and VPS26A in shoot gravitropism (Hashiguchi et al., 2010), VPS35B and VPS26B in maintaining innate immunity in plants (Munch et al., 2015), VPS29 in the transport of Sugar- Dependent-1 (SDP1) from peroxisomes to oil bodies during seedling development (Thazar-Poulot et al., 2015), and SNX1 in the endosomal trafficking if IRT1 in Arabidopsis roots (Ivanov et al., 2014). Together, these results support diverse roles for both the large and small retromer subunits in endosomal trafficking pathways that control development in plants.

Evolutionary divergence of VPS26 function in eukaryotes

Phylogenetic analysis of genes encoding the VPS26 large retromer protein has shown that VPS26C/DSCR3 represents a third VPS26 gene family member that is evolutionarily conserved and is part of a smaller, monophyletic clade distinct from the *VPS26A* and

VPS26B homologs across plant and animal species (Koumandou et al., 2011). In Arabidopsis, VPS26C forms a retromer-like complex with VPS35A and VPS29 that is important in regulation of polarized growth in root hairs (Jha et al., 2018). VPS26C also interacts genetically with an endosomal trafficking pathway from early endosomes to lytic vacuole involving the SNARE VTI13 (Larson et al., 2014) as a loss-of-function allele of *vps26c* was able to suppress the root hair growth and cell wall organization phenotypes of the *vti13* mutant. VPS26C orthologs exhibit conservation in biochemical function as the human *VPS26C/DSCR3* sequence is able to complement the *vps26c* mutant phenotype in Arabidopsis (Jha et al., 2018). Consistent with these results, the human DSCR3/VPS26C protein has recently been characterized in human cell culture where it has been shown to form a complex with VPS29 and a VPS35-like protein (McNally et al., 2017).

Proteomic and genetic analysis of the VPS26C complex in human cell culture has also shown that the VPS26C "retriever" complex participates in endosomal trafficking pathways distinct from the retromer complex in humans (McNally et al., 2017). Differences in retromer and retriever function are mediated in part by the cargo proteins that they recycle to the TGN or plasma membrane, respectively, as well as the cargo adaptor used to recruit these two complexes to the endosomal membrane (McNally et al., 2017). The functional conservation of VPS26C orthologs raises the interesting possibility that VPS26C in Arabidopsis may function in endosomal trafficking pathways that are distinct from the retromer complex. Further investigation will be needed to determine the cargo and adaptor proteins that associate with the VPS26C complex in plants and whether it traffics cargo to the plasma membrane instead of the TGN.

Genetic Crosstalk between Retromers and the VTI family of SNAREs

The VTI family of SNAREs participate in trafficking cargo to the lytic or storage vacuole in Arabidopsis (Sanmartin et al., 2007; Larson et al., 2014). Both VTI11 and VTI13 function in endosomal trafficking pathways to the lytic vacuole while VTI12 traffics cargo to the storage vacuole in Arabidopsis. Null mutants for each of these SNAREs exhibit unique phenotypes, suggesting that they have distinct functions in plants. *vti11* exhibits a defect in leaf vasculature (Shirakawa et al., 2009) and aberrant central lytic vacuole formation (Sanmartín et al., 2007). These mutants also show a shoot agravitropic phenotype establishing the role of VTI11 in endosomal trafficking pathways required to maintain shoot gravitropism in plants (Yano et al., 2003). Null mutants of *VTI12* display no developmental phenotype when grown on a nutrient dense medium, but have accelerated senescence when grown on nutrient-deficient media, revealing VTI12's role in plant autophagy (Surpin et al., 2003). *vti12* plants also exhibit abnormal accumulation of 12S globulin precursors in siliques, supporting a role for VTI12 in trafficking of vacuolar storage proteins (Sanmartín et al., 2007). *vti13* is defective in root hair growth and cell wall organization in root epidermal cells and root hairs of Arabidopsis (Larson et al., 2014).

Recent studies have linked the anterograde trafficking pathways to the lytic vacuole involving VTI11 and VTI13 with endosomal trafficking pathways mediated by the retromer. Hashiguchi et al. (2010) performed a suppressor screen of *vti11* and found that mutations within genes encoding the core retromer proteins VPS35A and VPS26A were sufficient to suppress the *vti11* shoot agravitropic 'zigzag' phenotype in double mutants. Although the mechanism of this genetic interaction has not been defined, Hashiguchi et al.

(2010) discuss the possibility that mis-sorting of membranes to vacuoles, due to the loss of the retromer function in *vti11 vps26a* or *vti11 vps35a* double mutants, may result in a recovery of vacuolar dynamics necessary for the movement of amyloplasts in endodermal cells resulting in a restoration of shoot gravitropism. A similar interaction between mutations in a retromer subunit and a SNARE has been described by Jha et al. (2018), where a loss-of-function mutation for *VPS26C* was shown to restore the root hair growth and wall organization phenotype of *vti13.* While the cellular mechanism responsible for this suppression is currently unknown, it is interesting to note that VPS35A physically interacts both with VPS26A and VPS26C in Arabidopsis (Zelazny et al., 2013; Jha et al., 2018) and that VPS35B and VPS35C cannot substitute for VPS35A in endosomal trafficking pathways controlling shoot gravitropism (Hashiguchi et al., 2010). VPS35A function has also been shown to be required for trafficking of cargo to the lytic vacuole (Nodzyński et al., 2013), indicating that retromer function may be required for both multiple trafficking pathways between the lytic vacuole and the TGN. An understanding of the coordination of endosomal trafficking pathways required for trafficking of cargo between the TGN and lytic vacuole and the identity of other proteins involved in these pathways will be required to determine cellular mechanisms that mediate these diverse developmental processes.

REFERENCES

Appel, J. R., Ye, S., Tang, F., Sun, D., Zhang, H., Mei, L., and Xiong, W.-C. (2018) Increased Microglial Activity, Impaired Adult Hippocampal Neurogenesis, and Depressive-like Behavior in Microglial VPS35-Depleted Mice. *The Journal of Neuroscience: The Official Journal of the Society for Neuroscience*, ***38*(26),** 5949–5968.

Bai, Z., and Grant, B. D. (2015) A TOCA/CDC-42/PAR/WAVE functional module required for retrograde endocytic recycling. *Proceedings of the National Academy of Sciences of the United States of America*, ***112*(12),** E1443-1452.

Bonifacino, J. S., and Hurley, J. H. (2008) Retromer. *Current Opinion in Cell Biology*, ***20*(4),** 427–436.

Braschi, E., Goyon, V., Zunino, R., Mohanty, A., Xu, L., and McBride, H. M. (2010) Vps35 mediates vesicle transport between the mitochondria and peroxisomes. *Current Biology, **20*(14),** 1310–1315.

Bugarcic, A., Zhe, Y., Kerr, M. C., Griffin, J., Collins, B. M., and Teasdale, R. D. (2011) Vps26A and Vps26B Subunits Define Distinct Retromer Complexes. *Traffic*, ***12*(12),** 1759–1773.

Burda, P., Padilla, S. M., Sarkar, S., and Emr, S. D. (2002) Retromer function in endosome-to-Golgi retrograde transport is regulated by the yeast Vps34 PtdIns 3-kinase. *Journal of Cell Science*, ***115*(20),** 3889–3900.

Chen, D., Xiao, H., Zhang, K., Wang, B., Gao, Z., Jian, Y., andYang, C. (2010) Retromer is required for apoptotic cell clearance by phagocytic receptor recycling. *Science*, ***327*(5970),** 1261–1264.

Collins, B.M. (2008) The structure and function of the retromer protein complex. *Traffic*, **9**, 1811-1822.

Gallon, M., Clairfeuille, T., Steinberg, F., Mas, C., Ghai, R., Sessions, R. B., and Cullen, P. J. (2014). A unique PDZ domain and arrestin-like fold interaction reveals mechanistic details of endocytic recycling by SNX27-retromer. *Proceedings of the National Academy of Sciences of the United States of America*, ***111*(35),** E3604-3613.

Gambardella, S., Biagioni, F., Ferese, R., Busceti, C. L., Frati, A., Novelli, G., Rugierri, S., and Fornai, F. (2016) Vacuolar Protein Sorting Genes in Parkinson's Disease: A Re-appraisal of Mutations Detection Rate and Neurobiology of Disease. *Frontiers in Neuroscience*. **10**, 532-542.

Haft, C.R., de la Luz Sierra, M., Bafford, R., Lesniak, M.A., Barr, V.A. and Taylor, S.I. (2000) Human orthologs of yeast vacuolar protein sorting proteins Vps26, 29, and 35: assembly into multimeric complexes. *Mol. Biol. Cell*, **11**, 4105–4116.

Harbour, M. E., and Seaman, M. N. J. (2011) Evolutionary variations of VPS29, and their implications for the heteropentameric model of retromer. *Communicative & Integrative Biology*, ***4*****(5),** 619–622.

Harterink, M., Port, F., Lorenowicz, M. J., McGough, I. J., Silhankova, M., Betist, M. C., and Korswagen, H. C. (2011) A SNX3-dependent retromer pathway mediates retrograde transport of the Wnt sorting receptor Wntless and is required for Wnt secretion. *Nature Cell Biology*, ***13*****(8),** 914–923.

Hashiguchi, Y., Niihama, M., Takahashi, T., Saito, C., Nakano, A., Tasaka, M. and Morita, M.T. (2010) Loss-of-function mutations of retromer large subunit genes suppress the phenotype of an Arabidopsis *zig* mutant that lacks Qb-SNARE VTI11. *Plant Cell,* **22**, 159–172.

Horazdovsky, B.F., Davies, B.A., Seaman, M.N., McLaughlin, S.A., Yoon, S. and Emr, S.D. (1997) A sorting nexin-1 homologue, Vps5p, forms a complex with Vps17p and is required for recycling the vacuolar protein-sorting receptor. *Mol. Biol. Cell*, **8**, 1529–1541.

Ivanov, R., Brumbarova, T., Blum, A., Jantke, A.-M., Fink-Straube, C., and Bauer, P. (2014) SORTING NEXIN1 is required for modulating the trafficking and stability of the Arabidopsis IRON-REGULATED TRANSPORTER1. *The Plant Cell*, ***26*****(3),** 1294–1307.

Jaillais, Y., Santambrogio, M., Rozier, F., Fobis-Loisy, I., Miège, C. and Gaude, T. (2007) The retromer protein VPS29 links cell polarity and organ initiation in plants. *Cell,* **130**, 1057–1070.

Jha, S.G., Larson, E.R., Humble, J., Domozych, D. S., Barrington, D.S., and Tierney, M.L. (2018) Vacuolar Protein Sorting 26C encodes an evolutionarily conserved large retromer subunit in eukaryotes that is important for root hair growth in Arabidopsis thaliana. *Plant J,* **94 (4)**, 595-611

Kleine-Vehn, J., Dhonukshe, P., Sauer, M., Brewer, P.B., Wiśniewska. J., Paciorek, T., Benková, E. and Friml, J. (2008a) ARF GEF-dependent transcytosis and polar delivery of PIN auxin carriers in Arabidopsis. *Curr. Biol.* **8**, 526-31.

Koumandou, V.L., Klute, M.J., Herman, E.K., Nunez-Miguel, R., Dacks, J.B. and Field, M.C. (2011) Evolutionary reconstruction of the retromer complex and its function in *Trypanosoma brucei*. *J. Cell Sci*. **124**, 1496–1509.

Kvainickas, A., Jimenez-Orgaz, A., Nägele, H., Hu, Z., Dengjel, J. and Steinberg, F. 2017 Cargo-selective SNX-BAR proteins mediate retromer trimer independent retrograde transport. *J Cell Biol.* **216**, 3677-3693.

Larson, E.R., Domozych, D.S. and Tierney, M.L. (2014) SNARE VTI13 plays a unique role in endosomal trafficking pathways associated with the vacuole and is essential for cell wall organization and root hair growth in arabidopsis. *Annals of Botany,* **114**, 1147–1159.

McNally, K. E., Faulkner, R., Steinberg, F., Gallon, M., Ghai, R., Pim, D., Langton, P., Pearson, N., Danson, C. M., Nagelle, H., Morris, L. L., Singla, A., Overlee, B. L., Heesom, K. J., Sessions, R., Banks, L., Collins, B. M., Berger, I., Billadeau, D. D., Burstein, E., and Cullen, P. J. (2017) Retriever is a Multiprotein Complex for Retromer-independent Endosomal Cargo Recycling. *Nat. Cell Biol.* **19**, 1214-1225.

Morita, M. T., Kato, T., Nagafusa, K., Saito, C., Ueda, T., Nakano, A., and Tasaka, M. (2002) Involvement of the Vacuoles of the Endodermis in the Early Process of Shoot Gravitropism in Arabidopsis. *The Plant Cell*. **14**, 47–56.

Munch, D., Teh, O.-K., Malinovsky, F.G., Liu, Q., Vetukuri, R.R., El Kasmi, F., Brodersen, P., Hara-Nishimura, I., Dangl, J.L., Petersen, M., Mundy, J. and Hofius, D. (2015) Retromer contributes to immunity-associated cell death in Arabidopsis. *Plant Cell,* **27**, 463–479.

Niihama, M., Uemura, T., Saito, C., Nakano, A., Sato, M. H., Tasaka, M., and Morita, M. T. (2005) Conversion of Functional Specificity in Qb-SNARE VTI1 Homologues of Arabidopsis. *Current Biology*. **15**, 555–560.

Nodzyński, T., Feraru, M.I., Hirsch, S., De Rycke, R., Niculaes, C., Boerjan, W., Van Leene, J., De Jaeger, G., Vanneste, S. and Friml, J. (2013) Retromer Subunits VPS35A and VPS29 Mediate Prevacuolar Compartment (PVC) Function in Arabidopsis. *Mol. Plant*, **6**, 1849–1862.

Oliviusson, P., Heinzerling, O., Hillmer, S., Hinz, G., Tse, Y.C., Jiang, L. and Robinson, D.G. (2006) Plant retromer, localized to the prevacuolar compartment and microvesicles in Arabidopsis, may interact with vacuolar sorting receptors. *Plant Cell*, **18**, 1239-1252.

Pourcher, M., Santambrogio, M., Thazar, N., Thierry, A.M., Fobis-Loisy, I., Miège, C., Jaillais, Y. and Gaude, T. (2010) Analyses of sorting nexins reveal distinct retromer-subcomplex functions in development and protein sorting in Arabidopsis thaliana. *Plant Cell*, **22**, 3980–3991.

Sanmartín, M., Ordóñez, A., Sohn, E.J., Robert, S., Sánchez-Serrano, J.J., Surpin, M.A., Raikhel, N.V. and Rojo, E. (2007) Divergent functions of VTI12 and VTI11 in trafficking to storage and lytic vacuoles in Arabidopsis. *Proc. Natl. Acad. Sci.USA*. **104**, 3645–3650.

Seaman, M.N., Marcusson, E.G., Cereghino, J.L., and Emr, S.D. (1997) Endosome to Golgi retrieval of the vacuolar protein sorting receptor, Vps10p, requires the function of the VPS29, VPS30, and VPS35 gene products. *J. Cell Biol.* **137**, 79–92.

Seaman, M. N., McCaffery, J. M., and Emr, S. D. (1998) A membrane coat complex essential for endosome-to-Golgi retrograde transport in yeast. *The Journal of Cell Biology*. **142**, 665–681.

Seaman, M. N. J. (2004) Cargo-selective endosomal sorting for retrieval to the Golgi requires retromer. *The Journal of Cell Biology*, ***165*(1),** 111–122.

Shirakawa, M., Ueda, H., Shimada, T., Nishiyama, C., and Hara-Nishimura, I. (2009) Vacuolar SNAREs Function in the Formation of the Leaf Vascular Network by Regulating Auxin Distribution. *Plant and Cell Physiology*. **50,** 1319–1328.

Siegenthaler, B. M., & Rajendran, L. (2012) Retromers in Alzheimer's disease. *Neuro-Degenerative Diseases*. **10,** 116–121.

Simonetti, B., Danson, C.M., Heesom, K.J. and Cullen, P.J. (2017) Sequence-dependent cargo recognition by SNX-BARs mediates retromer-independent transport of CI-MPR. *J. Cell Biol.* **216**, 3695-3712.

Surpin, M., Zheng, H., Morita, M.T., Saito, C., Avila, E., Blakeslee, J.J., Bandyopadhyay, A., Kovaleva, V., Carter, D., Murphy, A., Tasaka, M. and Raikhel, N. (2003) The VTI family of SNARE proteins is necessary for plant viability and mediates different protein transport pathways. *Plant Cell,* **15**, 2885–2899.

Swarbrick, J. D., Shaw, D. J., Chhabra, S., Ghai, R., Valkov, E., Norwood, S. J., and Collins, B. M. (2011) VPS29 Is Not an Active Metallo-Phosphatase but Is a Rigid Scaffold Required for Retromer Interaction with Accessory Proteins. *PLoS ONE*, ***6*(5).**

Tammineni, P., Jeong, Y. Y., Feng, T., Aikal, D., and Cai, Q. (2017) Impaired axonal retrograde trafficking of the retromer complex augments lysosomal deficits in Alzheimer's disease neurons. *Human Molecular Genetics*, ***26*(22),** 4352–4366.

Thazar-Poulot, N., Miquel, M., Fobis-Loisy, I. and Gaude, T. (2015) Peroxisome extensions deliver the Arabidopsis SDP1 lipase to oil bodies. *Proc. Natl. Acad. Sci. USA,* **112**, 4158–4163.

Wang, H., Toh, J., Ho, P., Tio, M., Zhao, Y., and Tan, E.-K. (2014) In vivo evidence of pathogenicity of VPS35 mutations in the Drosophila. *Molecular Brain*, ***7*,** 73.

Williams, E. T., Glauser, L., Tsika, E., Jiang, H., Islam, S., and Moore, D. J. (2018) Parkin mediates the ubiquitination of VPS35 and modulates retromer-dependent endosomal sorting. *Human Molecular Genetics*.

Yamazaki, M., Shimada, T., Takahashi, H., Tamura, K., Kondo, M., Nishimura, M. and Hara-Nishimura, I. (2008) Arabidopsis VPS35, a Retromer Component, is Required for Vacuolar Protein Sorting and Involved in Plant Growth and Leaf Senescence. *Plant Cell Physiol.* **49:** 142–156.

Yano, D., Sato, M., Saito, C., Sato, M. H., Morita, M. T., and Tasaka, M. (2003) A SNARE complex containing SGR3/AtVAM3 and ZIG/VTI11 in gravity-sensing cells is important for Arabidopsis shoot gravitropism. *Proceedings of the National Academy of Sciences of the United States of America*, ***100*****(14),** 8589–8594.

Zelazny, E., Santambrogio, M., Pourcher, M., Chambrier, P., Berne-Dedieu, A., Fobis-Loisy, I., Miege, C., Jallais, Y. and Gaude, T. (2013) Mechanisms governing the endosomal membrane recruitment of the core retromer in Arabidopsis. *J Biol. Chem.* **288,** 8815–8825.

Zhang, D., Isack, N. R., Glodowski, D. R., Liu, J., Chen, C. C.-H., Xu, X. Z. S., and Rongo, C. (2012) RAB-6.2 and the retromer regulate glutamate receptor recycling through a retrograde pathway. *The Journal of Cell Biology*, ***196*****(1),** 85–101.

Zheng, H., von Mollard, G. F., Kovaleva, V., Stevens, T. H., Raikhel, N. V., and Kaiser, C. (1999) The Plant Vesicle-associated SNARE AtVTI1a Likely Mediates Vesicle Transport from the Trans-Golgi Network to the Prevacuolar Compartment. *Molecular Biology of the Cell*. ***10***, 2251–2264.

CHAPTER 2

Vacuolar Protein Sorting 26C encodes an evolutionarily conserved large retromer subunit in eukaryotes that is important for root hair growth in *Arabidopsis thaliana*

Suryatapa Ghosh Jha[a], Emily R. Larson[a], Jordan Humble[a], David S. Domozych[b], David S. Barrington[a], Mary L. Tierney[a,1]

[a] Department of Plant Biology, University of Vermont, Burlington, Vermont 05405

[b] Skidmore College, Saratoga Springs, New York 12866

[1] Corresponding author's email: mary.tierney@uvm.edu

Note:

I would like to acknowledge the contributions of Dr. David Domozych (Skidmore College) for the data presented in Figure 7 and Dr. David Barrington (University of Vermont - Plant Biology) for the data presented in Figure 8, of Chapter 2.

All other experimental data shown in this chapter was produced and analyzed by Suryatapa Ghosh Jha.

SUMMARY

The large retromer complex participates in diverse endosomal trafficking pathways and is essential for plant developmental programs including cell polarity, programmed cell death, and shoot gravitropism in Arabidopsis. Here we demonstrate that an evolutionarily conserved VPS26 protein (VPS26C; At1G48550) functions in a complex with VPS35A and VPS29 necessary for root hair growth in Arabidopsis. Bimolecular Fluorescence Complementation showed that VPS26C forms a complex with VPS35A in the presence of VPS29 and this is supported by genetic studies showing that *vps29* and *vps35a* mutants exhibit altered root hair growth. Genetic analysis also demonstrated an interaction between a *VPS26C* trafficking pathway and one involving the SNARE *VTI13*. Phylogenetic analysis indicates that *VPS26C*, with the notable exception of grasses, has been maintained in the genomes of most major plant clades since its evolution at the base of eukaryotes. To test the model that *VPS26C* orthologs in animal and plant species share a conserved function, we generated transgenic lines expressing GFP fused with the *VPS26C* human ortholog (*HsDSCR3*) in a *vps26c* background. These studies illustrate that *GFP-HsDSCR3* is able to complement the *vps26c* root hair phenotype in Arabidopsis, indicating a deep conservation of cellular function for this large retromer subunit across plant and animal kingdoms.

SIGNIFICANCE

A large retromer complex protein, representative of an ancient clade of *VPS26* sequences, is required for root hair growth in Arabidopsis. VPS26C function is conserved across eukaryotes and contributes to polarized growth and cell wall organization in plants.

INTRODUCTION

Endosomal trafficking pathways affects many developmental processes in plants through the internalization of proteins at the plasma membrane, trafficking of cargo to the lytic and storage vacuoles and recycling of plasma membrane components (Geldner et al., 2001; Surpin et al., 2003; Sanmartin et al., 2007; Kleine-Vehn et al., 2008a, 2008b). The polarized growth of root hairs has been shown to depend on endosomal trafficking pathways (Voigt et al., 2005; Ovecka et al., 2005; Preuss et al., 2006; Larson et al., 2014a) and represents a powerful system to characterize cellular components that are essential for tip growth and cell wall organization in plants. The retromer complex functions in endosomal trafficking of membrane receptors from endosomes to the Golgi in yeast (Seaman et al., 1997) and consists of multi-protein complexes that are broadly conserved across eukaryotes (Oliviusson et al., 2006; Koumandou et al., 2011). Recently, a phylogenetic analysis of *Vacuolar Protein Sorting 26* (*VPS26)* genes, encoding a member of the large retromer complex, identified a monophyletic clade of sequences including Arabidopsis *VPS26C* (At1g48550), that represent an ancient clade which evolved prior to the divergence of animals and plants (Koumandou et al., 2011). The identification of *VPS26C* orthologs in both animal and plant species within this ancient clade led us to investigate two questions: what is the function of *VPS26C* in Arabidopsis, and is the function of *VPS26C* orthologs conserved across eukaryotes?

Retromers were first characterized in yeast (Horazdovsky et al., 1997; Seaman et al., 1997; Nothwehr and Hindes, 1997; Paravacini et al., 1992) as a complex required for transporting membrane proteins from the late endosome to the *trans*-Golgi network (TGN) and are

composed of a large cargo-binding subunit consisting of VPS35, VPS29 and VPS26 proteins, and a small subunit consisting of sorting nexin dimers (VPS5 in yeast; SNX1/2 in animals and plants). Yeast and mammalian systems encode a single *VPS35* and *VPS29* gene while two *VPS26* paralogs have been identified as large retromer subunits in several mammalian systems (Edgar & Polak, 2000; Haft et al., 2000; Kerr et al., 2005). In contrast, Arabidopsis encodes three VPS35 proteins, two VPS26 proteins and three sorting nexins (Jaillais et al., 2006; Oliviusson et al., 2006; Pourcher et al., 2010). Initial studies in yeast and mammalian systems suggested that a pentameric retromer complex composed of both the small and large subunits is required for endosomal trafficking of cargo from late endosomes to the TGN (Seaman et al., 1997). However, more recent studies suggest that the large and small subunits of the retromer in both mammalian and plant systems may also function independently in regulating specific trafficking pathways (Pourcher et al., 2010; Gallon and Cullen, 2015).

In Arabidopsis, genetic analysis of the role of the large retromer complex indicates that it is essential for multiple processes in plant development, including cell polarity and organ initiation (Jaillais et al., 2007), immunity-associated cell death (Munch et al., 2015) and oil body biogenesis and breakdown during vegetative growth (Thazar-Poulot et al., 2015). Additionally, the large retromer complex, consisting of VPS26A and VPS35A, is critical for shoot gravitropism in Arabidopsis and has been shown to share a genetic pathway with the SNARE protein VTI11 (Hashiguchi et al., 2010), that functions in anterograde membrane trafficking pathways between the TGN and the late endosome/vacuole (Zheng et al. 1999).

The large retromer complex was initially proposed to traffic vacuolar sorting receptors (VSRs) from the pre-vacuolar compartment(s) (PVC) to the TGN (Yamazaki et al., 2008; Kang et al., 2012). However, recent studies indicate that VSRs in plants bind their ligands in the ER and Golgi and are trafficked to the TGN where the bound ligands dissociate from their receptors and the free VSRs are recycled back to the Golgi (Kunzl et al., 2016; Fruholz et al., 2017). These data support a model in which sorting nexins, localized to the TGN, may be involved in the retrograde sorting of VSRs in plants (Robinson et al., 2016). This is consistent with recent studies in animal systems (Kvainickas et al., 2017; Simonetti et al., 2017), where sorting nexin (SNX) heterodimers are responsible for the retrograde trafficking of the mannose-6-phosphate receptor (CI-MPR) from endosomal membranes to the TGN, in a process that is independent of the large retromer subunit.

The subcellular localization of the large retromer complex in plants is still controversial (for review, see Robinson and Neuhaus, 2016). VPS35 proteins have been localized to both multivesicular bodies (MVBs)/PVCs (Oliviusson et al., 2006; Yamazaki et al., 2008; Munch et al., 2015) as well as an endosomal compartment that lacks VSRs (Yamazaki et al., 2008). In contrast, VPS29 has been localized to the TGN along with sorting nexins (Jallais et al., 2006, 2007; Niemes et al., 2010). These differences in subcellular localization may be due to the large retromer complex protein member studied (VPS35 vs VPS29) or may suggest that different versions of the large retromer complex associate with distinct membrane populations in Arabidopsis during growth.

The presence of multiple *VPS35* and *VPS26* paralogs in Arabidopsis and other eukaryotes presents the opportunity for different versions of the large retromer complex to regulate

distinct endosomal trafficking pathways. In mouse, *VPS26A* and *VPS26B* are non-redundant in function as deletion of *VPS26A* results in embryonic lethality while *VPS26B* knockout mice appear normal (Kim et al., 2010). In Arabidopsis by comparison, whereas *vps26a* and *vps26b* single mutants appear similar to wild type in their growth habit, growth of the *vps26a vps26b* double mutant is severely compromised (Zelazny et al., 2013) suggesting that *VPS26A* and *VPS26B* may share some redundancy in function. Nonetheless, genetic and cell biology approaches have identified several unique functions for *VPS26* and *VPS35* paralogs in Arabidopsis. For example, VPS35A and VPS29 were found to be important for trafficking of membrane proteins to the PVC (Nodzynski et al., 2013) while mutations in V*PS35A* and *VPS26A* are capable of suppressing the shoot gravitropic phenotype of *vti11* mutants (Hashiguchi et al., 2010). In contrast, *vps35b* and *vps26b* are defective in immunity-associated cell death and autophagy (Munch et al., 2015).

In this paper, we establish that VPS26C (At1G48550) is a component of the large retromer complex in Arabidopsis and is required for root hair growth. We provide evidence for a genetic interaction between the endosomal pathways defined by the *VPS26C*-retromer complex and the SNARE *VTI13* in maintaining root hair growth. We also demonstrate that the human *VPS26C* ortholog, *HsDSCR3*, is able to complement the *vps26c* root hair growth phenotype. These results define a new member of the VPS26 family of proteins in plants, provide evidence that the *VPS26C/DSCR3* clade share

deeply conserved cellular function in eukaryotes and establish a role for the large retromer complex in regulating root hair growth in Arabidopsis.

RESULTS

A VPS26C-VPS29-VPS35A large retromer complex is required for root hair growth

The *VPS26C* gene represents the only Arabidopsis member of an ancient gene family shared by animals and plants (Koumandou, 2011). In order to determine its function, we examined the phenotype of two T-DNA insertion mutants identified in the ABRC collection that were confirmed to be nulls based on qRT/PCR (Figure S1). Analysis of *vps26c* root hair growth indicated that the mutant alleles were indistinguishable from wild type seedlings when grown on MS medium alone (Figure 1) but that *vps26c-1* and *vps26c-2* exhibit much shorter root hairs when grown on MS medium containing 200 mM mannitol (Figures 1A, B). Root hairs of *vps26c*-1 seedlings, expressing a *GFP-VPS26C* fusion under the transcriptional control of either the 35S promoter (Figure S2) or the *VPS26C* endogenous promoter (Figures 1A, B) were indistinguishable from those of wild type seedlings when grown in the presence of mannitol (Figures 1A, B). Similar results were observed when *GFP-VPS26C* was expressed in the *vps26c*-2 background (Figure S2). In addition, expression of the *GFP-VPS26C* fusion under the transcriptional control of the 35S promoter did not cause any root hair growth aberrations in a wild type background (Figure S2)

Due to the sensitivity of *vps26c* root hair growth to mannitol, we also compared root hair growth of *vps26c* to wild type seedlings grown on MS media supplemented with 30 mM NaCl. Low concentrations of NaCl have been shown to reduce root hair growth in Arabidopsis, in part through an impact on the tip-localized Ca^{+2} gradient (Halperin et al., 2003; Wang et al., 2008). Root hairs of both *vps26c* mutant alleles were shorter than those

of wild type seedlings when grown on MS media supplemented with 30 mM NaCl and this phenotype was complemented by the expression of *GFP-VPS26C* in the *vps26c* mutant background (Figures 1A, C). To confirm that this phenotype was due to sodium, we compared wild type and *vps26c* seedlings grown on medium supplemented with 30 mM potassium chloride (Figure S3) and observed no difference in root hair length, suggesting that *vps26c* root hair growth is sensitive to sodium. These results indicate that *VPS26C* function contributes to root hair growth and that the *vps26c* root hair phenotype is sensitive to osmotic and salt stress.

The observation that *vps26c* exhibited a root hair phenotype on media supplemented with mannitol and NaCl led us to hypothesize that *VPS26C* function may be critical for polarized growth under conditions of abiotic stress. To examine this model, we performed qRT-PCR to analyze the expression of *VPS26C* in wild type seedling roots grown on MS medium and MS medium supplemented with mannitol or NaCl (Figure 2). We found that the *VPS26C* transcript is down-regulated in seedlings grown in the presence of mannitol or NaCl (Figure 2A). These data corroborate the difference in wild type root hair length observed by Halperin et al. (2003) for seedlings grown on MS media supplemented with NaCl (Figure S4). We also compared this expression with that of *VSP26A* and *VPS26B* in wild type Arabidopsis roots grown on these three media. In contrast to *VPS26C*, qRT-PCR analysis indicated that *VPS26A* and *VPS26B* transcripts were both up-regulated by 200 mM mannitol whereas only *VPS26A* showed an up-regulation in the presence of 30 mM NaCl in seedling roots while *VPS26B* remained unaffected (Figures 2B, C). These results show that mannitol and NaCl selectively down-regulate *VPS26C* in Arabidopsis seedling roots.

Further they show that a reduced level of the *VPS26C*, either due to the presence of mannitol or NaCl in the growth media or loss of *VPS26C* in the T-DNA insertion null mutants, negatively impacts growth of root hairs in Arabidopsis. We also used qRT-PCR to investigate whether *VPS26A* or *VPS26B* were differentially expressed in roots of *vps26c* seedlings when compared to wild type seedling roots (Figure 2D). We found that *VPS26A* transcripts are up-regulated in *vps26c* roots relative to wild type while *VPS26B* transcript levels were down-regulated in *vps26c* (Figure 2D).

To genetically dissect the role of other large retromer complex proteins in root hair growth, we analyzed T-DNA insertion mutants for the other genes encoding the large retromer complex in Arabidopsis. Mutant alleles for each of the *VPS35* and *VPS26* family members (*VPS35A; vps35a-2, VPS35B; vps35b-3, VPS35C; vps35c-2, VPS26A; vps26a-3,* and *VPS26B; vps26b-1*) and for *VPS29 (vps29-6)*, a single copy gene in Arabidopsis, were obtained from the ABRC. qRT-PCR was used to show that each of these mutants was a null or significantly down-regulated (Figure S1 A, B, D-G). Mutant and wild type seedlings were then grown for five days on MS medium and MS medium supplemented with 200 mM mannitol, and the length of their root hairs was compared (Figure 3). Among these mutants only *vps35a-2*, *vps29-6*, and *vps26c-1* showed a significant decrease in root hair length when compared to wild type seedlings. Interestingly, under normal MS media conditions *vps35a-2* and *vps29-6* root hairs were also shorter than those of wild type seedlings (Figure S5). These data provide genetic evidence indicating that VPS26C, VPS35A and VPS29 are part of a large retromer complex that functions in a pathway important for root hair growth in Arabidopsis.

We observed no other developmental phenotypes in *vps26c* mutants when compared to wild type plants when these two genotypes were grown to seed in growth chambers. In addition, qRT-PCR analysis suggested that the *VPS26C* is expressed at comparatively similar levels in various organs throughout growth (Figure S6), a pattern consistent with existing microarray data (bar.utoronto.ca/efp/cgi-bin/efpWeb.cgi). These results suggest that while VPS26C may function in many cell types throughout plant growth, the VPS26C-large retromer complex may have a specialized role in maintaining polarized growth in root hairs.

VPS26C is part of the large retromer complex containing VPS35A and VPS29.

The large retromer complex in eukaryotes is composed of VPS35, VPS29 and VPS26 where VPS26 and VPS35 physically interact with each other in mammalian systems (Collins, 2008). To examine whether VPS26C associates with VPS35 as part of a large retromer complex *in planta*, we used Bimolecular Fluorescence Complementation (BiFC), whereby *VPS26C* was used to generate a fusion with the N-terminal portion of YFP (N-YFP-VPS26C) and the three Arabidopsis *VPS35* genes were each used to create fusions with the C–terminal portion of YFP (C-YFP-VPS35) (Figure 4). *Nicotiana benthamiana* leaves were then transfected with both an *Agrobacterium tumefaciens* strain containing a N-YFP-VPS26C construct and an *A. tumefaciens* strain containing a plasmid in which a VPS35 gene family member was fused to the C-terminal portion of YFP (C-YFP-VPS35). Using this assay, we showed that VPS26C interacted in a BiFC complex exclusively with VPS35A (Figure 4B). No evidence for a large retromer complex was observed between VPS26C and either VPS35B or VPS35C (Figures 4C, D). In addition, as was seen by

Zelazny et al. (2013) and Munch et al. (2015), a positive BiFC interaction between VPS26 and VPS35 required the simultaneous expression of VPS29 in this assay (Figure 4E). We also observed a positive BiFC interaction between VPS26A and VPS35A that depended on the co-expression of VPS29-mCherry (Figure 4A), as has previously been reported by Zelazny et al. (2013). These results demonstrate that VPS26C colocalizes with VPS35A in the presence of VPS29 *in planta* as a large retromer complex and corroborate our genetic studies described above, predicting that VPS26C, VPS29 and VPS35A form a large retromer complex required for root hair growth in Arabidopsis.

Confocal analysis of Arabidopsis seedlings expressing VPS26C: GFP-VPS26C in a *vps26c* background indicated that VPS26C localizes, at least in part, to a membrane compartment in Arabidopsis roots (Figure 5A, 5B). We used Brefeldin A sensitivity as an assay to investigate whether VPS26C may be localized to the TGN, as Niemes et al. (2010) have localized VPS29 to both the TGN and the core of a BFA-sensitive compartment. BFA has been shown to inhibit GTP exchange factors (Peyroche et al., 1999; Richter et al., 2007, 2011) and disrupts trafficking pathways between the ER and Golgi as well as endocytosis from the plasma membrane to the TGN. Five-day-old seedlings expressing GFP-VPS26C in a *vps26c* background were incubated in either vehicle alone or 100 μM BFA diluted in 1X MS media for 90 minutes (Figure 5A). As a positive control, transgenic seedlings expressing the TGN marker VTI12-YFP were also incubated in vehicle alone or 100 μM BFA diluted in MS media for 90 min (Fig. 5A). While VTI12-YFP formed "BFA bodies" when incubated in the presence of Brefeldin A, VPS26C exhibited no sensitivity to BFA, as its cellular distribution appeared similar in both BFA-treated and control seedlings

(Figure 5A). This data indicates that VPS26C is not localized to a BFA-sensitive compartment in Arabidopsis roots.

The large retromer subunit VPS35A has been shown to localize to late endosomal membranes and physically interact with RABG3f, a Rab7 homolog sensitive to wortmannin (Zelazny et al., 2013; Singh et al., 2014). Wortmannin targets both PI3K and PI4K at concentrations higher than 1 μM and causes swelling and fusion of late endosomal membranes in Arabidopsis roots (Jaillais et al., 2008; Niemes et al., 2010; Takac et al., 2012). Therefore, to investigate whether VPS26C is associated with a late endomembrane compartment, we examined the sensitivity of GFP-VPS26C localization to wortmannin in Arabidopsis roots (Figure 5). Five-day-old seedlings expressing GFP-VPS26C in a *vps26c* background were incubated in either vehicle alone or 40 μM wortmannin, diluted in 1X MS media for 90 minutes (Figure 5B). As a positive control, transgenic seedlings expressing RABG3f-mCherry were also incubated in vehicle alone or 40 μM wortmannin diluted in MS media for 90 minutes (Figure 5B). While RABG3f exhibited sensitivity to wortmannin treatment by swelling of endosomal vesicles, and forming "donut-shaped" structures, VPS26C cellular organization was unaffected. This data suggests that the membrane compartments associated with VPS26C are distinct from endosomal compartments sensitive to wortmannin in Arabidopsis roots.

The large retromer complex subunit VPS26C and SNARE VTI13 are part of a shared endosomal trafficking pathway important for tip growth in Arabidopsis

Three members of the VTI family of SNARES in Arabidopsis have been characterized. VTI11 and VTI12 function in endosomal pathways important for trafficking cargo towards the lytic and storage vacuole, respectively (Sanmartin et al., 2007; Surpin et al., 2003), and VTI13 is required for root hair growth and localizes to the early endosome and vacuole membrane (Larson et al., 2014a). Previous genetic studies using a suppressor screen of the *vti11* shoot gravitropic phenotype resulted in the identification of mutations in *VPS26A* and *VPS35A* (Hashiguchi et al., 2010), indicating a genetic interaction between a VPS26A/VPS29/VPS35A retromer-dependent pathway and a VTI11 anterograde pathway trafficking cargo to the lytic vacuole. These studies prompted us to investigate whether VTI13 and VPS26C, both required for root hair growth, also function in a shared endosomal trafficking pathway. To address this, we generated a *vti13 vps26c* double mutant and compared root hair growth of *vti13 vps26c* with the single mutants and wild type seedlings. We found that both *vti13* and *vps26c* exhibited significantly shorter root hairs than wild type seedlings when grown in the presence of 200 mM mannitol, and these phenotypes were partially suppressed in the *vti13 vps26c* double mutant (Figure 6). These results provide genetic evidence for a shared trafficking pathway involving the SNARE VTI13 and retromer component VPS26C that contributes to root hair growth in Arabidopsis. In addition, our results suggest that the VTI family of SNAREs may function in endosomal trafficking pathways in conjunction with the large retromer complex to control various aspects of plant development.

The observation that *vps26c* is defective in root hair growth and shares a genetic interaction with *VTI13* led us to investigate whether VPS26C function might also be essential for cell wall organization in roots of Arabidopsis. We have previously shown that in contrast to wild type seedlings, root epidermal and hair cells of *vti13* mutants exhibit no surface labeling with LM15, a monoclonal antibody that recognizes a xyloglucan epitope in the cell wall (Larson et al., 2014a). To explore this question, we used live tissue labeling (Larson et al., 2014b) and confocal microscopy to probe xyloglucan organization on the surface of root epidermal cells and root hairs in *vps26c* mutants and the *vti13 vps26c* double mutant. Interestingly, when the *vps26c* mutation was introduced into a *vti13* background, root epidermal cells and root hairs were labeled with LM15, unlike the *vti13* mutant alone (Figure 7). The suppression of the *vti13* phenotype with respect to root hair growth and cell wall organization in the *vti13 vps26c* double mutant provides additional data to reinforce a model in which VPS26C and VTI13 contribute to a shared endosomal pathway regulating root hair growth and wall organization.

VPS26C orthologs show deep functional conservation in plants and animals

In Arabidopsis, VPS26A and VPS26B share 91% identity at the amino acid sequence level (Figure S7), function redundantly in many aspects of plant development (Zelazny et al., 2013), and are part of a large clade of sequences that includes orthologs from plant and animal species (Koumandou et al., 2011). Two genomic models are provided for *VPS26C* in Arabidopsis. To distinguish between these models and determine the predicted amino acid sequence of VPS26C, we sequenced *VPS26C* cDNA generated using RNA isolated from the *vps26c* mutant expressing a *GFP-VPS26C* fusion as a template. This allowed us

to define the genomic model used for *VPS26C* expression in Arabidopsis (Figure S7A). The cDNA sequence shows an alignment with one of the predicted mRNA sequences in NCBI, with accession number NM_103751.3, predicting a protein of 327 amino acids. When the predicted VPS26C amino acid sequence is compared with that of ATVPS26A and ATVPS26B, it was found that VPS26C shares only 20% and 22% amino acid identity with VPS26A and VPS26B, respectively (Figure S7B). This divergence in amino acid sequence between the *VPS26* family members in Arabidopsis is also reflected by a recent phylogenetic analysis of *VPS26* orthologs in eukaryotes (Koumandou et al., 2011) that indicates *VPS26C* is present in a separate clade from *VPS26A* and *VPS26B*. Moreover, the phylogenetic analysis of Koumandou et al. (2011) supports an ancient duplication event within the *VPS26* gene family prior to the diversification of plants and animals, giving rise to two eukaryotic lineages, the *VPS26A/B* clade and the *VPS26C/DSCR3* clade.

To examine the diversity of plant orthologs specifically within the *VPS26C/DSCR3* clade, we queried plant genome and transcriptome databases and generated a phylogenetic tree based on predicted amino acid sequences. These analyses identified a single *VPS26C* ortholog in *Amborella trichopoda*, a species sister to other extant angiosperms, as well as in many eudicots (Figure 8). Surprisingly, unlike *VPS26A* and *VPS26B* genes (Koumandou et al. 2011), *VPS26C* sequences were not identified from any of the grass genomes examined. Based on copy number and the amino acid tree topology, our data support the loss of *VPS26C* specifically in the lineage leading to monocots, or at least within the grass clade of monocots.

To examine the sequence conservation of VPS26C/DSCR3 orthologs, we compared the amino acid sequence of VPS26C from Arabidopsis with that predicted for the DSCR3 protein from humans (HsDSCR3) (Figure 9). An alignment of these sequences indicated that the proteins are 40% identical at the amino acid sequence level (Figure 9A). The identification of *VPS26C* orthologs in both animal and plant species led us to examine whether the function of these orthologs is conserved across eukaryotes. To this end, we transformed *vps26c-1* and *vps26c-2* with a 35S-driven GFP fusion to the human ortholog, *DSCR3*, and examined its ability to complement the Arabidopsis *vps26c* root hair growth phenotype. Comparison of root hair length between wild type, the *vps26c* mutant, and the *vps26c* mutant expressing *HsDSCR3/VPS26C* showed that expression of the human sequence is sufficient to complement the root hair growth phenotype of *vps26c* in Arabidopsis (Figures 9B and C; Figure S2h). These results support a model in which the function of the human *DSCR3* ortholog is similar to *VPS26C* from plants.

DISCUSSION

VPS26C encodes a large retromer subunit essential for root hair growth

In this paper, we have characterized *VPS26C* as a new member of the *VPS26* family in Arabidopsis and have shown that loss-of-function alleles of *VPS26C* have a negative effect on root hair elongation in the presence of environmental stresses, such as mannitol or NaCl (Figure 1). BiFC analysis supported the role of VPS26C as part of a large retromer complex by showing that VPS35A was the sole member of the VPS35 protein family to form a complex with VPS26C and that this interaction required co-expression of AtVPS29 (Figure 4). The lack of interaction between VPS26C and VPS35B or VPS35C in the BiFC assay, two proteins which are encoded by the same family of genes and those sharing significant homology with *VPS35A*, in addition to the positive control showing a previously characterized interaction between VPS35A and VPS26A using this assay (Zelazny et al., 2013), provides strong evidence for the specificity of these interactions (Kudla and Bock, 2016). The formation of the VPS35A/VPS29/VPS26C protein complex *in planta,* therefore, demonstrates yet another retromer complex functioning in plant systems.

An examination of T-DNA insertion mutants for the known retromer subunits in Arabidopsis showed that only *vps26c*, *vps35a* and *vps29* exhibited a root hair growth defect (Figure 3). The root hair phenotype of *vps26c* was the most severe in this assay. For VPS29, the milder root hair growth phenotype is likely due to our use of a *vps29* allele that is slightly leaky (Figure S1), while the less severe phenotype of *vps35a* may be due to the ability of VPS35B or VPS35C to substitute in part for VPS35A function *in vivo*. In contrast, the severe phenotype of *vps26c* in these studies may be due to the inability of

VPS26A or VPS26B to compensate for the loss of VPS26C in regulating root hair growth (Figure 1). While *VPS26A* transcript is upregulated in the *vps26c* mutant (Figure 2), the amino acid sequence similarity between these two proteins is relatively low (Figure S7), suggesting that they may not have redundant functions.

While the genetic analysis of *vps26c* alleles in Arabidopsis initially suggested to us that a VPS26C-large retromer complex functions in endosomal trafficking pathways in response to abiotic stress, the down-regulation of *VPS26C* expression in roots of seedlings grown on media supplemented with mannitol and NaCl indicates that VPS26C-retromer function may be coordinated with other cellular mechanisms required for root hair growth. Halperin et al. (2003) has shown that treatment of root hairs with low concentrations of NaCl also reduces root hair growth in Arabidopsis through a disruption of a tip-localized Ca+2 gradient. While we confirmed that root hair growth in wild type seedlings was affected by low concentrations of NaCl under our growth conditions (Figure S4), *vps26c* exhibited even shorter root hairs and both the mannitol and Na-induced phenotypes were complemented by a GFP-VPS26C fusion. The sensitivity of *vps26c* mutant root hairs to osmotic and salt stress suggests that this large retromer complex [VPS26C/VPS29/VPS35A] may function in a coupled manner with other cellular pathways required for root hair growth in Arabidopsis.

VPS26C functions in a cellular pathway that interacts with SNARE VTI13

A small gene family in Arabidopsis encoding the VTI-SNARES function in distinct processes during plant growth. VTI11 is essential for shoot gravitropism (Yano et al., 2003)

and loss-of-function mutations in retromer subunits *VPS35A* and *VPS26A* are able to suppress the *vti11* shoot agravitropic phenotype (Hashiguchi et al., 2010). We have previously shown that VTI13 is essential for root hair growth and root epidermal cell wall organization in Arabidopsis (Larson et al., 2014a). Here, we show that the *vti13 vps26c* double mutant partially suppresses the root hair growth defect that is exhibited by each of the single mutants (Figure 6). This result indicates a genetic interaction between *VTI13*- and *VPS26C*-dependent pathways. These data also support a model in which trafficking pathways to the lytic vacuole that involve the SNARES *VTI11* and *VTI13* are coordinated with the function of distinct VPS26-large retromer complexes.

While a cellular mechanism to explain these genetic interactions has not yet been determined for either *VTI11* or *VTI13*, several possibilities exist. It is possible that mutations in large retromer subunits enhance the ability of other VTI-family members to substitute for VTI13 function in root hair growth. This model has been put forward for the genetic interaction between *VTI11* and a large retromer complex containing *VPS26A* and *VPS35A* (Hashiguchi et al., 2010). We have shown that *VPS26A* transcript is up-regulated in roots of *vps26c* suggesting that *VPS26A* may function to partially suppress the root hair phenotype in the *vti13 vps26c* double mutant. However, other potential mechanisms need to be considered. The large retromer complex protein *VPS35A* regulates trafficking of cargo to the lytic vacuole (Nodzyński et al., 2013) and *VPS35B* function is required for normal function of late endocytic compartments in plants (Munch et al., 2015). Thus large retromer complex function may be required for both anterograde and retrograde trafficking pathways between the lytic vacuole and the TGN.

We had previously shown that epidermal cell wall organization of *vti13* root epidermal cells and hairs is defective in xyloglucan organization (Larson et al., 2014a). Interestingly, we found that when a *vps26c* mutation is introduced into the *vti13* background, xyloglucan staining is indistinguishable from that of wild type (Figure 7). The observation that xyloglucan can be detected in roots of the *vti13 vps26c* double mutant indicates that the defect in *vti13* wall organization is not due to defects in xyloglucan synthesis. While future experiments will be needed to define a cellular mechanism responsible for the *vti13* and *vps26c* root hair phenotypes, this data supports a model in which the *vps26c* mutant can suppress both the *vti13* root hair growth phenotype and xyloglucan organization phenotype within the *vti13 vps26c* double mutant.

VPS26C associates with endosomal membranes insensitive to Brefeldin A and wortmannin

VPS35A has been localized to the pre-vacuolar membrane and is required for the trafficking of membrane proteins in plants (Nodzynski et al., 2013) while VPS35B has been localized to a wortmannin-sensitive, late endosomal compartment in Arabidopsis (Munch et al., 2015). In addition, proteomic studies have localized VPS35A and VPS35B to a RABG3f-enriched compartment (Zelazny et al., 2013; Heard et al. 2015), consistent with their presence on late endosomal membranes. In contrast, Niemes et al., 2010, has localized VPS29 to the TGN in Arabidopsis while Jaillais et al. (2007) found VPS29 to localize to a wortmannin-sensitive compartment together with SNX1 and RABF2b. To investigate the nature of the membrane compartment associated with VPS26C in roots, we contrasted the cellular distribution of GFP-VPS26C and VTI12-YFP in control seedlings

and seedlings treated with Brefeldin A. We also compared control seedlings and seedlings expressing GFP-VPS26C or RABG3f-mCherry treated with wortmannin (Figure 5A, B). These studies showed that while VTI12-YFP, a TGN marker (Sanderfoot et al., 2001), was sensitive to BFA and RABG3f-mCherry, a late endosomal marker (Singh et al., 2014), was sensitive to wortmannin, the cellular distribution of GFP-VPS26C on cellular membranes was unaffected by either of these compounds in root epidermal cells.

Recent analysis of the subcellular localization of VPS26C (DSCR3) in human cell culture indicates that a VPS26C/VPS29/VPS35L protein complex resides on endosomal membranes, with VPS26C directly interacting with SNX17 while the classical retromer complex in humans involves an interaction between VPS35 and the WASH complex in association with SNX27 (McNally et al., 2017). These authors also demonstrated that the human complex containing VPS26C, termed the "retriever", is responsible for recycling a distinct subset of proteins to the plasma membrane when compared to the classical retromer complex in humans (McNally et al., 2017). These results open up the possibility that VPS26C in Arabidopsis may also be part of a "retriever" complex in plants and may not share a similar intracellular localization with previously studied large retromer complexes. Future experiments, focused on identifying membrane proteins that associate with the VPS26C/VPS29/VPS35A complex in plants, their intracellular location and the cargo that may be recycled by this complex will assist in demonstrating the identity of the membranes that this complex localizes to, as well as define its role in endosomal trafficking pathways required for polarized growth in root hairs.

VPS6C shares a conserved cellular function across eukaryotes

Amino acid sequence comparisons showed that while VPS26C shares low amino acid sequence similarity with VPS26A and VPS26B in Arabidopsis (Figure S7), it shares significant similarity with DSCR3-like sequences present in both animals and plants (Koumandou et al., 2011). We used phylogenetic analysis to show that a single *VPS26C* gene is found in the genomes of most land plants surveyed (Figure 8), although it appears to be absent from the genomes of monocots for which genomic data are available. This raises the interesting question of whether V*PS26A* and/or *VPS26B* can compensate for the loss of *VPS26C* in retromer-dependent pathways controlling monocot tip growth, or whether monocots utilize a different endocytic trafficking pathway to regulate root hair growth. Further experiments will be required to determine if functional orthologs of the Arabidopsis VPS26C protein exist in monocot species.

Comparison of ATVPS26C and HSDSCR3 amino acid sequences indicated a conservation of protein sequence between these orthologs (Figure 9). Therefore, we asked whether VPS26C/DSCR3 orthologs are conserved in function across animal and plant kingdoms. We found that a *GFP-HsDSCR3* fusion was able to complement the root hair growth phenotype of *vps26c-1* and *vps26c-2,* indicating that the human ortholog can carry out all the functions of *VPS26C* needed for root hair growth (Figure 9).

The ability of HsDSCR3 to complement the *vps26c* root hair phenotype in Arabidopsis suggests that VPS26C/DSCR3 proteins have a conserved function in eukaryotic cells. A VPS26C/HsDSCR3 complex, termed the “retriever” has been characterized within human

cells and has been shown to function in an endosomal trafficking pathway that involves the recycling of a number of membrane proteins (McNally et al., 2017). A proteomic analysis of the VPS26C-retriever complex was shown to include a minimum of 10 proteins involved in ARP2/3 activation and membrane binding (McNally et al., 2017). Interestingly, many of these proteins do not have homologs in plants. Thus, future studies will be necessary to identify other proteins that interact with the VPS26C/VPS35A/VPS29 complex in a cellular pathway regulating polarized growth and cell wall organization in Arabidopsis.

EXPERIMENTAL PROCEDURES

Plant material, T-DNA insertion verification, and growth conditions

Analysis of wild type and SALK mutant lines was performed using the Columbia-0 ecotype of Arabidopsis. The growth medium for Arabidopsis seedlings consisted of 1X Murashige-Skoog (MS) salts (Murashige and Skoog, 1962), 1% (w/v) sucrose, 5 mM 4-morpholineethanesulfonic acid sodium salt (MES), pH 6, 1X Gamborg's vitamin solution, and 1.3% (w/v) agarose (Invitrogen). For plants grown to maturity, seeds were sown on soil (Transplanting mix, Gardener's Supply, Intervale Rd, Burlington, VT) and placed in Conviron MTR30 growth chambers (Conviron, Winnipeg, CA, USA), using cool-white lights (80 μmol/m^2/sec; Licor photometer LI-189) under a 16:8 h light: dark cycle at 19° C. Two *vps26c* T-DNA mutant alleles, SALK_100616 (*vps26c-1*) and SALK_036953 (*vps26c-2*), were obtained from the Arabidopsis Biological Research Center (ABRC) and PCR was used to confirm the T-DNA insertion in *VPS26C* (AT1G48550; NCBI Reference sequence: NC_003070.9) (Figure S8). To generate the *vti13 vps26c* double mutant, *vps26c-1* homozygotes were crossed with *vti13* homozygotes and F2 plants were genotyped for the two mutations using PCR. Seedlings homozygous for both the *vps26c* and *vti13* T-DNA insertion alleles were grown to seed and T3 seedlings were analyzed for root hair growth. Primer sequences used for genomic PCR are listed in Table S1.

The *vps26c-1* and *vps26c-2* mutants were transformed separately with *35S:GFP-VPS26C* and *VPS26C:GFP-VPS26C* and transgenic lines containing these constructs were selected for BASTA resistance. T3 homozygous lines expressing the *GFP-VPS26C* constructs were analyzed for complementation of the *vps26c* mannitol/NaCl root hair phenotype. In

addition, *vps26c* mutants were transformed with the *VPS26C* human ortholog (*35S:GFP-HsDSCR3*) and seedlings from homozygous lines expressing *GFP-HsDSCR3* were analyzed for complementation of *vps26c* root hair phenotypes.

Characterization of root hair phenotypes

Seeds were sterilized using 20% (v/v) bleach, followed by 5-6 washes in sterile distilled water. The sterilized seeds were stored in sterile water overnight in the dark at 4° C before plating them on solid media. Seedlings were grown on MS medium using petri plates placed vertically under continuous white light at 20°C for five days. Where indicated, 200 mM mannitol or 30 mM NaCl was included in the growth medium. To characterize root hair shape and growth, seedlings were mounted in sterile water on glass slides. Images were taken using a Nikon Eclipse TE200 inverted microscope with SPOT imaging software (Diagnostic Instruments). The length of 10-15 root hairs/seedling for at least 10 seedlings per genotype were measured, using the calibrating tool in the SPOT software, and a Student's *t*-test was used for statistical analysis.

Construction of GFP-VPS26C fusions

To generate the *35S: GFP-VPS26C* construct, *VPS26C* was amplified by PCR using genomic DNA and primers described in Supplementary Table 1. The *VPS26C* PCR product was cloned into pENTR (Invitrogen) and was subsequently recombined into pB7WGF2 to create a *35S: GFP-VPS26C* fusion. This construct was transformed into *E.coli,* DH5α, and subsequently into *Agrobacterium tumefacians,* GV3101, and was used to transform

35S:GFP-VPS26C into Arabidopsis using the floral dip method (Clough & Bent, 1998; Zhang et al., 2006).

To generate the *GFP-HsDSCR3* fusion, cloned *HsDSCR3* cDNA was purchased from Origene technologies (Cat. No.- RC210755) and used as a template for PCR amplification with primers described in Table S1. The *HsDSCR3* PCR product was cloned into pENTR (Invitrogen) and transformed into *Escherichia coli,* strain DH5α. The insert was confirmed by PCR, and subsequently recombined into pB7WGF2 using Gateway technology, according to manufacturer's instructions. The *GFP-HsDSCR3* construct in pB7WGF2 was transformed into *A. tumefaciens* and then into Arabidopsis as described above.

To generate a *VPS26C: GFP-VPS26C* construct, 2 kb of genomic sequence upstream of the V*PS26C* translation start codon was amplified using primers containing a SacI and a SpeI restriction site at their respective 5'-ends (see Table S1). The *VPS26C* promoter PCR product was cloned into pENTR (Invitrogen), digested with SacI and SpeI, and ligated upstream of *GFP-VPS26C* in the B7WGF2 backbone that had previously been digested with SacI and SpeI to remove the 35S promoter. The *VPS26C: GFP-VPS26C* construct was transformed into *E. coli* DH5α and subsequently into *A. tumefacians,* strain GV3101 for transformation into Arabidopsis.

RNA isolation and transcript analysis using RT-PCR and qRT-PCR

For transcript expression analysis across the developmental stages of Arabidopsis, 7-day-old seedling roots, 7-day-old whole seedlings, leaves (45-day-old plant, 10-12 leaved

rosette, bolted), stems, open flowers and green siliques were collected for three biological replicates. For null mutant analysis, seven-day-old seedlings were pooled from each genotype and three biological replicates were generated for RNA extraction. For all other RT-PCR and qRT-PCR assays, five-day-old seedling roots were used for RNA isolation. Roots from approximately 200 seedlings were pooled for each genotype and treatment and three biological replicates were generated. Root tissue was excised from the seedlings leaving only the differentiation, elongation, and meristematic regions of the root. All isolated tissues were frozen, ground in liquid nitrogen, and stored at -80°C. Total RNA was extracted using a Qiagen RNeasy Plant Mini Kit, quantified using a nanodrop (ThermoScientific) followed by generation of first strand cDNA using Superscript II Reverse Transcriptase (Invitrogen), according to the manufacturer's instructions. For semi-quantitative RT-PCR, root cDNA was used as a template, and PCR products were amplified using Phusion polymerase (New England Biolabs) according to the manufacturer's instructions. For quantitative RT-PCR, the first-strand cDNA was diluted 1:10 and then used as a template with iTaq Universal SYBR green Supermix (Bio-Rad). An Applied Biosystems Step-one Plus instrument was used to run the qRT-PCR. Three technical and three biological replicates were used for each qRT-PCR cycle. The differential expression values of transcripts were standardized against the transcript expression of *EF1α* and *ACT2* housekeeping genes. The sequence of primers used for RT- and qRT-PCR are described in Supplemental Table 1.

BiFC analysis

Full-length genomic clones were amplified for *VPS26A, VPS26C, VPS29, VPS35A*, *VPS35B* and *VPS35C* using Arabidopsis seedlings. The primers used for each of the PCR reactions are listed in TableS1. *VPS26A* and *VPS26C* were each cloned into the destination vector pSAT4-DEST-nEYFP-C1 (CD3-1089, ABRC) to create N-terminal YFP fusion constructs. *VPS35A*, *VPS35B* and *VPS35C* were each cloned into destination vector pSAT5-DEST-cEYFP-C1 (CD3-1097, ABRC) to form C-terminal YFP fusion constructs. *VPS29* was amplified using primers containing KpnI and BamHI restriction enzyme sequences at their 5'-ends and cloned into pENTR (Invitrogen). Both *VPS29* in pENTR and the destination vector pSAT6-mCherry-C1-B (CD3-1105, ABRC) were digested with KpnI and BamHI, gel purified and a mCherry-VPS29 fusion was generated using T4 DNA ligase and the pSAT6 backbone. All constructs were transformed into *E.coli* strain DH5α. The presence of VPS sequences was confirmed using PCR, followed by transformation into *A. tumefaciens,* strain GV2260 before transfecting into *Nicotiana benthamiana* leaves.

N. benthamiana leaves were co-transformed with two *A. tumefaciens* strains containing a N-terminal YFP-VPS26C fusion and a C-terminal YFP fusion to either *VPS35A*, *VPS35B*, or *VPS35C* in a manner similar to that described by Munch et al. (2015) with the following changes. N-terminal *YFP-VPS26A* was co-transformed with a C-terminal YFP fusion to *VPS35A* as a positive control. All transformations also included an *A. tumefaciens* strain containing *VPS29* fused with *mCherry.* Overnight cultures of *A. tumefaciens* containing the various YFP fusions were grown with appropriate antibiotic selection at 28°C, pelleted and resuspended in 10mM magnesium chloride to reach a final OD600=1.5. Two

microliters of 100 mM acetosyringone was added per ml of resuspended bacterial culture. Bacterial suspensions were incubated at room temperature in the dark for 4 hours without shaking and then infiltrated into the abaxial side of fully expanded 4-week-old *N. benthamiana* leaves (1 ml of culture/leaf). Infected plants were grown under continuous light at 20°C for 2-3 days after which leaf tissue was imaged using confocal microscopy.

Confocal microscopy and drug treatment

Confocal images were obtained using a Zeiss LSM 510 META confocal laser-scanning microscope. The LSM META software was used to acquire images, which were then processed using ImageJ (https://imageJ.net/Citing). The GFP-VPS26C lines were excited with a 488 nm laser and emissions were captured using a 505-530nm band pass filter. The YFP protein fusions for BiFC assays were excited with a 514 nm laser and emissions were captured using a 530-600 nm band pass filter. The mCherry fusion in the BiFC assays was excited with an additional laser of 545 nm and emissions were acquired using a 560-615 nm band pass filter. All signals were captured sequentially and superimposed in a final composite image.

To investigate the sensitivity of VPS26C to BFA or wortmannin, five-day-old seedlings were incubated in multi-well plates with either vehicle alone, or with 100 μM BFA or 40 μM wortmannin diluted in 1X MS medium for 90 minutes before imaging using confocal microscopy. Excitation and emission wavelengths for YFP, GFP and mCherry fusions were as described above. VTI12-YFP (WAVE 13Y; CS781654) and RabG3f-mCherry

(WAVE 5R; CS781670) were used as positive controls for the BFA and wortmannin sensitivity assays, respectively.

Immunohistochemistry of roots and root hairs of Arabidopsis

For immunofluorescence analysis of roots hairs, the protocol described in Larson et al. (2014b) was employed. Briefly, whole roots were washed 3X (5 min each) in fresh MS medium and then placed in blocking solution consisting of 1% nonfat Carnation Instant Milk in MS for 30 min with gentle agitation. After washing 3X with MS, the roots were placed in the primary antibody label consisting of LM15 (Plant Probes; Leeds, UK) diluted 1/10 in MS for 90 min. After three washes with MS and a 30 min block (see above), the roots were then incubated in the secondary antibody label consisting of anti-rat TRITC (Sigma Chemical; St. Louis, MO) diluted 1/75 in MS for 90 min. The roots were then washed 3X with MS, positioned in the well of immunoslide (EMS; Ft. Washington, PA) containing 50 µL MS and then covered with a glass coverslip.

Roots were observed with an Olympus Fluoview 1200 confocal laser scanning microscope (CLSM) using a 559 laser and TRITC filter set with an excitation range of 515-550nm and an emission range of 600-640nm. Intensity levels of LM15-labeled root hair walls were adjusted using the Hi-Lo pseudocolor control of the CLSM. The captured image was then changed to green pseudocolor. Root hair images were captured at a maximum intensity under conditions that did not show any saturation signals. In these experiments, a small level of non-specific labeling was observed in root epidermal cells. All labeling was repeated 3X and the control included the elimination of the primary antibody step.

Phylogenetic Analysis of VPS26C sequences

For phylogenetic analyses, gene sequences of *VPS26C* from fifteen angiosperm genomes were downloaded from Phytozome (v.12.1) or NCBI. Predicted VPS26C amino acid sequences were first aligned with the program Muscle, as implemented in Geneious version 10.1 (Kearse et al., 2012). The final six positions in the alignment were trimmed from five accessions to yield sequences of uniform length. To improve posterior-probability support for the phylogeny, the amino-acid alignment was reconstructed with all parameters at default values except the gap-open score, which was set to 0 to yield the maximum allowable number of gaps. All sites in the alignment with gaps (55 of 336) were removed from the dataset, because support values were further improved. The alignment from which the gaps were removed is provided in Table S2.

Phylogenetic analysis was performed using the program MrBayes 3.2.6 (Ronquist et al., 2012) running on EXSEDE via the Cipres Portal (Miller et al., 2010). A Markov Chain Monte Carlo analysis was performed for the amino acid sequences with four independent Markov chains run for five million generations; trees were sampled every 1000 generations. Stationarity was determined using the log-likelihood scores for each run plotted against generation in the program Tracer version 1.5 (Rambaut and Drummond, 2007). 25% of the trees were discarded as a burn-in phase, and a 50% majority-rule consensus tree was calculated for the remaining trees. The species sister to all remaining angiosperms (*Amborella trichopoda)* was used as the outgroup for the phylogenetic analyses (Stevens, 2012).

Statistical Analysis

Statistical analyses were done using a Student's *t*-Test, where pairwise comparison was performed between genotypes, or treatments. For example, root hair growth measurements were compared in a pair-wise fashion between wild type and each of the mutants individually, and significance was accepted at the $P<0.05$ level.

Accession numbers

The sequence and T-DNA insertion details mentioned in this publication are available at the Arabidopsis Information Resource (TAIR) and are indicated by the following accession numbers. The mutant alleles and SALK T-DNA insertion lines used for genetic studies are denoted in parentheses, respectiely: *VPS26A*, AT5G53530 (*vps26a-3,* CS831947); *VPS26B*, AT4G27690 (*vps26b-1,* SALK_142592; Zelazny et al., 2013); *VPS26C*, AT1G48550 (*vps26c-1*, SALK_100616; *vps26c-2*, SALK_036953); *VPS29*, AT3G47810 (*vps29-6,* SALK_051994); *VPS35A*, AT2G17790 (*vps35a-2,* SALK_079196); *VPS35B*, AT1G75850 (*vps35b-3,* SALK_052160); *VPS35C*, AT3G51310 (*vps35c-2,* SALK_099733); *VTI13*, AT3G29100 (SALK_075261)

ACKNOWLEDGEMENTS

Jordan Humble identified the root hair phenotype of *vps26c* alleles in response to mannitol. Emily Larson generated the *VPS26C: GFP-VPS26C* construct and performed crosses to generate the *vti13 vps26c* double mutant. David Barrington generated a phylogenetic tree for *VPS26C* orthologs in plants. David Domozych performed the immunohistochemistry using LM15 monoclonal antibodies to characterize the distribution of xyloglucans on the surface of epidermal cells in wild type, *vti13*, *vps26c* and *vti13 vps26c* seedling roots. Suryatapa Ghosh Jha analyzed the *vps26c* alleles for their response to mannitol and NaCl in the media and other retromer mutant phenotypes, generated complemented lines for both *vps26c-1* and *vps26c-2*, performed BiFC analysis of VPS26C *in planta*, confocal microscopy analysis, qRT/PCR analysis of *VPS26C* expression during plant plant growth and cloned and complemented the *vps26c* alleles with the *VPS26C/DSCR3* human ortholog. Suryatapa Ghosh Jha wrote the first draft of the manuscript; Mary Tierney edited the manuscript and supervised the research. The authors have no conflict of interest to declare.

We thank Jeanne Harris, Jill Preston and Georgia Drakakaki for insightful comments and suggestions on the manuscript. We also thank Georgia Drakakaki for providing us seeds of the VTI12-YFP (Wave 13Y) line. Imaging work was done at the Microscope Imaging Facility at the University of Vermont. Confocal microscopy was performed on a Zeiss 510 META laser scanning confocal microscope supported by NIH Award Number 1S10RR019246 from the National Center for Research Resources. USDA-Hatch Grants

VT-H02001 and VT-H02311 and funds from the Department of Plant Biology, University of Vermont, supported this research.

REFERENCES

Clough, S.J. and Bent, A.F. (1998) Floral dip: a simplified method for Agrobacterium-mediated transformation of *Arabidopsis thaliana*. *Plant J.* **16**, 735–743.

Collins, B.M. (2008) The structure and function of the retromer protein complex. *Traffic*, **9**, 1811-1822.

Edgar, A.J. and Polak, J.M. (2000) Human homologues of yeast vacuolar protein sorting 29 and 35. *Biochem. Biophys. Res. Comm.* **277**, 622–630.

Früholz, S. and Pimpl, P. (2017) Analysis of Nanobody-Epitope Interactions in Living Cells via Quantitative Protein Transport Assays. *Methods Mol. Biol.* **1662**,171-182.

Gallon, M. and Cullen, P.J. (2015) Retromer and sorting nexins in endosomal sorting. *Biochem. Soc. Trans.* **43**, 33–47.

Geldner, N., Friml, J., Stierhof, Y.-D., Jürgens, G. and Palme, K. (2001) Auxin transport inhibitors block PIN1 cycling and vesicle trafficking. *Nature*, **413**, 425-428.

Haft, C.R., de la Luz Sierra, M., Bafford, R., Lesniak, M.A., Barr, V.A. and Taylor, S.I. (2000) Human orthologs of yeast vacuolar protein sorting proteins Vps26, 29, and 35: assembly into multimeric complexes. *Mol. Biol. Cell*, **11**, 4105–4116.

Halperin, S.J., Gilroy, S. and Lynch, J.P. (2003) Sodium chloride reduces growth and cytosolic calcium, but does not affect cytosolic pH, in root hairs of *Arabidopsis thaliana* L. *J. Exp. Bot.* **54**, 1269–1280.

Hashiguchi, Y., Niihama, M., Takahashi, T., Saito, C., Nakano, A., Tasaka, M. and Morita, M.T. (2010) Loss-of-function mutations of retromer large subunit genes suppress the phenotype of an Arabidopsis *zig* mutant that lacks Qb-SNARE VTI11. *Plant Cell,* **22**, 159–172.

Heard, W., Sklenář, J., Tomé, D.F., Robatzek, S. and Jones, A.M. (2015) Identification of Regulatory and Cargo Proteins of Endosomal and Secretory Pathways in Arabidopsis thaliana by Proteomic Dissection. *Mol Cell Proteomics*, **14**, 1796-1813.

Horazdovsky, B.F., Davies, B.A., Seaman, M.N., McLaughlin, S.A., Yoon, S. and Emr, S.D. (1997) A sorting nexin-1 homologue, Vps5p, forms a complex with Vps17p and is required for recycling the vacuolar protein-sorting receptor. *Mol. Biol. Cell*, **8**, 1529–1541.

Jaillais, Y., Fobis-Loisy, I., Miege, C., Rollin, C. and Gaude, T. (2006) AtSNX1 defines an endosome for auxin-carrier trafficking in Arabidopsis. *Nature*, **443**, 106–109.Jaillais, Y., Santambrogio, M., Rozier, F., Fobis-Loisy, I., Miège, C. and Gaude, T. (2007) The

retromer protein VPS29 links cell polarity and organ initiation in plants. *Cell,* **130**, 1057–1070.

Jaillais, Y., Fobis-Loisy, I., Miège, C. and Gaude, T. (2008) Evidence for a sorting endosome in Arabidopsis root cells. *Plant J.* **53**, 237-47.

Kang, H., Kim, S.Y., Song, K., Sohn, E.J., Lee, Y., Lee, D.W., Hara-Nishimura, I. and Hwang, I. (2012) Trafficking of vacuolar proteins: the crucial role of Arabidopsis vacuolar protein sorting 29 in recycling vacuolar sorting receptor. *Plant Cell*, **24**, 5058–5073.

Kearse, M., Moir, R., Wilson, A., Stones-Havas, S., Cheung, M., Sturrock, S., Buxton, S., Cooper, A., Markowitz, S., Duran, C., Thierer, T., Ashton, B., Mentjies, P. and Drummond, A. (2012) Geneious Basic: an integrated and extendable desktop software platform for the organization and analysis of sequence data. *Bioinformatics,* **28**, 1647–1649. https://www.geneious.com

Kerr, M.C., Bennetts, J.S., Simpson, F., Thomas, E.C., Flegg, C., Gleeson, P.A., Wicking, C. and Teasdale, R.D. (2005) A novel mammalian retromer component, Vps26B. *Traffic*, **6**, 991–1001.

Kim, E., Lee, Y., Lee, H.J., Kim, J.S., Song, B.S., Huh, J.W., Lee, S.R., Kim, S.U., Kim, S.H., Hong, Y., Shim, I. and Chang, K.T. (2010) Implication of mouse Vps26b-Vps29-Vps35 retromer complex in sortilin trafficking. *Biochem. Biophys. Res. Comm.* **403**, 167–171.

Kleine-Vehn, J., Dhonukshe, P., Sauer, M., Brewer, P.B., Wiśniewska. J., Paciorek, T., Benková, E. and Friml, J. (2008a) ARF GEF-dependent transcytosis and polar delivery of PIN auxin carriers in Arabidopsis. *Curr. Biol.* **8**, 526-31.

Kleine-Vehn, J., Langowski, L., Wisniewska, J., Dhonukshe, P., Brewer, P.B. and Friml, J. (2008b) Cellular and molecular requirements for polar PIN targeting and transcytosis in plants. *Mol. Plant*, **1**, 1056-66.

Koumandou, V.L., Klute, M.J., Herman, E.K., Nunez-Miguel, R., Dacks, J.B. and Field, M.C. (2011) Evolutionary reconstruction of the retromer complex and its function in *Trypanosoma brucei*. *J. Cell Sci*. **124**, 1496–1509.

Künzl, F., Früholz, S., Fäßler, F., Li, B. and Pimpl, P. (2016) Receptor-mediated sorting of soluble vacuolar proteins ends at the trans-Golgi network/early endosome. *Nature Plants* **2,** 16017.

Kvainickas, A., Jimenez-Orgaz, A., Nägele, H., Hu, Z., Dengjel, J. and Steinberg, F. 2017 Cargo-selective SNX-BAR proteins mediate retromer trimer independent retrograde transport. *J Cell Biol.* **216**, 3677-3693.

Larson, E.R., Domozych, D.S. and Tierney, M.L. (2014a) SNARE VTI13 plays a unique role in endosomal trafficking pathways associated with the vacuole and is essential for cell wall organization and root hair growth in arabidopsis. *Annals of Botany,* **114**, 1147–1159.

Larson, E.R., Tierney, M.L., Tinaz, B. and Domozych, D.S. (2014b) Using monoclonal antibodies to label living root hairs: a novel tool for studying cell wall microarchitecture and dynamics in Arabidopsis. *Plant Methods,* **10**, 30.

McNally, K. E., Faulkner, R., Steinberg, F., Gallon, M., Ghai, R., Pim, D., Langton, P., Pearson, N., Danson, C. M., Nagelle, H., Morris, L. L., Singla, A., Overlee, B. L., Heesom, K. J., Sessions, R., Banks, L., Collins, B. M., Berger, I., Billadeau, D. D., Burstein, E., and Cullen, P. J. (2017) Retriever is a Multiprotein Complex for Retromer-independent Endosomal Cargo Recycling. *Nat. Cell Biol.* **19**, 1214-1225.

Miller, M.A., Pfeiffer, W. and Schwartz, T. (2010) Creating the CIPRES Science Gateway for inference of large phylogenetic trees. pp 1-8 in Proceedings of the Gateway Computing Environments Workshop (GCE), 14 Nov. 2010, New Orleans, LA.

Munch, D., Teh, O.-K., Malinovsky, F.G., Liu, Q., Vetukuri, R.R., El Kasmi, F., Brodersen, P., Hara-Nishimura, I., Dangl, J.L., Petersen, M., Mundy, J. and Hofius, D. (2015) Retromer contributes to immunity-associated cell death in Arabidopsis. *Plant Cell,* **27**, 463–479.

Murashige, T. and Skoog, F. (1962) A revised medium for rapid growth and bio assays with tobacco tissue cultures. *Physiol. Plant.* **15**, 473-497.

Niemes, S., Langhans, M., Viotti, C., Scheuring, D., San Wan Yan, M., Jiang, L., Hillmer, S., Robinson, D.G. and Pimpl, P. (2010) Retromer recycles vacuolar sorting receptors from the trans-Golgi network. *Plant J.* **61**, 107-121.

Nodzyński, T., Feraru, M.I., Hirsch, S., De Rycke, R., Niculaes, C., Boerjan, W., Van Leene, J., De Jaeger, G., Vanneste, S. and Friml, J. (2013) Retromer Subunits VPS35A and VPS29 Mediate Prevacuolar Compartment (PVC) Function in Arabidopsis. *Mol. Plant*, **6**, 1849–1862.

Nothwehr, S.F. and Hindes, A.E. (1997) The yeast VPS5/GRD2 gene encodes a sorting nexin-1-like protein required for localizing membrane proteins to the late Golgi. *J. Cell Sci.* **110**, 1063–1072.

Oliviusson, P., Heinzerling, O., Hillmer, S., Hinz, G., Tse, Y.C., Jiang, L. and Robinson, D.G. (2006) Plant retromer, localized to the prevacuolar compartment and microvesicles in Arabidopsis, may interact with vacuolar sorting receptors. *Plant Cell*, **18**, 1239-1252.

Ovecka, M., Lang, I., Baluska, F., Ismail, A., Illes, P. and Lichtscheidl, I.K. (2005) Endocytosis and vesicle trafficking during tip growth of root hairs. *Protoplasma*, **226**, 39–54.

Paravicini, G., Horazdovsky, B.F. and Emr, S.D. (1992) Alternative pathways for the sorting of soluble vacuolar proteins in yeast: a vps35 null mutant missorts and secretes only a subset of vacuolar hydrolases. *Mol. Biol. Cell*, **3**, 415–427.

Peyroche, A., Antonny, B., Robineau, S., Acker, J., Cherfils, J. and Jackson, C. L. (1999) Brefeldin A Acts to Stabilize an Abortive ARF–GDP–Sec7 Domain Protein Complex: Involvement of Specific Residues of the Sec7 Domain. *Mol. Cell*, **3**, 275–285.

Pourcher, M., Santambrogio, M., Thazar, N., Thierry, A.M., Fobis-Loisy, I., Miège, C., Jaillais, Y. and Gaude, T. (2010) Analyses of sorting nexins reveal distinct retromer-subcomplex functions in development and protein sorting in Arabidopsis thaliana. *Plant Cell*, **22**, 3980–3991.

Preuss, M.L., Schmitz, A.J., Thole, J.M., Bonner, H.K., Otegui, M.S. and Nielsen, E. (2006) A role for the RabA4b effector protein PI-4Kβ1 in polarized expansion of root hair cells in *Arabidopsis thaliana*. *J. Cell Biol.* **172**, 991–998.

Rambaut, A. and Drummond, A.J. (2007) *Tracer.* Version 1.5. http://beast.bio.ed.ac.uk/Tracer

Richter, S., Geldner, N., Schrader, J., Wolters, H., Stierhof, Y.D., Rios, G., Koncz, C., Robinson, D.G. and Jürgens, G. (2007). Functional diversification of closely related ARF-GEFs in protein secretion and recycling. *Nature*, **448**, 488-92.

Richter, S., Müller, L.M., Stierhof, Y.D., Mayer, U., Takada, N., Kost, B., Vieten, A., Geldner, N., Koncz, C. and Jürgens, G. (2011) Polarized cell growth in Arabidopsis requires endosomal recycling mediated by GBF1-related ARF exchange factors. *Nat. Cell Biol.* **14**, 80-6.

Robinson, D.G. and Neuhaus, J.M. (2016) Receptor-mediated sorting of soluble vacuolar proteins: myths, facts, and a new model. *J. Exp. Bot.* **67**, 4435-4449.

Ronquist, F., Teslenko, M., van der Mark, P., Ayres, D.L., Darling, A., Höhna, S., Larget, B., Liu, L., Suchard, M.A. and Huelsenbeck, J.P. (2012) MrBayes 3.2: efficient Bayesian phylogenetic inference and model choice across a large model space. *Syst. Biol.* **61**, 539–542.

Sanderfoot, A.A., Kovaleva, V., Bassham, D.C. and Raikhel, N.V. (2001) Interactions between syntaxins identify at least five SNARE complexes within the golgi/prevacuolar system of the Arabidopsis cell. *Mol. Biol. Cell,* **12**, 3733-3743.

Sanmartín, M., Ordóñez, A., Sohn, E.J., Robert, S., Sánchez-Serrano, J.J., Surpin, M.A., Raikhel, N.V. and Rojo, E. (2007) Divergent functions of VTI12 and VTI11 in trafficking to storage and lytic vacuoles in Arabidopsis. *Proc. Natl. Acad. Sci.USA,* **104**, 3645–3650.

Seaman, M.N., Marcusson, E.G., Cereghino, J.L., and Emr, S.D. (1997) Endosome to Golgi retrieval of the vacuolar protein sorting receptor, Vps10p, requires the function of the VPS29, VPS30, and VPS35 gene products. *J. Cell Biol.* **137**, 79–92.

Simonetti, B., Danson, C.M., Heesom, K.J. and Cullen, P.J. (2017) Sequence-dependent cargo recognition by SNX-BARs mediates retromer-independent transport of CI-MPR. *J. Cell Biol.* **216**, 3695-3712.

Singh, M.K., Kruger, F., Beckmann, H., Brumm, S., Vermeer, J.E.M., Munnik, T., Mayer, U., Stierhof, Y-D., Grefen, C., and Schumacher, K. (2014) Protein Delivery to Vacuole Requires SAND Protein- Dependent Rab GTPase Conversion for MVB-Vacuole Fusion. *Curr. Biol.* **24**, 1383-1389.

Stevens, P. F. (2001 onwards) Angiosperm Phylogeny Website. Version 12, July 2012. http://www.mobot.org/MOBOT/research/APweb/

Surpin, M., Zheng, H., Morita, M.T., Saito, C., Avila, E., Blakeslee, J.J., Bandyopadhyay, A., Kovaleva, V., Carter, D., Murphy, A., Tasaka, M. and Raikhel, N. (2003) The VTI family of SNARE proteins is necessary for plant viability and mediates different protein transport pathways. *Plant Cell,* **15**, 2885–2899.

Takac, T., Pechan, T., Samajova, O., Ovecka, M., Richter, H., Eck, C., Niehaus, K., and Samaj, J. (2012) Wortmannin Treatment induces changes in Arabidopsis root proteome and post-Golgi compartments. *J. Proteome Res.* **11**, 3127-3142.

Thazar-Poulot, N., Miquel, M., Fobis-Loisy, I. and Gaude, T. (2015) Peroxisome extensions deliver the Arabidopsis SDP1 lipase to oil bodies. *Proc. Natl. Acad. Sci. USA,* **112**, 4158–4163.

Voigt, B., Timmers, A.C., Šamaj, J., Hlavacka, A., Ueda, T., Preuss, M., Nielsen, E., Mathur, J., Emans, N., Stenmark, H., Nakano, A., Baluska, F. and Menzel D. (2005) Actin-based motility of endosomes is linked to the polar tip growth of root hairs. *Euro. J. Cell Biol.* **84**: 609–621.

Wang, Y., Zhang, W., Li, K., Sun, F., Han, C., Wang, Y. and Li, X. (2008) Salt-induced plasticity of root hair development is caused by ion disequilibrium in *Arabidopsis thaliana*. *J. Plant Res.* **121:** 87–96.

Yamazaki, M., Shimada, T., Takahashi, H., Tamura, K., Kondo, M., Nishimura, M. and Hara-Nishimura, I. (2008) Arabidopsis VPS35, a Retromer Component, is Required for Vacuolar Protein Sorting and Involved in Plant Growth and Leaf Senescence. *Plant Cell Physiol.* **49:** 142–156.

Zelazny, E., Santambrogio, M., Pourcher, M., Chambrier, P., Berne-Dedieu, A., Fobis-Loisy, I., Miege, C., Jallais, Y. and Gaude, T. (2013) Mechanisms governing the

endosomal membrane recruitment of the core retromer in Arabidopsis. *J Biol. Chem.* **288:** 8815–8825.

Zhang, X., Henriques, R., Lin, S.S., Niu, Q.W. and Chua, N.H. (2006) Agrobacterium-mediated transformation of *Arabidopsis thaliana* using the floral dip method. *Nat. Protocols*, **1:** 641–646.

Zheng, H., von Mollard, G.F., Kovaleva, V., Stevens, T. H., and Raikhel, N. V. (1999) The Plant Vesicle-associated SNARE AtVTI1a Likely Mediates Vesicle Transport from the Trans-Golgi Network to the Prevacuolar Compartment. *Mol. Biol. Cell*, **10:** 2251–2264.

FIGURE LEGENDS

Figure 1.

vps26c is defective in root hair growth when grown in the presence of mannitol or NaCl.

(A) Wild type, *vps26c-1, vps26c-2* and *vps26c-1* seedlings expressing VPS26C: GFP-VPS26C were grown on 1X MS medium, pH 6, 1X MS medium, pH6 supplemented with 200 mM mannitol, and 1X MS medium, pH 6 supplemented with 30mM NaCl for 5 days after which root hairs were imaged using bright field microscopy. Both *vps26c* mutants exhibited root hairs indistinguishable from wild type when seedlings were grown on standard MS medium, but showed reduced root hair length when either mannitol or NaCl was added to the medium. The *vps26c* root hair growth phenotypes were complemented in *vps26c*-1 mutant lines expressing *VPS26C: GFP-VPS26C* for both media conditions. Three independent transgenic lines expressing *VPS26C: GFP-VPS26C* in a *vps26c-1* background exhibited similar root hair growth phenotypes. Bars= 100 μm

(B) Average root hair length (μm) of 5-day-old seedlings grown on 1X MS medium, pH 6 (black bars) and on 1X MS medium, pH6 supplemented with 200 mM mannitol (grey bars). Twenty seedlings per genotype per treatment were scored and 10-15 root hairs per seedling were measured for each biological replicate. The graph shows an average of three biological replicates. Asterisks indicate statistical significance according to the Student's *t*-test, where wild type was compared in a pair-wise manner with each of the genotypes for each treatment ($P < 0.05$). Error bars represent the standard error of the mean of three biological replicates.

(C) Average root hair length of 5-day-old seedlings grown on 1X MS medium, pH 6 (black) and 1X MS medium, pH 6 supplemented with 30 mM NaCl (grey). Twenty seedlings per treatment per genotype were scored and 10-15 root hairs per seedling were measured for each biological replicate. The graph shows an average of three biological replicates. Asterisks indicate statistical significance according to the Student's *t*-test, where wild type was compared in a pair-wise manner with each of the genotypes individually for each treatment ($P < 0.05$). Error bars represent the standard error of the mean of three biological replicates.

Figure 2.

Differential expression of *VPS26* family members in wild type seedlings grown under different media conditions

(A) qRT-PCR was used to quantitate *VPS26C* transcript levels present in roots of wild type seedlings grown on 1X MS medium, pH 6, or 1X MS medium, pH 6 supplemented with either 200 mM mannitol or 30 mM NaCl. Seedlings grown in the presence of either mannitol or NaCl showed a down-regulation of *VPS26C* expression when compared to wild type seedlings grown on MS alone. Asterisks indicate statistical significance according to the Student's *t*-test, where a pair-wise comparison was performed between *VPS26C* transcript levels from roots of seedlings grown on MS media and each of the treatments ($P < 0.05$). Error bars represent the standard error of the mean of three biological replicates, run in triplicate.

(B and C) qRT-PCR analysis of *VPS26A* **(B)** and *VPS26B* **(C)** transcript levels in roots of wild type seedlings grown on 1X MS medium, pH 6 or seedlings grown on 1X MS medium, pH 6 supplemented with either 200 mM mannitol or 30 mM NaCl. In contrast to *VPS26C*, wild type seedlings grown in the presence of either mannitol or NaCl showed an induction of *VPS26A* expression when compared to wild type seedlings grown on MS alone. This upregulation is also observed in the expression of *VP26B* in roots of wild type seedlings grown on media containing mannitol. Asterisks indicate statistical significance according to the Student's *t*-test, where pair-wise comparisons were performed betweenVPS26A or VPS26B transcript levels from roots of seedlings grown on MS media and the level of these same transcripts in roots of seedlings grown under each treatment condition ($P < 0.05$). Error bars represent the standard error of the mean of three biological replicates, run in triplicate.

(D) *VPS26B* in wild type vs. *vps26c* seedling roots grown on 1X MS medium, pH 6. *VPS26A* transcript levels were induced in *vps26c* roots when compared to wild type roots, whereas *VPS26B* transcript levels were down regulated in *vps26c* roots when compared to the wild type roots. Asterisks indicate statistical significance according to the Student's *t*-test, where pair-wise comparisons were performed betweenVPS26A or VPS26B transcript levels from roots of wild type seedlings grown on MS media and the level of these same transcripts in roots of *vps26c* seedlings grown on MS media ($P < 0.05$). Error bars represent the standard error of mean of three biological replicates, run in triplicate.

Figure 3.

Large retromer complex mutants *vps35a-2, vps29-6* and *vps26c-1* share a defect in root hair growth.

(A) Average root hair lengths (μm) of T-DNA insertion mutants for the large retromer complex were compared to those of wild type seedlings grown on 1X MS medium, pH 6 supplemented with 200 mM mannitol. Root hairs of 20 seedlings per treatment per genotype were scored and 10-15 root hairs per seedling were measured for each biological replicate. The data represents the average of three biological replicates. Asterisks denote statistical significance ($P < 0.05$), determined by the Student's *t*-test, where wild type root hair length was compared in a pair-wise manner with that for each of the retromer mutants individually. Error bars represent the standard error of mean for the three biological replicates.

(B) *vps26c-1, vps29-6* and *vps35a-2* and wild type seedlings were grown on 1X MS medium, pH 6 supplemented with 200 mM mannitol for five days and were imaged using bright field microscopy to characterize root hair growth. Root hair length of the *vps26c-1*, *vps29-6* and *vps35a-2* mutant seedlings was significantly reduced when compared to wild type seedlings. Bars=100 μm. Error bars represent the standard error of mean for the three biological replicates.

Figure 4.

VPS26C forms a complex with the core retromer component VPS35 in a VPS29 dependent manner

VPS26C-YN was co-transfected with mCherry-VPS29 and individually with each of the VPS35-YC constructs, using *Agrobacterium tumefaciens,* strain GV2260 into fully expanded 3-week-old *N. benthamiana* leaves. As a positive control, VPS26A-YN was shown to interact with VPS35A-YC, demonstrating the effectiveness of this approach (A). Bimolecular fluorescent complementation was used to demonstrate the formation of an *in planta* complex between VPS26C-YN and VPS35A-YC, detected by the presence of YFP fluorescence (B). This complex also co-localized with mCherry-VPS29 (A and B). No fluorescent signal was detected for either VPS35B-YC or VPS35C-YC when co-expressed with VPS26C-YN and mCherry-VPS29 in *Nicotiana benthamiana* leaves (C, and D, respectively). In addition, no fluorescent signal was detected when VPS29 was not co-expressed in the cells containing VPS26C-YN and VPS35A-YC fusions (E). Lastly, when only VPS26C-YN was co-expressed with mCherry-VPS29 (F), no fluorescent signal was detected. YN= N-terminal end of YFP, YC= C-terminal end of YFP. Bars = 10 μm

Figure 5.

VPS26C localizes to membrane compartments in Arabidopsis roots that are insensitive to both Brefeldin A and wortmannin.

(A) To determine if GFP-VPS26C localized to the TGN, we treated both the transgenic seedlings expressing the TGN marker VTI12-YFP and transgenic lines expressing GFP-

VPS26C with 100 μM Brefeldin A (BFA) for 90 min. VTI12-YFP was sensitive to BFA, forming "BFA-bodies" in response to this treatment while GFP-VPS26C showed no sensitivity to BFA. Bars =10 μm

(B) To determine whether GFP-VPS26C localized to late endosomes, we treated transgenic seedlings expressing the late endosome marker RABG3f-mCherry and seedlings expressing GFP-VPS26C with 40 μM wortmannin for 90 minutes. While RABG3f showed sensitivity to wortmannin by forming dilated, donut-shaped structures (highlighted in the inset), the localization pattern of GFP-VPS26C was unaffected by wortmannin treatment. Bars = 10 μm

Figure 6.

The *vps26c* mutant suppresses the polarized root hair growth phenotype of *vti13*

(A) Wild type, *vps26c-1, vti13* and *vti13 vps26c* double mutant seedlings were grown on 1X MS media, pH 6 supplemented with 200 mM mannitol for five days and imaged using bright field microscopy. Root hairs of the *vti13 vps26c* double mutant were longer than either *vti13* or *vps26c*, indicating a suppression of the polarized growth defect of *vti13* in the double mutant. Bars = 100 μm

(B) Root hair lengths of wild type, *vps26c*, *vti13* and *vti13 vps26c* mutants grown for five days on 1X MS medium supplemented with 200 mM mannitol. *vps26c* and *vti13* show a reduction in root hair length, whereas root hair length of the *vti13 vps26c* double mutant is not significantly different from wild type. Root hairs of 20 seedlings per genotype were scored, and 10-15 root hairs per seedling were measured for each biological replicate. An average of three biological replicates is displayed above. Asterisks indicate statistical

significance (P<0.05), determined by the Student's *t*-test, where wild type was compared in a pair-wise manner with each of the mutant genotypes individually. Error bars represent the standard error of mean for the three biological replicates.

Figure 7.

Cell wall organization of xyloglucan in roots of *vps26c* and the *vti13 vps26c* double mutant is distinct from that of *vti13*.

Wild type, *vps26c-1, vti13,* and *vti13 vps26c* seedlings were grown on 1X MS medium, pH 6 for 5 days and labeled with LM15, a monoclonal antibody that recognizes a xyloglucan epitope in cell walls. Root epidermal cells and root hairs of wild type and *vps26c* seedlings label similarly with LM15 whereas *vti13* root epidermal cells and root hairs do not exhibit significant LM15 labeling (as previously described in *Larson et al., 2014*). LM15 labeling of xyloglucan in root epidermal cells and root hairs is restored in the *vti13 vps26c* double mutant, indicating that the *vps26c* mutation can suppress the *vti13* cell wall phenotype.

Figure 8.

VPS26C genes are single copy in most representative angiosperms but have likely been lost in monocots.

50% majority rule Bayesian phylogram of angiosperm *VPS26C*-like genes. Bayesian posterior probabilities are given on each interior branch. Branch lengths are in substitutions; the scale is provided below the tree.

Figure 9.

AtVPS26C and HsDSCR3 orthologs share 40% amino acid identity and a conserved function in Arabidopsis.

(A) Alignment of ATVPS26C and HSDSCR3 illustrates that these orthologs share 40% amino acid sequence identity. Legend: (*): fully conserved residues; (:) conserved residues with strongly similar properties; (.) conserved residues having less similar properties.

(B, C) Wild type, *vps26c-1* and *vps26c-1* seedlings expressing *35S:GFP-HsDSCR3* were grown on MS media, pH 6 supplemented with 200 mM mannitol for 5 days after which root hair growth was imaged using bright field microscopy. Fifteen seedlings per genotype were scored and 10-15 root hairs per seedling were measured for each biological replicate. The graph represents the average of three biological replicates. Three independent transgenic lines expressing *GFP-HsDSCR3* in the *vps26c* mutant background were examined. Asterisks denote statistical significance ($P<0.05$), according to Student's *t*-test, where wild type root hair length was compared in a pair-wise manner with root hair length of *vps26c-1* and *vps26c-1* seedlings complemented with GFP-HsDSCR3 individually. Error bars represent the standard error of mean for the three biological replicates.

SHORT LEGENDS FOR SUPPORTING INFORMATION

Table S1: List of Primers

Table S2: Alignment of VPS26C sequences used to generate VPS26C phylogeny (consistent with Figure 7)

Figure S1: T-DNA mutant lines of retromer subunits exhibited strongly reduced gene expression.

Figure S2: Overexpression of VPS26C does not affect root hair growth in wild type seedlings and VPS26C/DSCR3 GFP-fusions complement the vps26-2 root hair phenotype.

Figure S3: Root hair length is unaffected when seedlings are grown in MS media supplemented with KCl.

Figure S4: Supplementation of MS media with mannitol and NaCl results in a reduction in root hair length in wild type seedlings.

Figure S5: vps35a and vps29 exhibit shorter root hairs than wild type seedlings independent of media conditions.

Figure S6: qRT/PCR analysis of VPS26C expression in Arabidopsis thaliana.

Figure S7: Genomic model for VPS26C and alignment of VPS26C with gene family members VPS26A and VPS26B.

Figure S8: Genotyping of WT, vps26c-1, and vps26c-2 expressing the GFP-VPS26C/DSCR3 fusions using gene-specific primers and genomic PCR.

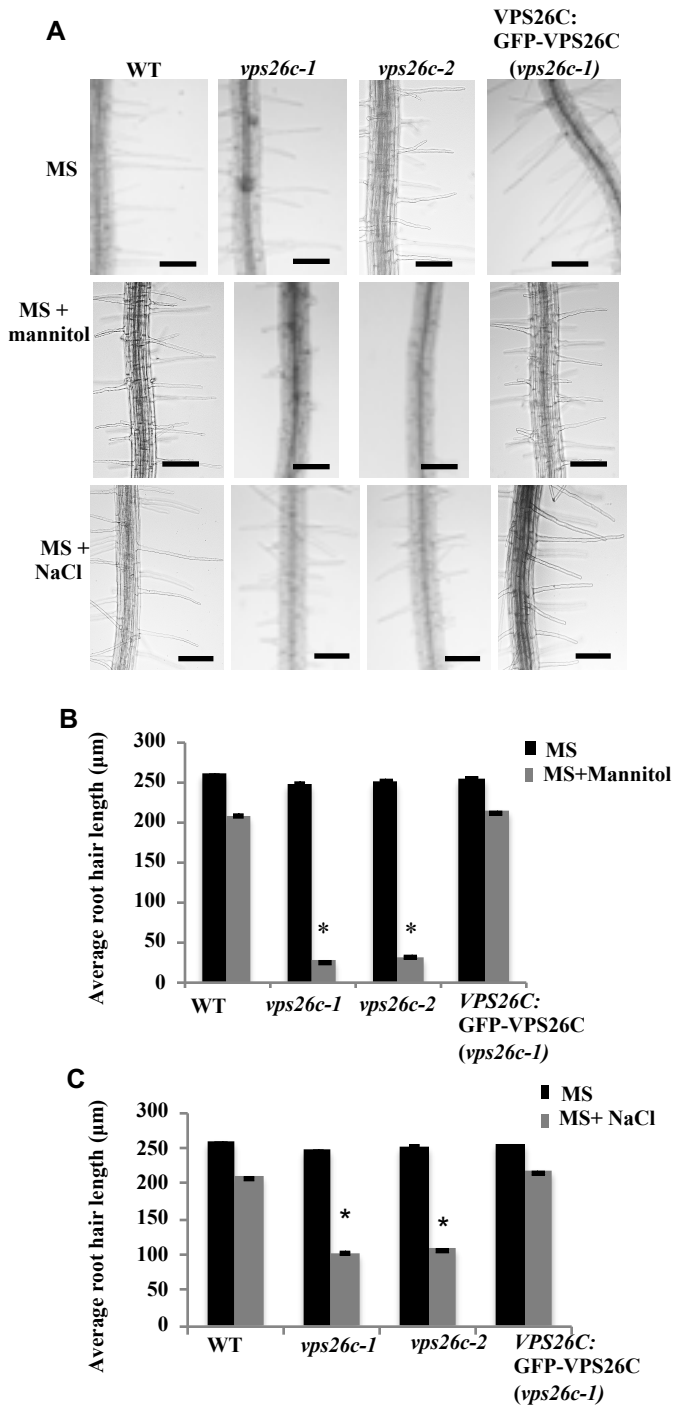
A
WT
vps26c-1
vps26c-2
VPS26C:
GFP-VPS26C
(vps26c-1)
MS
MS +
mannitol
MS +
NaCl
B
Average root hair length (µm)
300
250
200
150
100
50
0
MS
MS+Mannitol
*
*
WT
vps26c-1
vps26c-2
VPS26C:
GFP-VPS26C
(vps26c-1)
C
Average root hair length (µm)
300
250
200
150
100
50
0
MS
MS+ NaCl
*
*
WT
vps26c-1
vps26c-2
VPS26C:
GFP-VPS26C
(vps26c-1)

Figure 1.

vps26c is defective in root hair growth when grown in the presence of mannitol or NaCl.

(A) Wild type, *vps26c-1, vps26c-2* and *vps26c-1* seedlings expressing VPS26C: GFP-VPS26C were grown on 1X MS medium, pH 6, 1X MS medium, pH 6 supplemented with 200 mM mannitol, and 1X MS medium, pH 6 supplemented with 30mM NaCl for 5 days after which root hairs were imaged using bright field microscopy. Both *vps26c* mutants exhibited root hairs indistinguishable from wild type when seedlings were grown on standard MS medium, but showed reduced root hair length when either mannitol or NaCl was added to the medium. The *vps26c* root hair growth phenotypes were complemented in *vps26c*-1 mutant lines expressing *VPS26C:GFP-VPS26C* for both media conditions. Three independent transgenic lines expressing *VPS26C:GFP-VPS26C* in a *vps26c-1* background exhibited similar root hair growth phenotypes. Bars= 100 μm

(B) Average root hair length (μm) of 5-day-old seedlings grown on 1X MS medium, pH 6 (black bars) and on 1X MS medium, pH 6 supplemented with 200 mM mannitol (grey bars). Twenty seedlings per genotype per treatment were scored and 10-15 root hairs per seedling were measured for each biological replicate. The graph shows an average of three biological replicates. Asterisks indicate statistical significance according to the Student's *t*-test, where wild type was compared in a pair-wise manner with each of the genotypes for each treatment ($P < 0.05$). Error bars represent the standard error of the mean of three biological replicates.

(C) Average root hair length of 5-day-old seedlings grown on 1X MS medium, pH 6 (black) and 1X MS medium, pH 6 supplemented with 30 mM NaCl (grey). Twenty seedlings per treatment per genotype were scored and 10-15 root hairs per seedling were measured for each biological replicate. The graph shows an average of three biological replicates. Asterisks indicate statistical significance according to the Student's *t*-test, where wild type was compared in a pair-wise manner with each of the genotypes individually for each treatment ($P < 0.05$). Error bars represent the standard error of the mean of three biological replicates.

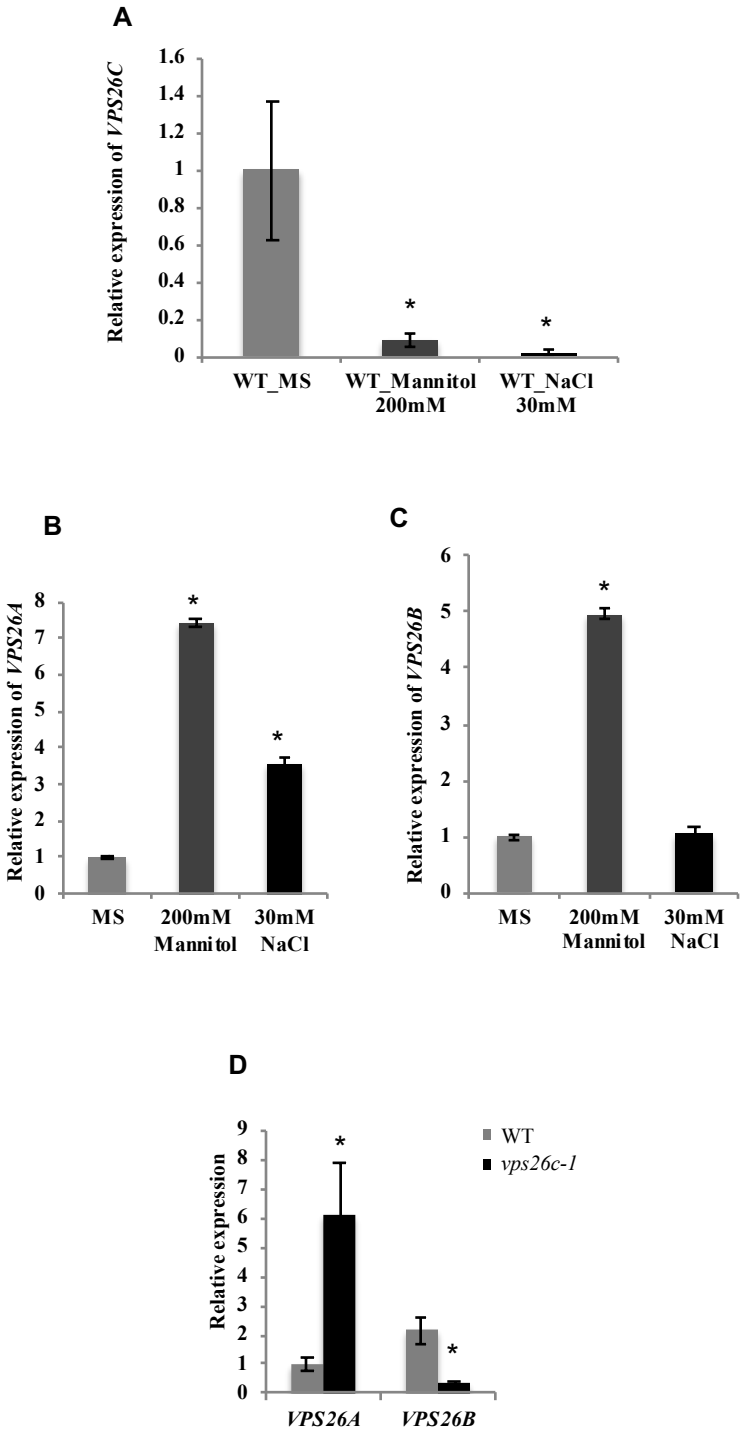
A
Relative expression of VPS26C
1.6
1.4
1.2
1
0.8
0.6
0.4
0.2
0
*
*
WT_MS
WT_Mannitol 200mM
WT_NaCl 30mM
B
Relative expression of VPS26A
8
7
6
5
4
3
2
1
0
*
*
MS
200mM Mannitol
30mM NaCl
C
Relative expression of VPS26B
6
5
4
3
2
1
0
*
MS
200mM Mannitol
30mM NaCl
D
Relative expression
9
8
7
6
5
4
3
2
1
0
*
*
WT
vps26c-1
VPS26A
VPS26B

Figure 2.

Differential expression of *VPS26* family members in wild type seedlings grown under different media conditions.

(A) qRT-PCR was used to quantitate *VPS26C* transcript levels present in roots of wild type seedlings grown on 1X MS medium, pH 6, or 1X MS medium, pH 6 supplemented with either 200 mM mannitol or 30 mM NaCl. Seedlings grown in the presence of either mannitol or NaCl showed a down-regulation of *VPS26C* expression when compared to wild type seedlings grown on MS alone. Asterisks indicate statistical significance according to the Student's *t*-test, where a pair-wise comparison was performed between VPS26C transcript levels from roots of seedlings grown on MS media and each of the treatments ($P < 0.05$). Error bars represent the standard error of the mean of three biological replicates, run in triplicate.

(B and C) qRT-PCR analysis of *VPS26A* **(B)** and *VPS26B* **(C)** transcript levels in roots of wild type seedlings grown on 1X MS medium, pH 6 or seedlings grown on 1X MS medium, pH 6 supplemented with either 200 mM mannitol or 30 mM NaCl. In contrast to *VPS26C*, wild type seedlings grown in the presence of either mannitol or NaCl showed an induction of *VPS26A* expression when compared to wild type seedlings grown on MS alone. This upregulation is also observed in the expression of *VP26B* in roots of wild type seedlings grown on media containing mannitol. Asterisks indicate statistical significance according to the Student's *t*-test, where pair-wise comparisons were performed betweenVPS26A or VPS26B transcript levels from roots of seedlings grown on MS media and the level of these same transcripts in roots of seedlings grown under each treatment condition ($P < 0.05$). Error bars represent the standard error of the mean of three biological replicates, run in triplicate.

(D) qRT-PCR analysis demonstrating the differential expression of *VPS26A* and *VPS26B* in wild type vs. *vps26c* seedling roots grown on 1X MS medium, pH 6. *VPS26A* transcript levels were induced in *vps26c* roots when compared to wild type roots, whereas *VPS26B* transcript levels were down regulated in *vps26c* roots when compared to the wild type roots. Asterisks indicate statistical significance according to the Student's *t*-test, where pair-wise comparisons were performed betweenVPS26A or VPS26B transcript levels from roots of wild type seedlings grown on MS media and the level of these same transcripts in roots of seedlings grown on MS media ($P < 0.05$). Error bars represent the standard error of mean of three biological replicates, run in triplicate.

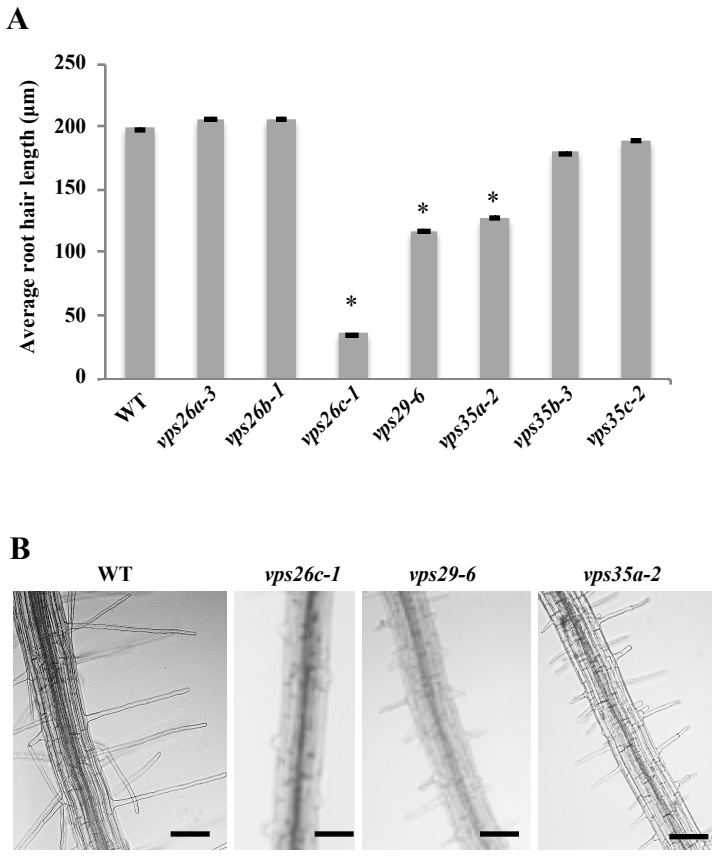
A
Average root hair length (µm)
250
200
150
100
50
0
*
*
*
WT
vps26a-3
vps26b-1
vps26c-1
vps29-6
vps35a-2
vps35b-3
vps35c-2
B
WT
vps26c-1
vps29-6
vps35a-2

Figure 3.

Large retromer complex mutants *vps35a-2, vps29-6* and *vps26c-1* share a defect in root hair growth.

(A) Average root hair lengths (μm) of T-DNA insertion mutants for the large retromer complex were compared to those of wild type seedlings grown on 1X MS medium, pH 6 supplemented with 200 mM mannitol. Root hairs of 20 seedlings per treatment per genotype were scored and 10-15 root hairs per seedling were measured for each biological replicate. The data represents the average of three biological replicates. Asterisks denote statistical significance ($P < 0.05$), determined by the Student's *t*-test, where wild type root hair length was compared in a pair-wise manner with that for each of the retromer mutants individually. Error bars represent the standard error of the mean of three biological replicates.

(B) *vps26c-1, vps29-6* and *vps35a-2* and wild type seedlings were grown on 1X MS medium, pH 6 supplemented with 200 mM mannitol for five days and were imaged using bright field microscopy to characterize root hair growth. Root hair length of the *vps26c-1*, *vps29-6* and *vps35a-2* mutant seedlings was significantly reduced when compared to wild type seedlings. Bars= 100 μm

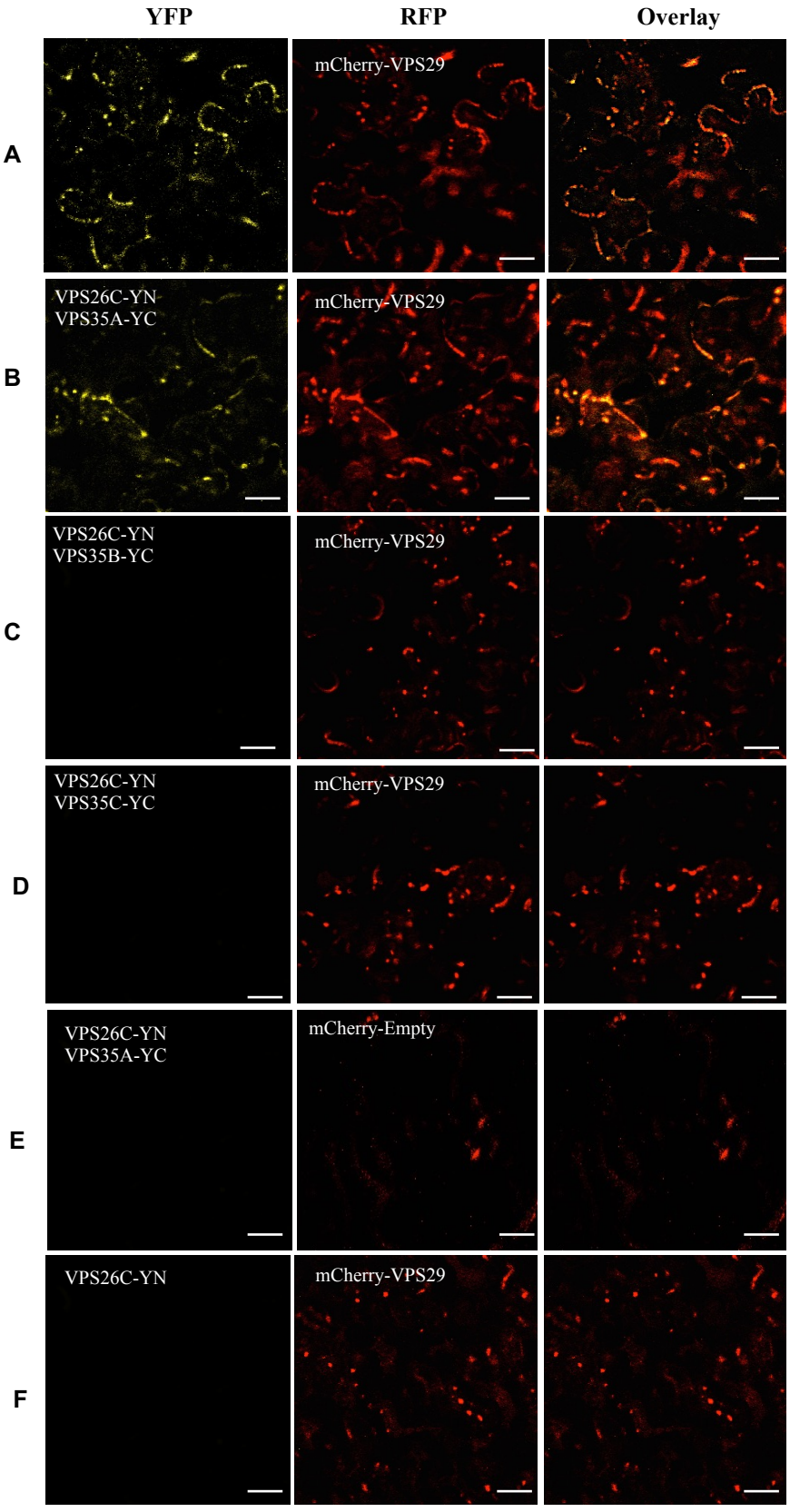
YFP
RFP
Overlay
A
mCherry-VPS29
B
VPS26C-YN
VPS35A-YC
mCherry-VPS29
C
VPS26C-YN
VPS35B-YC
mCherry-VPS29
D
VPS26C-YN
VPS35C-YC
mCherry-VPS29
E
VPS26C-YN
VPS35A-YC
mCherry-Empty
F
VPS26C-YN
mCherry-VPS29

Figure 4.

VPS26C forms a complex with the core retromer component VPS35 in a VPS29 dependent manner.

VPS26C-YN was co-transfected with mCherry-VPS29 and individually with each of the VPS35-YC constructs, using *Agrobacterium tumefaciens,* strain GV2260 into fully expanded 3-week-old *N. benthamiana* leaves. A known interaction, VPS26A-YN was shown to interact with VPS35A-YC, as a positive control demonstrating the working of this technique (A). Bimolecular fluorescent complementation was used to demonstrate an *in planta* interaction between VPS26C-YN and VPS35A-YC, detected by the presence of YFP fluorescence (B). All of these interactions were also demonstrated to be co-localizing with mCherry-VPS29 (A and B). No fluorescent signal was detected for either VPS35B-YC or VPS35C-YC when co-expressed with VPS26C-YN in *Nicotiana benthamiana* leaves (C, and D, respectively). In addition, no fluorescent signal was detected when VPS29 was not co-expressed in the cells containing VPS26C-YN and VPS35A-YC fusions (E).Lastly, when only VPS26C-YN was co-expressed with mCherry-VPS29 (F), no fluorescent signal was detected. YN= N-terminal end of YFP, YC= C-terminal end of YFP. Bars = 10 μm

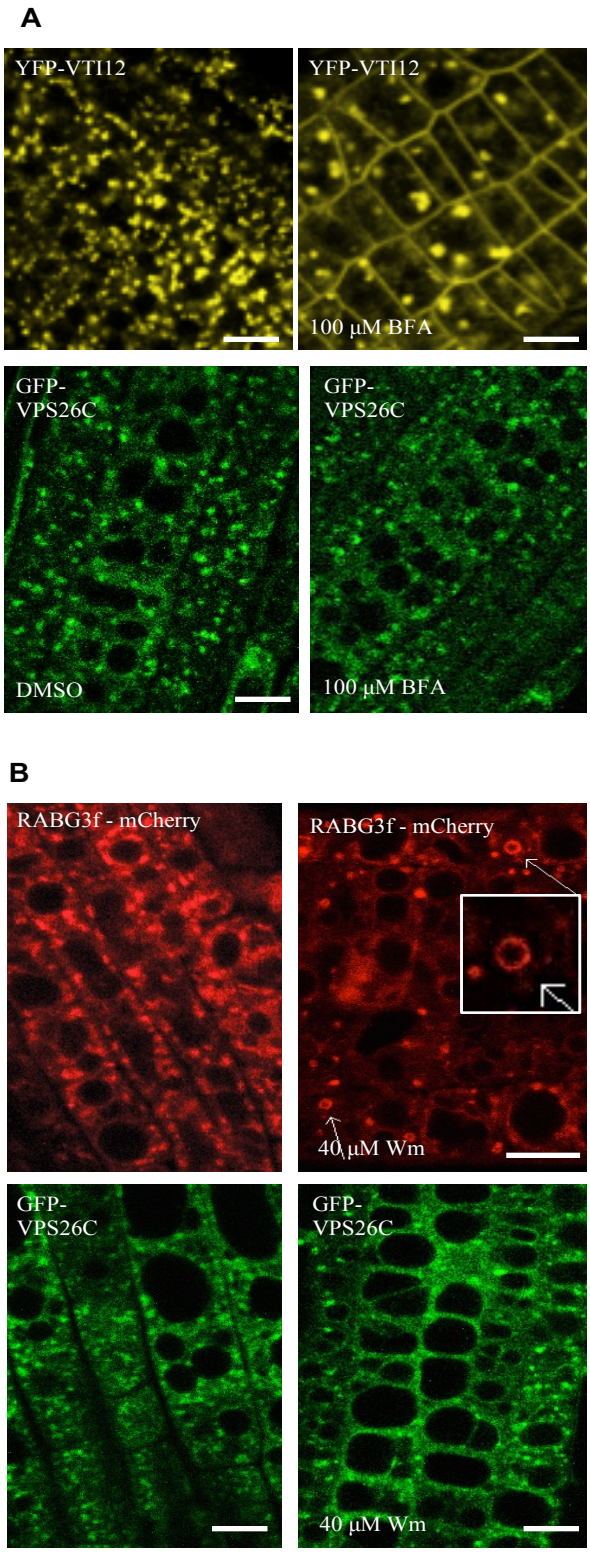
A
YFP-VTI12
YFP-VTI12
100 µM BFA
GFP-
VPS26C
DMSO
GFP-
VPS26C
100 µM BFA
B
RABG3f - mCherry
RABG3f - mCherry
40 µM Wm
GFP-
VPS26C
GFP-
VPS26C
40 µM Wm

Figure 5.

VPS26C localizes to membrane compartments in Arabidopsis roots that are insensitive to both Brefeldin A and wortmannin.

(A) To determine if GFP-VPS26C localized to the TGN, we treated both the transgenic seedlings expressing the TGN marker VTI12-YFP and transgenic lines expressing GFP-VPS26C with 100 μM Brefeldin A (BFA) for 90 min. VTI12-YFP was sensitive to BFA, forming "BFA-bodies" in response to this treatment while GFP-VPS26C showed no sensitivity to BFA. Bars =10 μm

(B) To determine whether GFP-VPS26C localized to late endosomes, we treated transgenic seedlings expressing the late endosome marker RABG3f-mCherry and seedlings expressing GFP-VPS26C with 40 μM wortmannin for 90 minutes. While RABG3f showed sensitivity to wortmannin by forming dilated, donut-shaped structures (highlighted in the inset) , the localization pattern of GFP-VPS26C was unaffected by wortmannin treatment.
Bars = 10 μm

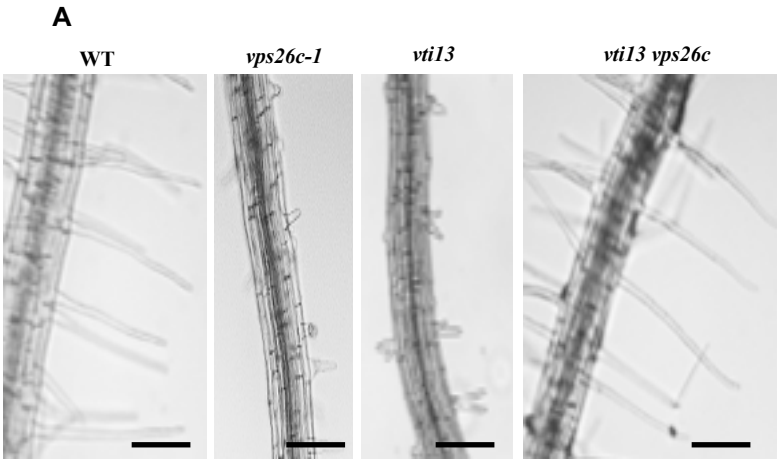
A
WT
vps26c-1
vti13
vti13 vps26c

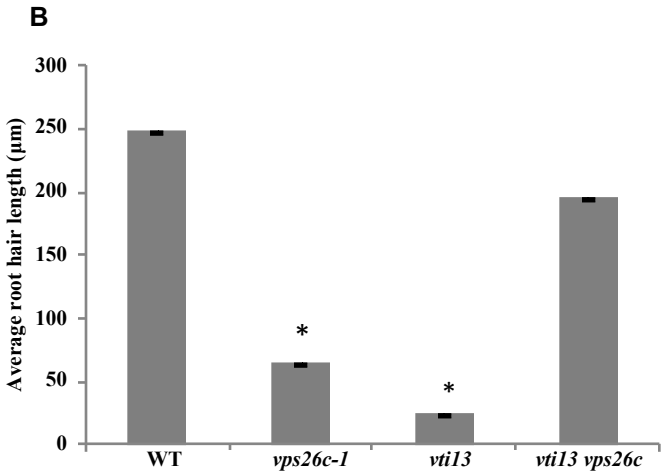
B
Average root hair length (µm)
300
250
200
150
100
50
0
*
*
WT
vps26c-1
vti13
vti13 vps26c

Figure 6.

The *vps26c* mutant suppresses the polarized root hair growth phenotype of *vti13*.

(A) Wild type, *vps26c-1, vti13* and *vti13 vps26c* double mutant seedlings were grown on 1X MS media, pH 6 supplemented with 200 mM mannitol for five days and imaged using bright field microscopy. Root hairs of the *vti13 vps26c* double mutant were longer than either *vti13* or *vps26c*, indicating a suppression of the polarized growth defect of *vti13* in the double mutant. Bars = 100 μm

(B) Root hair lengths of wild type, *vps26c*, *vti13* and *vti13 vps26c* mutants grown for five days on 1X MS medium supplemented with 200 mM mannitol. *vps26c* and *vti13* show a reduction in root hair length, whereas root hair length of the *vti13 vps26c* double mutant is not significantly different from wild type. Root hairs of 20 seedlings per genotype were scored, and 10-15 root hairs per seedling were measured for each biological replicate. An average of three biological replicates is displayed above. Asterisks indicate statistical significance ($P<0.05$), determined by the Student's *t*-test, where wild type was compared in a pair-wise manner with each of the mutant genotypes individually. Error bars represent the standard error of the mean of three biological replicates.

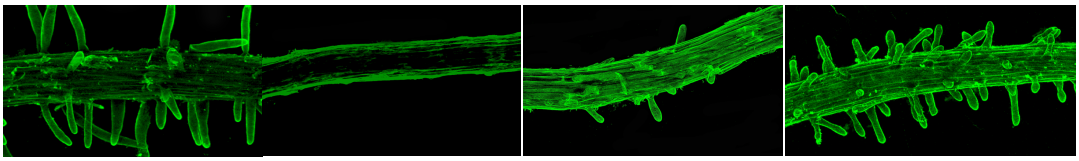

Figure 7.

Cell wall organization of xyloglucan in roots of *vps26c* and the *vti13 vps26c* double mutant is distinct from that of *vti13*.

Wild type, *vps26c-1, vti13,* and *vti13 vps26c* seedlings were grown on 1X MS medium, pH 6 for 5 days and labeled with LM15, a monoclonal antibody that recognizes a xyloglucan epitope in cell walls. Root epidermal cells and root hairs of wild type and *vps26c* seedlings label similarly with LM15 whereas *vti13* root epidermal cells and root hairs do not exhibit significant LM15 labeling (as previously described in *Larson et al., 2014*). LM15 labeling of xyloglucan in root epidermal cells and root hairs is restored in the *vti13 vps26c* double mutant, indicating that the *vps26c* mutation can suppress the *vti13* cell wall phenotype.

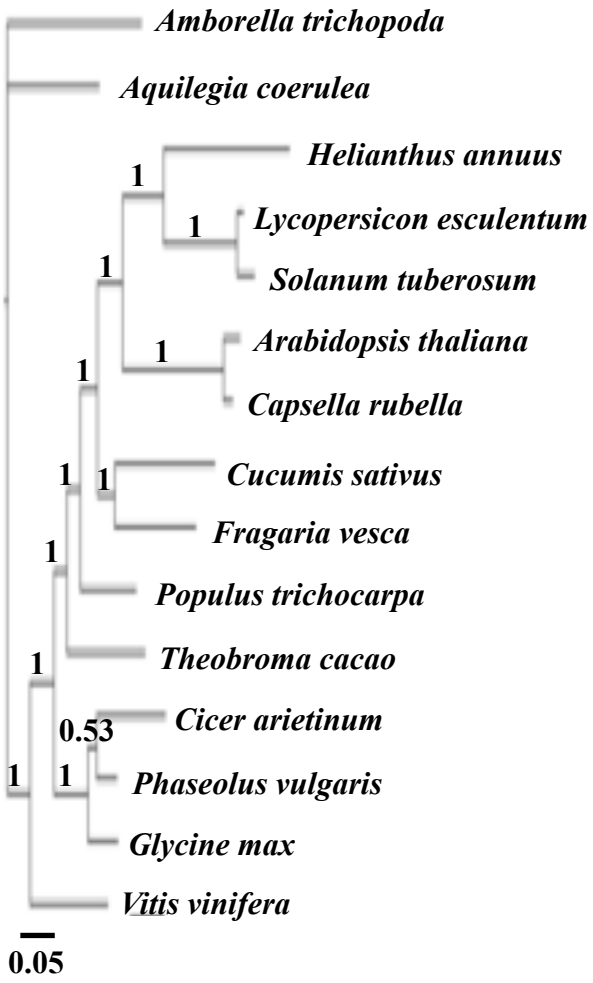

Figure 8.

VPS26C genes are single copy in most representative angiosperms, but have likely been lost in monocots.

50% majority rule Bayesian phylogram of angiosperm *VPS26C*-like genes. Bayesian posterior probabilities are given on each interior branch. Branch lengths are in substitutions; the scale is provided below the tree.

A

```
Arabidopsis      MATATTVNVKLSRSNRIYRSSEPVEGKIVIKSATSISHQAIRLSVNGSVNLQVRGGSAGV   60
Human            --MGTALDIKIKRANKVYHAGEVLSGVVVISSKDSVQHQGVSLTMEGTVNLQLSAKSVGV   58
                    .*::::*:.*:*::*::.* :.* :**.*  *:.**.: *:::*:****: . *.**

Arabidopsis      IESFYGVIKPIQIVKKTIEVKSSGKIPPGTTEIPFSLNLREPGEGIVEKFYETFHGTNIN   120
Human            FEAFYNSVKPIQIINSTIEMVKPGKFPSGKTEIPFEFPLHLKGNK---VLYETYHGVFVN   115
                 :*:**. :******::.***: . **:* *.*****.: *:  *:     :***:**. :*

Arabidopsis      IQYLLTADIPRGYLHKPLSATMEFIIESGRVDLPERPIPPEIVIFYI-TQDTQRHPLLPD   179
Human            IQYTLRCDMKRSLLAKDLTKTCEFIVHSAPQKGKFTPSPVDFTITPETLQNVKERALLPK   175
                 *** * .*: *. * * *: * ***:.*.  .    * * ::.*     *:.:.: ***.

Arabidopsis      IKTGGFRVTGKLATQCSLQDPLSGELTVEASSVPITSIDIHLLRVESIIVGERIVTETSL   239
Human            FLLRG----HLNSTNCVITQPLTGELVVESSEAAIRSVELQLVRVETCGCAEGYARDATE   231
                 :   *       :*:* : :**:***.**:*.. * *::::*:***:   .*  . :::

Arabidopsis      IQSTQIADGDVCRNMTLPIYVLLPRLLMCPSVFAGPFSVEFKVCITISFKSKLAKAQPKS   299
Human            IQNIQIADGDVCRGLSVPIYMVFPRLFTCPTLETTNFKVEFEVNIVVLLHPDHL------   285
                 **. *********.:::***:::***: **:: :  *.***:* *.: :: .

Arabidopsis      DPTAPRLWMALERLPLELVRTKRDQFSC   327
Human            ---------ITENFPLKLCRI-------   297
                           *.:**:* *
```

B

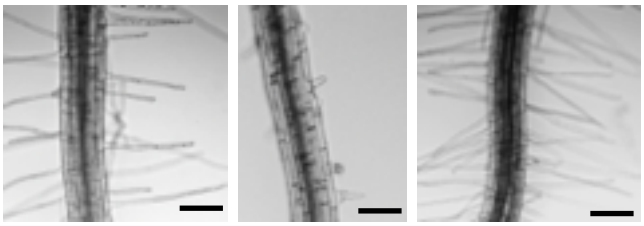

WT | *vps26c-1* | 35S:GFP-HsDSCR3 (*vps26c-1*)

C

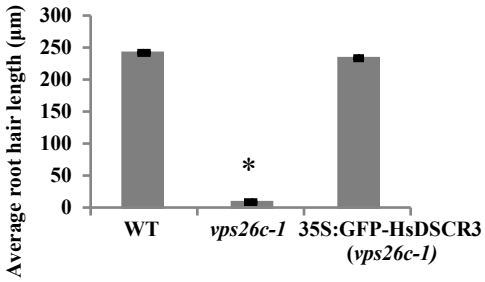

Figure 9.

AtVPS26C and *HsDSCR3* orthologs share 40% amino acid identity and a conserved function in Arabidopsis.

(A) Alignment of ATVPS26C and HSDSCR3 illustrates that these orthologs share 40% amino acid sequence identity. Legend: (*): fully conserved residues; (:) conserved residues with strongly similar properties; (.) conserved residues having less similar properties.

(B, C) Wild type, *vps26c-1* and *vps26c-1* seedlings expressing *35S:GFP-HsDSCR3* were grown on MS media, pH 6 supplemented with 200 mM mannitol for 5 days after which root hair growth was imaged using bright field microscopy. Fifteen seedlings per genotype were scored and 10-15 root hairs per seedling were measured for each biological replicate. The graph represents the average of three biological replicates. Three independent transgenic lines expressing *GFP-HsDSCR3* in the *vps26c* mutant background were examined. Asterisks denote statistical significance ($P<0.05$), according to Student's *t*-test, where wild type root hair length was compared in a pair-wise manner with root hair length of *vps26c-1* and *vps26c-1* seedlings complemented with GFP-HsDSCR3 individually. Error bars represent the standard error of the mean of three biological replicates.

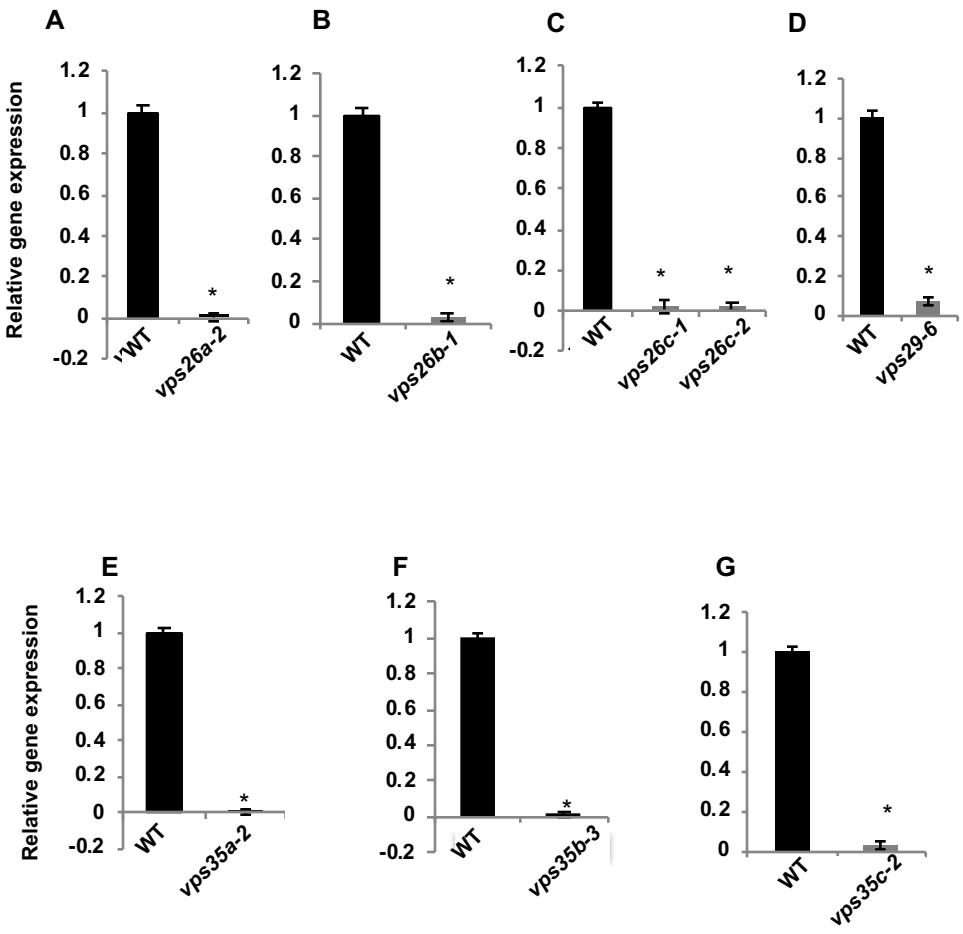

H

	WT	*mutant line*
vps26a-2	1	0.000148887
vps26b-1	1	0.027657675
vps26c-1	1	0.020535958
vps26c-2	1	0.020535958
vps29-6	1	0.06902534
vps35a-2	1	0.006267683
vps35b-3	1	0.007974088
vps35c-2	1	0.024387897

Figure S1.

T-DNA mutant lines of retromer subunits exhibited strongly reduced gene expression.

(A-G) qRT-PCR was used to compare the transcript level for individual retromer subunit genes in wild type seedlings and their respective T-DNA mutant lines. Seedlings were grown on 1X MS medium, pH 6 for 5 days and total RNA was isolated from seedlings for the qRT-PCR analysis. Error bars represent the standard error of mean of three biological replicates, run in triplicate. Asterisks indicate statistical significance according to the Student's *t*-test ($P < 0.05$), where wild type expression for the appropriate retromer transcript was compared in a pair-wise manner to the mutant genotypes. Error bars represent the standard error of mean of three biological replicates, run in triplicate.

(H) Relative gene expression values for each of the core retromer subunit mutants compared to wild type expression.

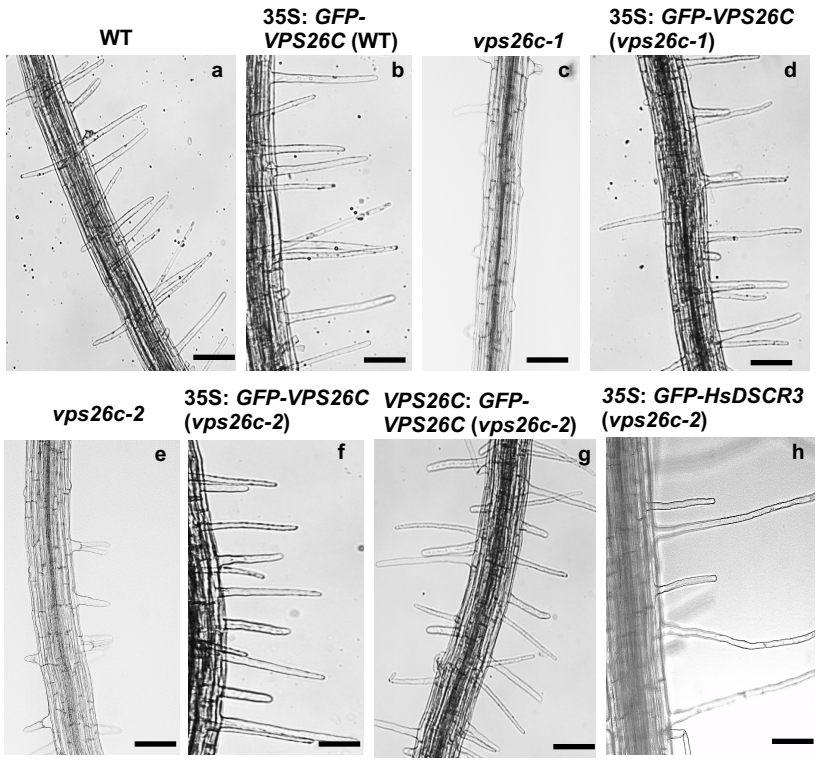

Figure S2.

Overexpression of VPS26C does not affect root hair growth in wild type seedlings and VPS26C/DSCR3 GFP-fusions complement the *vps26c* root hair phenotype.

Overexpression of GFP-VPS26C in a wild type background does not cause any root hair aberrations in the seedlings (a, b). Root hair phenotype in *vps26c*-1 (c) and *vps26c-2* (e) is complemented by expressing 35S: GFP-VPS26C (d, f). Introduction of GFP-VPS26C and GFP-HsDSCR3 fusions driven by the endogenous and the 35S promoters, respectively, also complement the phenotype in *vps26c-2* (g, h). (Bars = 100 μm)

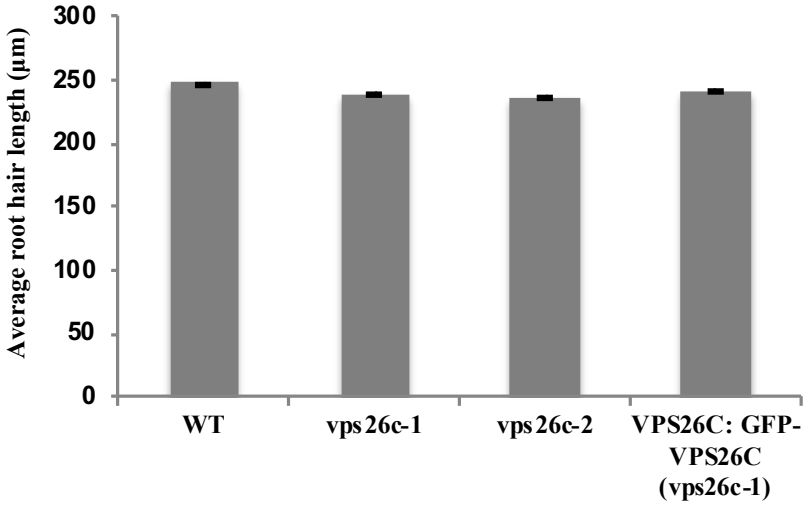

Figure S3.

Root hair length is unaffected when seedlings are grown on MS medium supplemented with KCl.

WT, *vps26c-1, vps26c-2* and *VPS26C: GFP-VPS26C (vps26c-1) seedlings* were grown on 1x MS media supplemented with 30 mM KCl for five days after which root hair growth was imaged using bright field microscopy. Twenty seedlings per treatment per genotype were scored and 10-15 root hairs per seedling were measured for each biological replicate. The graph shows an average of three biological replicates. Statistical analysis was done using the Student's *t*-test, where wild type was compared in a pair-wise manner with each of the genotypes individually for the treatment ($P < 0.05$). Error bars represent the standard error of mean of three biological replicates.

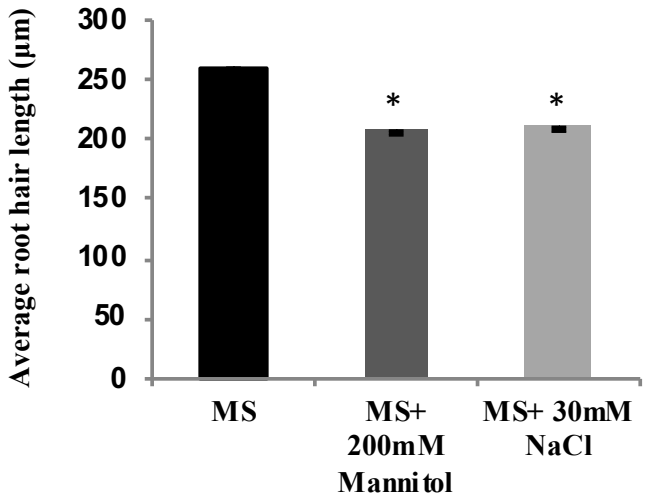

Figure S4.

Supplementation of MS media with mannitol and NaCl results in a reduction in root hair length in wild type seedlings.

Wild type seedlings grown on 1X MS medium, pH6 or 1X MS medium, pH6 supplemented with either 200 mM mannitol or 30 mM NaCl for 5 days after which root hair growth was imaged using bright field microscopy. Wild seedlings show a significant decrease in root hair length when mannitol or NaCl is present in the media. Twenty seedlings per treatment per genotype were scored and 10-15 root hairs per seedling were measured for each biological replicate. The graph shows an average of three biological replicates. Asterisks indicate statistical significance ($P < 0.05$) based on the Student's *t*-test, where root hair length of seedlings grown on MS medium was compared in a pair-wise manner with that of each of the treatments. Error bars represent the standard error of mean of three biological replicates.

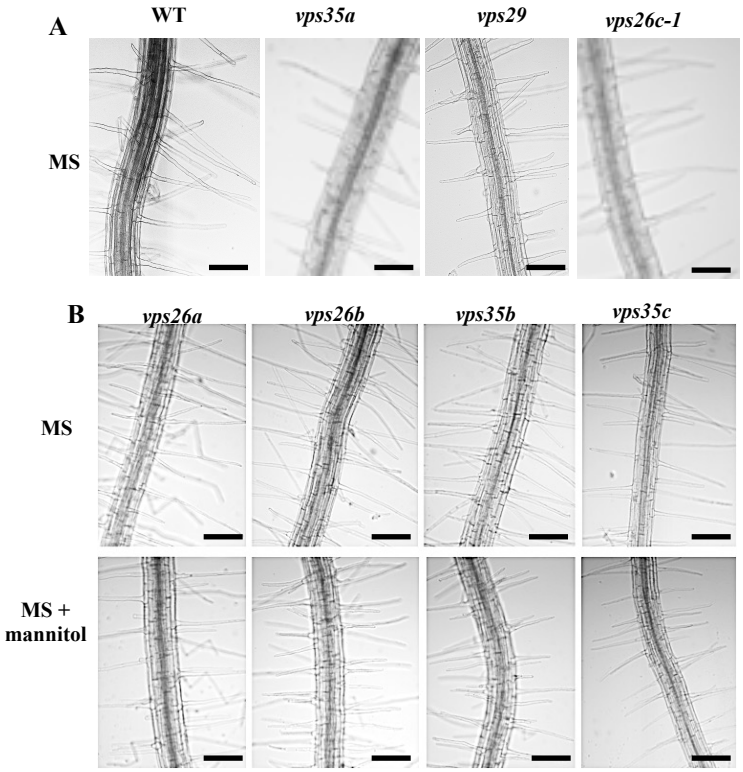
A
WT
vps35a
vps29
vps26c-1
MS
B
vps26a
vps26b
vps35b
vps35c
MS
MS +
mannitol

C

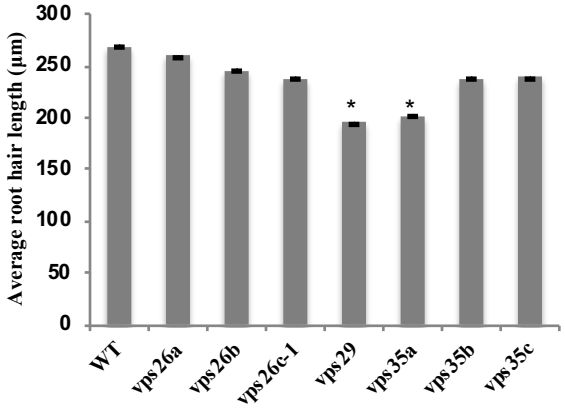
Average root hair length (µm)
300
250
200
150
100
50
0
*
*
WT
vps26a
vps26b
vps26c-1
vps29
vps35a
vps35b
vps35c

Figure S5.

vps35a and *vps29* exhibit shorter root hairs than wild type seedlings independent of media conditions.

(A) Wild type*, vps26c-1, vps29* and *vps35a* seedlings were grown for five days on 1X MS medium, pH6 after which root hair growth was imaged using bright field microscopy. In contrast to *vps26c* alleles, *vps35a* and *vps29* seedlings exhibited reduced root hair growth on this media.

(B) Wild type seedlings and T-DNA insertion mutants *vps26a, vps26b, vps35b* and *vps35c* were grown on 1X MS medium, pH6 (upper panel) and 1X MS medium, pH6 supplemented with 200 mM mannitol (lower panel) for five days after which root hair growth was imaged using bright field microscopy. In all cases, root hair length of each mutant was indistinguishable from wild type seedlings, independent of media conditions. Bars=100 μm

(C) Comparison of root hair lengths of the retromer complex mutants and wild type seedlings grown on 1X MS medium, pH6 for 5 days. Root hairs of 15 seedlings per treatment per genotype were scored for length measurements, and 10-15 root hairs per seedling were measured for each biological replicate. The graph represents the average of three biological replicates. Asterisks denote statistical significance ($P<0.05$) based on the Student's *t*-test, where wild type was compared in a pair-wise manner with each of the genotypes. Error bars represent the standard error of mean of three biological replicates.

.

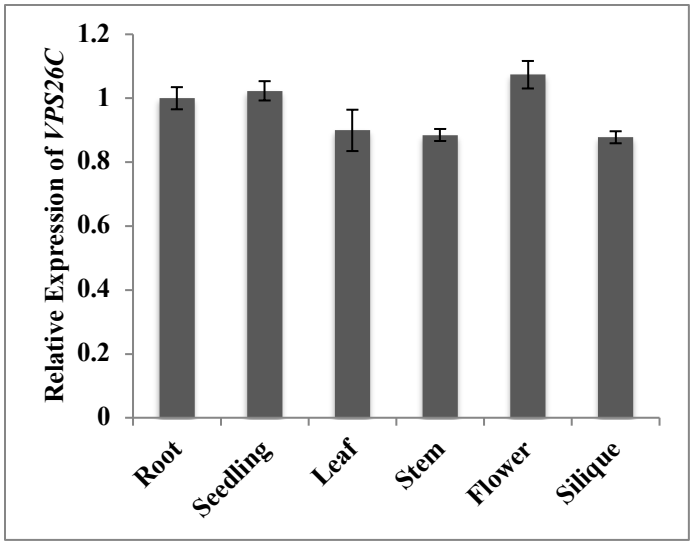

Figure S6:

Expression pattern of *VPS26C* in *Arabidopsis thaliana.*

qRT-PCR analysis of *VPS26C* transcript levels in different organs of Arabidopsis. Seven-day-old seedling roots, 7-day-old whole seedlings, leaves (45-day-old plant, 10-12 leaves/rosette), stems, open flowers and green siliques were used for this study. The level of *VPS26C* expression in root was compared in a pair-wise manner with *VPS26C* expression in each of the other tissues, using the Student's *t*-test. No significant differences in gene expression were observed among the tissues examined. Error bars represent the standard error of mean of three biological replicates.

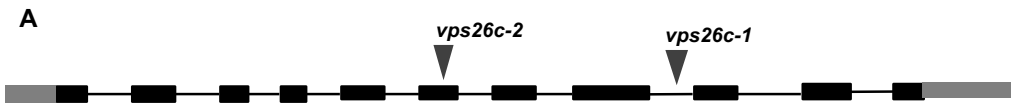

B

```
VPS26C      -------MATATTVNVK-----------------LSRSNRIYRSSEPVEGKIVIKSA--T
VPS26A      MNYLLGAFKPACNISITFTDGKNRKQVPTKKDNGQIVMNPLFQSQETIAGKINIEPYQGK
VPS26B      MNYLLGAFKPACNISITFSDGKNRKQVPMKKENGQTALVPLFHSQDTISGKVCIEPYQGK
                   :  * .:.:.                        :::*.: : **: *:    .

VPS26C      SISHQAIRLSVNGSVNLQVRGGSAGVIESFYGVIKPIQIVKKTIEVKSSGKIPPGTTEIP
VPS26A      KVEHNGVKVELLGQIEMYFDRGN---FYDFTSLVREI---------DVPGEIYE-RKTYP
VPS26B      KVEHNGVKVELLGQIEMYFDRGN---FYDFTSLVREL---------DVPGEIYE-RKTYP
            .:.*:.:::.: *.::: .  *.   : .* .::: :         .  *:*    .  *

VPS26C      FSLNLREPGEGIVEKFYETFHGTNINIQYLLTADIPRGYLHKPLSATMEFIIESGRVDLP
VPS26A      FE-------FSSVEMPYETYNGVNVRLRYVLKVTVTRGYAGSIVEYQ-DFVVR---NYVP
VPS26B      FE-------FPTVEMPYETYNGVNVRLRYVLKVTVTRGYAGSILEYQ-ELVVR---NYAP
            *.          **  ***::*.*:.::*:*.. : ***  . :.   ::::.      *

VPS26C      ERPIPPEIVIFYITQDTQRHPLLPDIKTGGFRVTGKLATQCSLQDPLSGELTVEASSVPI
VPS26A      LPPINNSIKMEVGIEDC---------LHIEFE---YNKSKYHLKDVILGKIYFLLVRIKI
VPS26B      LPDINNSIKMEVGIEDC---------LHIEFE---YNKSKYHLKDVILGKIYFLLVRIKM
               *  .* :    :*             *.      ::  *:* : *:: .    : :

VPS26C      TSIDIHLLRVESIIVGERIVTETSLIQSTQIADGDVCRNMTLPIYVLLPRLLMCPSV--F
VPS26A      KNMDLEIRRRESTGAGANTHVETETLAKFELMDGAPVRGESIPVRVFLTPYDLTPTHKNI
VPS26B      KNMDLEIRRRESTGAGANTHVETETLAKFELMDGTPVRGESIPVRLFLAPYDLTPTHRNI
            ..:*:.: * **  .* .  .**. : . :: **   *. ::*: ::*    : *:   :

VPS26C      AGPFSVEFKVCITISFKSKLAKAQPKSDPTAPRLWMALERLPLELVRTKRDQFSC
VPS26A      NNKFSVKYYLNLVLVDE------------EDRR-YFKQQ--EITLYRLKEETS—
VPS26B      NNKFSVKYYLNLVLVDE------------EDRR-YFKQQ--EITLYRLKEDASS-
             . ***:: : :.:  :              * ::  :   : * * *.:
```

Figure S7.

Arabidopsis VPS26C shares approximately 20% amino acid sequence identity with gene family members VPS26A and VPS26B.

(A) The gene model for *VPS26C* (At1G48550; NCBI accession: NM_103751.3), confirmed by comparing the gene's predicted cDNA sequence with the sequence of *VPS26C* cDNA amplified from a *vps26c* complemented line. The grey boxes denote the 5' and 3' UTRs, the black boxes indicate exons, and the black lines indicate introns. Triangles indicate T-DNA insertion sites corresponding to *vps26c-1* and *vps26c-2*.

(B) The predicted amino acid sequences of VPS26A, VPS26B and VPS26C were compared, where VPS26A and VPS26B shared 91% amino acid identity while VPS26A and VPS26B shared only 20% and 22% amino acid identity with VPS26C, respectively. Legend: (*) fully conserved residues (:) residues with strongly similar properties; (.) residues having less similar properties.

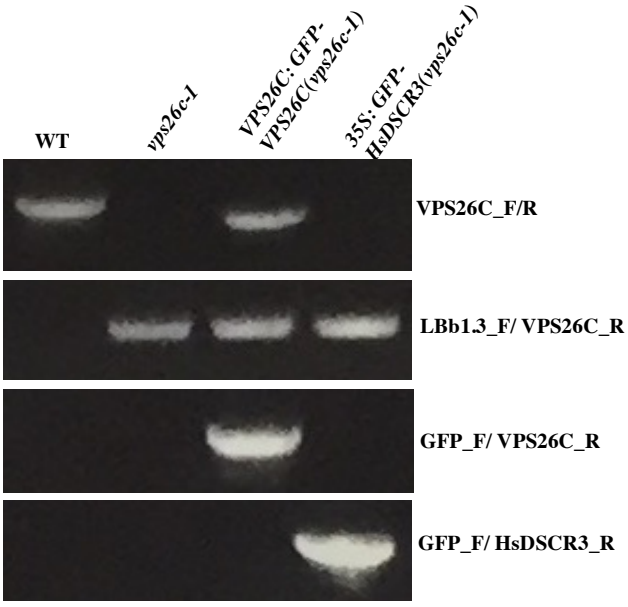

Figure S8.
Genotyping of WT, *vps26c-1,* and *vps26c-1* expressing the GFP-VPS26C/DSCR3 fusions using gene-specific primers and genomic PCR.

Genomic DNA was isolated from seedlings of wild type, *vps26c-1,* and transgenic lines expressing *VPS26C: GFP-VPS26C (vps26c-1 background)* and *35S: GFP-HsDSCR3 (vps26c-1 background)*. Genomic PCR was used with VPS26C F/R primers to confirm the presence of *VPS26C* gene in wild type seedlings and the complemented line expressing *GFP-VPS26C* (top panel), T-DNA insertions in all lines containing the *vps26c-1* allele were confirmed using primers LBb1.3_F/VPS26C_R. The presence of *GFP-VPS26C* and *GFP-HSDSCR3* in their respective complemented lines were detected using primers GFP_F/ VPS26C_R and GFP_F/ HsDSCR3_R, respectively (See Supplemental Table 1 for primer sequences used).

Supplemental Table 1: List of Primers

Purpose	Orientation	Sequence (Listed 5' to 3')
Genotyping VPS26C	F	ATGGCGACGGCGACGA
Genotyping VPS26C	R	TTAGCAGCTGAACTGATCTC
Diagnostic T-DNA insertion: LBb1.3	F	ATTTTGCCGATTTCGGAAC
VPS26C genomic sequence cloning	F	CACCATGGCGACGGCGACGA
VPS26C genomic sequence cloning	R	TTAGCAGCTGAACTGATCTC
VPS26C promoter cloning	F	CACCGAGCTCTGTTGGCCTGCTTTCTTT
VPS26C promoter cloning	R	ACTAGTTTTACTCACCGAGCTTAGC
Genotyping VTI13	F	TTGTTCTTTCCAGGTTAAGAAAATGG
Genotyping VTI13	R	TGAGTTTGAAGTACAAGATAAAGATA
Human ortholog HsDSCR3 cloning	F	CACCATGGGGACCGCCCTGGACATCAG
Human ortholog HsDSCR3 cloning	R	TTAAACCTTATCGTCGTCATCCTTGTAT
VPS26A genomic sequence cloning	F	CACCATGAATTATCTTCTTGGAGAAGCC
VPS26A genomic sequence cloning	R	AGATGTCTCTTCCTTGAGCCTGTACAAG
VPS26B genomic sequence cloning	F	CACCATGAATTATCTTCTTGGAGCTTT
VPS26B genomic sequence cloning	R	TCTTAGCCGGACATTCACAC
VPS29 genomic sequence cloning	F	CACCGGTACCATGGTGCTGGTATTGGC
VPS29 genomic sequence cloning	R	GGATCCCTACGGACCAGAGCTGG
VPS35A genomic sequence cloning	F	CACCATGATCGCAGACGGATCAGA
VPS35A genomic sequence cloning	R	CTATACTTTGATCGCCTGGTATCTC
VPS35B genomic sequence cloning	F	CACCATGAGAACGCTCGCCG
VPS35B genomic sequence cloning	R	TCACAGCTTGATAGGGTCAT
VPS35C genomic sequence cloning	F	CACCATGATCGCCGACGACG
VPS35C genomic sequence cloning	R	TCATTCAAACCATTCCATTT
RT-PCR VPS26C	F	GCTGTAGCTAAGCTCGGTGAGTAA
RT-PCR VPS26C	R	GGATCTTTGGTGCGTCTAGGAACA
QRT-PCR VPS26A	F	TCACTTCCTTGGTGCGTGAGA
QRT-PCR VPS26A	R	CGCACGTTCACGCCATTGTA
QRT-PCR VPS26B	F	CAGCTTGGAAGGTTCCCATGA
QRT-PCR VPS26B	R	TGCTCCACCTTTTTCCCTTGAT
QRT-PCR VPS26C	F	TGGCAAAATCCCTCCGGGAA
QRT-PCR VPS26C	R	CCTCGCGGTATATTACTGACTTGG
QRT-PCR VPS29	F	CGATCGCTGAGAAGATCCGC
QRT-PCR VPS29	R	ATGGAGATCCCCCAATGCCA
QRT-PCR VPS35A	F	ACTCAAAGGCCCAGGTGACT
QRT-PCR VPS35A	R	AAGTTTCGCTGCATACCCCG
QRT-PCR VPS35B	F	TGGATGAAACCAACGCGGAG
QRT-PCR VPS35B	R	CGTCGAGGTCCTCCTGTCAT
QRT-PCR VPS35C	F	AGAACCTTGTTGCACGGCTT
QRT-PCR VPS35C	R	GGCAAACGCTTAGGTCCTCC
QRT-PCR EF1α	F	TGAGCACGCTCTTCTTGCTTTCA
QRT-PCR EF1α	R	GGTGGTGGCATCCATCTTGTTACA
QRT-PCR ACT2	F	CTTGCACCAAGCAGCATGAA
QRT-PCR ACT2	R	CCGATCCAGACACTGTACTTCCTT

Supplemental Table 2. Alignment of VPS26C sequences used to generate VPS26C phylogeny (consistent with Fig. 8).

CHAPTER 3

Proteomic analysis of VTI13-endosomes suggests a possible mechanism for a VTI13-dependent endosomal pathway in regulating polarized growth and cell wall organization in *Arabidopsis thaliana*

Suryatapa Ghosh Jha[1], Bin Deng[2], Fan Zhang[2], and Mary L Tierney[1]

[1]Department of Plant Biology, University of Vermont.

[2]Department of Biology, University of Vermont

Note:

I would like to acknowledge Dr. Bin Deng and Dr. Fan Zhang (Vermont Genetics Network and University of Vermont – Department of Biology) for the conducting LC-MS/MS to identify protein sequences from the affinity purified fraction consisting of VTI13-endosomes.

All other experimental data shown in this chapter was produced and analyzed by Suryatapa Ghosh Jha.

ABSTRACT

Soluble NSF Attachment Receptors (SNAREs) are membrane proteins involved in tethering endomembrane vesicles to their target membranes, thus assisting in vesicle fusion. The VTI-SNARE family member VTI13 is essential for root hair growth and cell wall organization in Arabidopsis and localizes to early endosomes and the vacuole membrane. We have used affinity purification and proteomic analysis to identify proteins that are part of the VTI13 early endosome compartment and may share a function with VTI13 in polarized growth and cell wall assembly. Proteins associated with endocytic trafficking pathways as well as several ER-body proteins were enriched in the GFP-VTI13 fraction. qRT-PCR analysis showed that the transcripts for a subset of these proteins are differentially regulated in the absence of *VTI13*. Additionally, several of the proteins identified are essential for root hair growth. Together, this study identifies candidates that have essential functions in the VTI13 pathway in regulating polarized growth in *Arabidopsis thaliana*.

INTRODUCTION

Endomembrane trafficking pathways are essential for a variety of developmental processes in higher eukaryotes. These include both exocytic and endocytic vesicular trafficking pathways, endosomal transport of proteins from the plasma membrane to the lytic vacuole or lysosomes for degradation and the recycling of receptors from the late endosomal membranes to the Golgi and *trans*-Golgi network (TGN). Alterations in endomembrane trafficking pathways have been implicated in severe abnormalities in plant and animal development (Surpin and Raikhel, 2004; Morita et al., 2014; Zhang, 2008; Burd, 2011; Bercusson et al., 2017; Geldner, 2004). In plants, this includes *gnom*, a loss of function mutation in a membrane associated ARF-GEF that leads to inhibition of PIN1 endosomal trafficking and defects in auxin transport and homeostasis (Steinmann et al., 1999; Geldner et al., 2001), the VTI11 SNARE loss-of-function mutant *zig,* that is defective in trafficking of cargo to the lytic vacuole resulting in agravitropic defects in *Arabidopsis thaliana* (Sanmartin et al., 2007; Hashiguchi et al., 2010), loss of the large retromer subunit VPS35B leading to defects in innate immunity in plants and *vps26c*, a large retromer subunit mutant that is defective in root hair growth (Jha et al., 2108).

Soluble NSF Attachment Receptor (SNARE) proteins, initially identified in yeast, are involved in the process of membrane fusion during endosomal trafficking and are divided into two subgroups based on their structural motifs. Q-SNAREs (Qa, Qb, and Qc) are integral components of target membranes while R-SNAREs are primarily associated with the vesicle membranes. During the process of membrane fusion, Q- and R- SNAREs form a tight coiled-coil helical complex, with three Q-SNAREs and one R-SNARE, facilitating

the transfer of cargo between membrane compartments (Fasshauer et al.,1998; Fukuda et al., 2000; Niihama et al., 2005). The Arabidopsis genome encodes about 65 SNAREs that belong to several subfamilies (Kim and Brandizzi, 2012). SNAREs within each subfamily function in distinct endosomal trafficking pathways, although gene family members can sometimes exhibit functional redundancies (Sanderfoot, 2007).

A number of SNAREs have been shown to be critical for polarized growth in plants. For example, SYP123 and SYP132 are expressed exclusively in trichoblasts of Arabidopsis (Enami et al., 2009; Ichikawa et al., 2014). SYP123 has been shown to localize to an endosome compartment in trichoblasts that is Brefeldin A (BFA)-sensitive and to the plasma membrane of root hairs, suggesting a role in endosomal trafficking pathways important for polarized cell growth. These authors have also demonstrated that SYP123 and SYP132 form a ternary complex with each of the Vesicle-Associated Membrane Proteins VAMP721, VAMP722 and VAMP724 that localizes to the tip of growing root hairs (Ichikawa et al., 2014). SNARES have also been shown to play an important role in pathways regulating the assembly or organization of plant cell walls. SYP111 localizes to the cell plate and has been shown to participate in membrane fusion events during cell division (Lauber et al., 1997; Muller et al., 2004). Also, proteomic analysis of TGN containing the SNARE SYP61 has shown that this compartment contains several cellulose synthase subunits that are trafficked to the plasma membrane to facilitate cellulose synthesis during cell expansion (Drakakaki et al., 2012).

The VTI-family of SNARES in Arabidopsis has four gene family members, of which three have been characterized for their function during plant growth. VTI11 localizes to the TGN, prevacuolar membrane (PVC) and lytic vacuole (Sanderfoot et al., 2001) while VTI13 can be detected in the membranes of early endosomes and the lytic vacuole (Larson et al., 2014). In contrast, VTI12 is localized to the TGN and the membrane surrounding storage vacuoles (Surpin et al., 2003). T-DNA insertion mutants for each of these SNAREs exhibit unique phenotypes, suggesting that they have distinct functions in plants. VTI11 has been shown to be important for shoot gravitropism (Morita et al., 2002) and for proper development of leaf vasculature, which is controlled by auxin distribution in the leaf primordium (Shirakawa et al., 2009), while VTI12 plays a role in plant autophagy (Surpin et al., 2003). VTI13 is essential for polarized growth and cell wall organization in roots (Larson et al., 2014). In addition, the endosomal trafficking pathways involving *VTI11* and *VTI13* have been shown to exhibit a genetic interaction with a retrograde trafficking pathway controlled by different large retromer subunit proteins (Hashiguchi et al., 2010; Jha et al., 2018).

The primary goal of this study was to initiate a mechanistic dissection of the VTI13-endosomal trafficking pathway in *Arabidopsis thaliana* to better understand its role in controlling growth and cell wall organization. Proteomic approaches have been successfully used to identify proteins associated with distinct endosomal compartments in plants. Drakakaki et al. (2012) identified cellulose synthase (CESA) subunits as cargo molecules of the SYP61-TGN proteome and demonstrated the role of this compartment in CESA trafficking and cell wall biosynthesis. More recently, Heard et al. (2015) used GFP-

fusions to tag proteins known to associate with distinct endosomal compartments *in vivo*, and used immunoprecipation and proteomic analysis to identify and characterize the subcellular localization of several regulatory and cargo proteins controlling secretory and endocytic pathways in Arabidopsis. In this paper, we describe a proteomics analysis of transgenic Arabidopsis seedlings expressing 35S:GFP-VTI13 and identify proteins potentially associated with a VTI13 early endosome compartment. Further analysis of the function of these proteins may provide us with testable models regarding the role of the VTI13 early endosome in controlling polarized growth and cell wall organization in Arabidopsis.

RESULTS

Protein extraction and immunoprecipitation of a VTI13 compartment

VTI13 functions in an endosomal trafficking pathway that is critical for polarized growth and cell wall organization in Arabidopsis root epidermal cell walls (Larson et al., 2014). VTI13 localizes to the membrane of early endosomes (EE) and the lytic vacuole (Larson et al., 2014). To further investigate the function of early endosomes containing VTI13, we used immunoprecipitation followed by proteomic analysis to identify proteins associated with the VTI13 early endosomal compartment in Arabidopsis seedlings expressing 35S:GFP-VTI13 in a *vti13* genetic background. Untransformed wild type seedlings and seedlings expressing the 35S:GFP-VTI13 construct were grown for seven days under continuous light on MS media and harvested for protein extraction (Figure 10). Seedlings were ground in liquid nitrogen followed by homogenization buffer and the resulting extract was filtered through Miracloth. The filtrate was then centrifuged at 6000 x g for 10 min at 4°C. and proteins in the supernatant were used for affinity purification of GFP-VTI13 and associated proteins using Chromotek GFP-Trap Agarose beads (Figure 11). The protein extract was incubated with the GFP-trap agarose beads for 1 hour at 4°C on a nutator after which the beads were washed three times with the homogenization buffer without inclusion of the protease inhibitors and centrifuged to remove the buffer at 2500 x g for 4 minutes at 4°C. Proteins were eluted from the anti-GFP resin by incubation in SDS-PAGE buffer at 95°C for 10 minutes. The sample was centrifuged at 2500 x g for 5 minutes in a microcentrifuge and proteins in the supernatant were collected for further analysis. The presence of GFP-VTI13 in the final supernatant fraction was verified by Western blotting (Figure 12) prior to proteomic analysis.

Identification of proteins associated with VTI13 by liquid chromatography (LC)-tandem mass spectrometry (MS/MS)

The affinity purified protein extract isolated from seedlings expressing 35S:GFP-VTI13 and from wild type seedlings (control) was partially size-separated using SDS-PAGE until the sample had entered the first cm of the running gel. The polyacrylamide gel containing the sample was collected and proteins within the gel matrix were treated with trypsin followed by LC-MS/MS using Thermo Q-Exactive mass spectrometry at the UVM proteomics facility. The peptide spectra of proteins in the GFP-VTI13 and control samples were queried against the *Arabidopsis thaliana* protein database (uniprot.org) using the software Protein Discoverer, version 1.4. These studies identified seven proteins enriched in all three GFP-VTI13 biological replicates and 31 proteins enriched in two of the three replicates tested when compared to untransformed Col-0 (Table 1). Proteins identified in this study were separated into two major groups based on their predicted function. The first of these included a number of proteins known to function in endocytosis and endosomal trafficking in Arabidopsis (Table 1) and included Dynamin-related Proteins (DRP)1 (Kang et al., 2003), DRP2A (Jin et al., 2001), DRP2B (Fujimoto et al., 2008), two Clathrin heavy chain (CHC) proteins (Kitakura et al., 2011; Wu et al., 2015), a plasma membrane ATPases AHA1 and AHA2 (Merlot et al., 2007; Mlodzinska et al., 2015) and Patellin 1 (PATL1) (Paterman et al., 2004). The second group of proteins identified in these studies are ER body proteins that are predicted to function in plant defense response pathways (Yamada et al., 2011; Nakano et al., 2014). These included GDSL Esterase/Lipases (GELPs) (Nagano et al., 2008), beta-Glucosidases (BGLUs) (Hara-

Nishimura and Matsushima, 2003; Matsushima et al., 2003a; Matsushima et al., 2003b) and Jacalin-Related Lectins (JALs) (Nagano et al., 2008) (Table I).

Many genes encoding the proteins associated with the GFP-VTI13 immunocomplex are mis-regulated in *vti13*

As a first step in characterizing the genes corresponding to proteins identified in this proteome analysis, we analyzed their expression by qRT/PCR in 7-day-old wild type and *vti13* seedlings. The genes that were significantly misexpressed in the *vti13* mutant are listed in Table 2 (A and B). A subset of genes encoding proteins associated with endosomal trafficking, including *DRP1A, DRP2A, DRP2B,* and *CHC1* were found to be significantly down-regulated in *vti13* mutant seedlings. This suggests that these genes may function in endosomal trafficking pathways involving VTI13 in regulating growth. In contrast, *Patellin 1 (PATL1*) transcripts were significantly upregulated in *vti13*. *PATL1* encodes a protein involved in endomembrane trafficking and interaction with phosphoinositides (Peterman et al., 2014).

We also investigated the expression of genes encoding ER-body proteins associated with GFP-VTI13 in our proteomic study. Several of these proteins have been implicated in plant defense response pathways (Matsushima et al., 2002). ER-body proteins have been shown to be constitutively expressed in roots and seedlings of plants within the Brassicales, but their expression in leaves is wound-inducible (Hara-nishimura and Matsushima, 2003). We show that several of the genes encoding these proteins are misexpressed in *vti13*. BGLU21 and GELP22 are down-regulated in the *vti13* background, whereas BGLU25, JAL22 and

JAL34 are upregulated in *vti13*. The role of the ER-body proteins in a VTI13 proteome compartment requires further analysis, but these initial data suggest that VTI13 might play a role in trafficking of these ER-body proteins in Arabidopsis.

DRP2A and *DRP2B* are essential for root hair growth

DRP2A and DRP2B were enriched significantly in all three biological replicates of our proteomic data, prompting us to investigate the role of these two genes in root hair growth. Dynamin Related Proteins (DRPs) localize to the cell plate (Fujimoto et al., 2008) and to the tip of root hairs in Arabidopsis (Taylor, 2011) and are implicated to function in several post-Golgi trafficking pathways that regulate cell plate formation and cell growth (Huang et al., 2015). *DRP2A* and *DRP2B* have been shown to also redundantly play a role in gametophyte development (Backeus et al., 2010). The significant reduction in *DRP2A* and *DRP2B* expression in *vti13* led us to ask if these two genes, like *VTI13*, are important for controlling root hair growth. T-DNA insertion mutants of *DRP2A* (*drp2a:* SALK_018859C) and *DRP2B* (*drp2b:* SALK_003049) were used for these studies. Seedlings were grown under continuous light for 5 days on 1X MS medium, pH6, and on 1X MS medium, pH6, supplemented with 200 mM mannitol, after which they were analyzed for defects in root hair growth. Both *drp2a* and *drp2b* seedlings grown on both media exhibited aberrant root hair growth when compared to wild type seedlings (Figure 13). This result, along with the downregulation of DRP2A and DRP2B transcripts in *vti13,* suggest that *DRP2A* and *DRP2B may* function in a VTI13-dependent endosomal trafficking pathway essential for polarized growth in Arabidopsis.

DISCUSSION

The primary aim of this study was to use a proteomics approach as a starting point for developing a better understanding of the role of the VTI13-dependent endosomal trafficking pathway in regulating root hair growth in Arabidopsis. The two major groups of proteins were identified in this study: proteins implicated in regulating membrane trafficking pathways and ER body proteins. The Dynamin-related proteins (DRPs), Clathrin Heavy Chain proteins (CHCs), and Patellin (PATL1) have all been shown to function in membrane trafficking pathways important for plant development, while the Glucosidases (BGLUs), the GDSL Esterase/Lipases (GELPs) and the Jacalin-related Lectins (JALs) are associated with ER bodies in Arabidopsis and may function in plant defense response pathways.

Proteins involved in endosomal trafficking

DRP2A and DRP2B are important candidates in our study as these are significantly enriched in the VTI13-fraction in all of the three biological replicates tested in the proteomic analysis. Dynamins are GTPases that act as 'molecular scissors', where they break the mesh-like scaffold formed by clathrins at the site of vesicle invagination and pinch a vesicle off of the donor membrane. Studies have shown that DRP1A and DRP2B function redundantly in regulating cell plate formation and cell morphogenesis (Fujimoto et al., 2008), cell polarity (Stanislas et al., 2015) and in clathrin-coated vesicle (CCV) formation in plants (Fujimoto et al., 2010). DRP2 function also contributes to cellular pathways regulating gametophyte development (Backues et al., 2010) and in maintaining innate immune signaling pathways (Smith et al., 2014). DRP2A and DRP2B localize to the

endocytic vesicle formation sites in the plasma membrane, clathrin-rich TGN, and the cell plate (Taylor, 2011). In addition, treatment of seedlings with wortmannin, an inhibitor of phosphatidylinositol kinases, or disruption of the cytoskeleton through latrunculin B or oryzalin treatment results in an increased duration of DRP2A and DRP2B at the plasma membrane, supporting a role for DRP2A and DRP2B function in several endosomal trafficking pathways associated with post-Golgi trafficking in plants (Huang et al., 2015).

DRP2A and DRP2B have been shown to localize at the tip of root hairs by immunolabelling, a site where rapid endocytosis takes place (Taylor, 2011). Induced expression of a dominant negative form of either protein resulted in reduced endocytosis at the tip and a bulging root hair phenotype (Taylor, 2011). In our studies, *DRP2A* and *DRP2B* were significantly down-regulated in *vti13* seedlings when compared with wild type seedlings, suggesting that they may function in a common cellular pathway. In addition, both *dpr2a* and *drp2b* exhibited shorter root hairs when compared with wild type seedlings grown on MS medium. Based on our initial studies, we hypothesize that DRP2A and DRP2B may act in coordination with VTI13 in controlling the endocytic machinery important for root hair growth and cell wall organization. Further studies demonstrating co-localization of VTI13 with these proteins as well as analysis of cell wall organization of the *drp2a* and *drp2b* mutants will be important to test this model.

Clathrins are proteins composed of two Clathrin Heavy Chain (CHCs) and two Clathrin Light Chain (CLCs) subunits. These proteins form a scaffold at the site of vesicle invagination, both at the plasma membrane and endosomal membranes and participate in

clathrin-mediated endocytosis (Goud et al., 1991; Blackbourn and Jackson, 1996; Puertollano et al., 2001; Holstein, 2002; Baisa et al., 2013). In our study, *CHC1* is significantly down regulated in the *vti13* mutant background. Preliminary studies of a T-DNA insertion mutant allele, *chc1-1,* indicate that it also shows aberrant root hair growth when compared to wild type seedlings (Supplemental Table 1). These initial studies suggest that CHC1 may function in a VTI13-dependent pathway required for root hair growth in Arabidopsis. The presence of CHC1, DRP2A and DRPB in the VTI13 interactome suggest a coordinated role of these proteins in pathways linked to cell plate formation and cytokinesis, and/or endosomal trafficking in Arabidopsis. This is consistent with the observed role of VTI13 in maintaining proper cell wall organization in root epidermal cells (Larson et al., 2014).

Expression of the plasma membrane proton-ATPase *AHA2* is also negatively regulated in *vti13*. *AHA2* is involved in controlling H+ efflux in root tips (Yuan et al., 2017) as well as controlling root architecture in nitrogen deficient conditions (Mlodzinska et al., 2015). These studies implicate AHA2 as a potential cargo of VTI13 early endosomes. Further analysis including co-localization studies between AHA2 and VTI13 and genetic analysis of *aha2* mutant alleles will be required to establish a role of AHA2 in controlling root hair growth in a VTI13-dependent manner.

In contrast to the down-regulation of the *DRPs* and *CHC1* in the *vti13* mutants, the expression of *Patellin 1 (PATL1)* is upregulated in *vti13*. *PATL1* is a member of the Patellin gene family in Arabidopsis, consisting of six members. PATL1 is a peripheral membrane

protein, having the SEC14 and the Golgi dynamics (GOLD) domain, similar to membrane trafficking proteins in other eukaryotes (Peterman et al., 2004). PATL1 has been shown to interact with phosphoinositides and is involved in cell plate maturation. Our preliminary analysis of *patl1* mutants showing an aberrant root hair growth phenotype (Supplemental Table 1) and its mis-regulation in *vti13* makes *PATL1* an important target in elucidating the VTI13-dependent pathway controlling polarized growth.

ER-Body proteins

The ER body proteins are found broadly within members of the Brassicaceae (Hara-Nishimura, 2003) and are broadly classified into two groups: proteins constitutively expressed in roots and seedlings and wound-induced ER body proteins expressed in leaves (reviewed in Yamada et al., 2011). In Arabidopsis, the roots constitutively accumulate ER bodies, whereas other plant organs accumulate ER bodies as part of a wound response pathway. Under conditions where root tissues are damaged, the activation of ER bodies can occur, leading release of beta-glucosidases (BGLUs) from ER bodies and their possible interaction with JAL proteins in the cytosol. This results in the formation of protein aggregates that hydrolyze glucosides in the vacuole, leading to the formation of toxic products to ward off pathogens and other agents of attack (Nagano et al., 2005; Nagano et al., 2008). In their review of ER bodies, Yamada et al. (2011) argue that when generating protein extracts, homogenization of roots or seedlings can induce this same ER body activation pathway to form the BGLU-JAL protein aggregates. This concern needs to be considered in evaluating the identification of ER body proteins within the VTI13 proteome

as the presence of BGLUs and JALs in the VTI13-fraction could reflect an artefact of the tissue homogenization technique used.

While further analysis is required to evaluate the biological significance of ER-body protein association with the VTI13 early endosomes, we have shown that several of the genes that encode ER body proteins identified in this study are mis-regulated in the *vti13* mutant. These genes, B*GLU21*, *BGLU25*, *GELP22*, *JAL22* and *JAL34*, act in coordination in forming ER bodies as well as in functioning in plant defense pathways (Yamada et al., 2011). Moreover, Jacalins (JALs) are involved in regulating the size of the ER bodies containing BGLUs (Nagano et al., 2008). The mis-expression of several ER-body protein genes identified in our study provides preliminary support for a model in which the VTI13-early endosome may be involved in trafficking these proteins within Arabidopsis. It has also been suggested that the constitutive expression of ER-body proteins in seedlings and roots of members of the Brassicaceae may reflect a function unrelated to plant defense response pathways (Yamada et al., 2011). The mis-regulation of these specific ER-body proteins in *vti13* provides an opportunity to further define the function of these proteins in Arabidopsis seedlings and the role of their association with the VTI13 proteome.

In conclusion, this analysis has identified a number of proteins that associate with GFP-VTI13 using immunoaffinity purification that are candidate proteins associated with the VTI13 early endosome in Arabidopsis seedlings. A number of the genes encoding these proteins were also mis-regulated in *vti13*, suggesting that their expression is dependent on the VTI13 endosomal trafficking pathway. Of particular interest are DRP1A, DRP2A,

DRP2B and CHC1, proteins known to regulate aspects of membrane fusion in Arabidopsis and that may function with VTI13 in regulating root hair growth and cell wall organization by controlling endosomal trafficking pathways in seedlings. The preliminary data described here will be useful in building models and generating testable hypotheses concerning the function of the VTI13 early endosome in plants.

METHODS

Plant material and growth conditions

Analysis of wild type seedlings and SALK mutant lines was performed using the Columbia-0 ecotype of Arabidopsis. The growth medium for Arabidopsis seedlings consisted of 1X Murashige-Skoog (MS) salts (Murashige and Skoog, 1962), 1% (w/v) sucrose, 5 mM 4-morpholineethanesulfonic acid sodium salt (MES), pH 6, 1X Gamborg's vitamin solution, and 1.3% (w/v) agarose (Invitrogen). For plants grown to maturity, seeds were sown on soil (Transplanting mix, Gardener's Supply, Intervale Rd, Burlington, VT) and placed in Conviron MTR30 growth chambers (Conviron, Winnipeg, CA, USA), using cool-white lights (80 μmol/m^2/sec; Licor photometer LI-189) under a 16:8 h light: dark cycle at 19° C.

Protein extraction and affinity purification

Wild type seedlings and transgenic seedlings expressing *35S:GFP-VTI13* in the *vti13* mutant background were grown on 1X MS, pH6 medium containing 1.3% (w/v) agarose, 1X Gamborg's vitamins and 1% (w/v) sucrose for 7 days under continuous light at room temperature. The seedlings were then harvested by freezing them in liquid nitrogen and grinding in a mortar and pestle. The frozen, ground tissue was homogenized using a 1:2 ratio of fresh weight tissue to protein extraction buffer (150 mM HEPES pH7.5, 10 mM EDTA, 10 mM EGTA, 17.5% (w/v) sucrose, 7.5 mM KCl, 0.01% (v/v) Igepal CA-630, 10 mM dithiothreitol, 1% (v/v) protease inhibitors (E-64, Pepstatin, Aprotinin, Leupeptin, O-phenanthroline; Sigma-Aldrich). The homogenate was then filtered through two layers of

miracloth to remove cell debris. The filtrate was centrifuged at 6000 x *g* at 4°C for 20 min. and the supernatant was collected for affinity purification.

Three µL of Chromotek GFP-Trap agarose beads/per gram of fresh weight tissue were added to the supernatant and incubated for one hour at 4°C with gentle shaking using a nutator. The sample was then centrifuged at 2500 x *g* at 4°C to pellet the beads and the supernatant was discarded. The agarose beads were washed with 200 µL of the homogenization buffer (without the protease inhibitors) three times and after the last wash, the beads were resuspended in 25 µL of 2X SDS loading buffer (950 µL of 2X Laemmeli buffer (BioRad) and 50 µL of β-mercaptoethanol). The beads were incubated at 95°C for 10 min. to elute bound protein and the eluate was separated from the beads by spinning the sample at 2500 x *g* and pipetting the supernatant into a fresh tube. This affinity purified fraction was confirmed to contain GFP-VTI13 by Western blotting after which the samples were prepared for proteomic analysis.

SDS-PAGE and Western blotting

GFP-VTI13 was detected in the eluted fraction using SDS-PAGE (12% resolving gel, 5% stacking gel). Five µL of the eluate was loaded on the gel and the proteins were size-separated for 1.5 hours at 120V. The proteins were then transferred to an Immobilon-FL PVDF membrane using a Fisher Biotech semi-dry blotting unit for 1 hour at 65 mA. The membrane was washed three times with 1X Phosphate Buffered Saline with Tween-20 (PBST) (8 mM Na2HPO4, 2 mM KH2PO4, 150 mM NaCl, 3 mM KCl, 0.05% Tween-20) and blocked for an hour at 4°C in 1X blocking buffer (5 g non-fat dry milk per 100 mL of

1X PBS). The membrane was incubated overnight with shaking in a 1:5,000 dilution of anti-GFP primary antibody (polyclonal; rabbit; Molecular Probes – Life technologies) in blocking buffer, washed 3 times with 1X Phosphate Buffered Saline (PBS), and incubated for 1 hour with shaking in the dark with a 1:20,000 dilution of secondary antibody (Licor, IRDye 680RD goat anti-rabbit). The membrane was washed with 1X PBS three times before detecting the GFP-VTI13 protein using Licor Odyssey CLx imaging system.

Tryptic digestion of proteins

Protein samples eluted from the Chromotek-GFP-trap agarose beads were applied to a 12% (w/v) SDS-polyacrylamide gel containing a 5% (w/v) SDS-acrylamide stacking gel. The proteins in each sample were separated briefly by running the samples into the resolving gel for 15 min. at 120V. The portion of the resolving gel containing the protein samples was then cut into three individual pieces (top, middle and bottom) and provided to the UVM Proteomics Center for tryptic digestion and LC-MS/MS. Each piece of acrylamide was cut into 1 mm^3 cubes and washed with 50 mM NH_4HCO_3 in 50% (v/v) CH_3CN. Each group of gel cubes was then dehydrated in CH_3CN for 10 min. and dried in a Speed Vac. Protein samples were reduced by dithiothreitol (DTT) and alkylated by iodoacetamide (Spiess et al., 2011). A solution of 10 ng/µL trypsin in 50 mM NH_4HCO_3 was used to re-swell the gel pieces completely at 4°C for 30 min., followed by a 37°C digestion overnight. The digestion was terminated by adding 10% (v/v) formic acid. The sample was then centrifuged at 2800 x *g*, and the supernatant was collected for LC-MS/MS.

Mass Spectrometry

Protein samples were analyzed by tandem mass spectrometry by the UVM Proteomics Center. Briefly, 2 μL of tryptic-digested protein sample was analyzed on a Thermo Q-Exactive mass spectrometer coupled to an EASY-nLC system (Thermo Fisher). The spectra of peptides identified in this analysis were searched against the *Arabidopsis thaliana* protein database (*www.uniprot.org*) (protein count: 39369) by Proteome Discoverer (PD) 1.4.

Characterization of root hair phenotypes

Wild type and mutant seeds (see Table below) were sterilized using 20% (v/v) bleach, followed by 5-6 washes in sterile distilled water. The sterilized seeds were stored in sterile water overnight in the dark at 4°C before plating them on solid media. Seedlings were grown on MS medium using petri plates placed vertically under continuous white light at 20°C for five days. Where indicated, 200 mM mannitol was included in the growth medium. To characterize root hair shape and growth, seedlings were mounted in sterile water on glass slides. Images were taken using a Nikon Eclipse TE200 inverted microscope with SPOT imaging software (Diagnostic Instruments). The length of 10-15 root hairs/seedling for at least 10 seedlings per genotype were measured, using Image J and the calibrating tool in the SPOT software, and a Student's *t*-test was used for statistical analysis.

RNA isolation and transcript analysis using qRT-PCR

To measure mRNA transcript abundance for genes in our study, wild type Arabidopsis seedlings or mutant seedlings from the Arabidopsis T-DNA insertion collection were grown for 7 days and used to generate three biological replicates. Each replicate contained roots from approximately 200 seedlings. Seedlings were frozen, ground in liquid nitrogen, and stored at -80°C. Total RNA was extracted using a Qiagen RNeasy Plant Mini Kit, quantified using a nanodrop (Thermo Scientific) followed by generation of first strand cDNA using Superscript II Reverse Transcriptase (Invitrogen), according to the manufacturer's instructions. For quantitative RT-PCR, the first-strand cDNA was diluted 1:10 and then used as a template with iTaq Universal SYBR green Supermix (Bio-Rad). An Applied Biosystems Step-one Plus instrument was used to run the qRT-PCR. Three technical and three biological replicates were analyzed by qRT-PCR cycle. The differential expression values of transcripts were standardized against the transcript expression of *EF1α* and *ACT2* housekeeping genes. The sequence of primers used for qRT-PCR are described in Supplemental Table 3 (Table S3).

Accession numbers

Locus	Annotation	Accession No.	Allele
At5G42080	Dynamin related protein 1A (*DRP1A*)	CS835032	*drp1a*
At1G14830	Dynamin related protein 1C (*DRP1C*)	SALK_080307 SALK_088722	*drp1c*
At1G10290	Dynamin related protein 2A (*DRP2A*)	SALK_018859C	*drp2a*
At1G59610	Dynamin related protein 2B (*DRP2B*)	SALK_003049	*drp2b*
At3G11130	Clathrin Heavy Chain 1 (*CHC1*)	SALK_112213 SALK_103252	*chc1-1* *chc1-2*
At3G08530	Clathrin Heavy Chain 2 (*CHC2*)	SALK_151638	*chc2-3*
At2G18960	Plasma membrane ATPase 1 (*AHA1*)	SALK_065288C	*aha1-7*
At3G14780	GDSL esterase lipase	SALK_039970C	
At4G34450	Coatomer gamma 2 subunit	SALK_103820 SALK_103822	
At1G72150	Patellin 1 (*PATL1*)	SALK_080204	*patl1*
At2G38000	DNA J Chaperone	SALK_038497	
At3G20370	TRAF-like protein	SALK_030953	

ACKNOWLEDGEMENTS

We thank Gary Ward's lab and Anne Kelsen (University of Vermont, Department of Microbiology and molecular genetics) for kindly letting us use their lab equipment – Fisher Biotech semi dry blotting system for Western blots and the Licor imaging system for detecting proteins. We would also like to thank Jeanne Harris and Jill Preston for their careful review and insightful comments on the manuscript. USDA-Hatch Grants VT-H02001 and VT-H02311 and funds from the Department of Plant Biology, University of Vermont, supported this research.

REFERENCES

Backues, S. K., Korasick, D. A., Heese, A., and Bednarek, S. Y. (2010) The Arabidopsis dynamin-related protein2 family is essential for gametophyte development. *The Plant Cell*, ***22*(10),** 3218–3231.

Bercusson, A., de Boer, L., and Armstrong-James, D. (2017) Endosomal sensing of fungi: current understanding and emerging concepts. *Medical Mycology*, ***55*(1),** 10–15.

Burd, C. G. (2011) Physiology and pathology of endosome-to-Golgi retrograde sorting. *Traffic, **12*(8),** 948–955.

Collings, D. A., Gebbie, L. K., Howles, P. A., Hurley, U. A., Birch, R. J., Cork, A. H., and Williamson, R. E. (2008) Arabidopsis dynamin-like protein DRP1A: a null mutant with widespread defects in endocytosis, cellulose synthesis, cytokinesis, and cell expansion. *Journal of Experimental Botany*, ***59*(2),** 361–376.

Ebine, K., and Ueda, T. (2015) Roles of membrane trafficking in plant cell wall dynamics. *Frontiers in Plant Science*, ***6***.

Esch, L., and Schaffrath, U. (2017) An Update on Jacalin-Like Lectins and Their Role in Plant Defense. *International Journal of Molecular Sciences*, ***18*(7).**

Fujimoto, M., Arimura, S., Nakazono, M., and Tsutsumi, N. (2008) Arabidopsis dynamin-related protein DRP2B is co-localized with DRP1A on the leading edge of the forming cell plate. *Plant Cell Reports*, ***27*(10),** 1581–1586.

Geldner, N. (2004) The plant endosomal system--its structure and role in signal transduction and plant development. *Planta*, ***219*(4),** 547–560.

Geldner, N., Friml, J., Stierhof, Y.-D., Jürgens, G., and Palme, K. (2001) Auxin transport inhibitors block PIN1 cycling and vesicle trafficking. *Nature*, ***413*(6854),** 425–428.

Hara-Nishimura, I., and Matsushima, R. (2003) A wound-inducible organelle derived from endoplasmic reticulum: a plant strategy against environmental stresses? *Current Opinion in Plant Biology*, ***6*(6),** 583–588.

Hong, Z., Geisler-Lee, C. J., Zhang, Z., and Verma, D. P. S. (2003). Phragmoplastin dynamics: multiple forms, microtubule association and their roles in cell plate formation in plants. *Plant Molecular Biology*, ***53*(3),** 297–312.

Huang, J., Fujimoto, M., Fujiwara, M., Fukao, Y., Arimura, S.-I., and Tsutsumi, N. (2015) Arabidopsis dynamin-related proteins, DRP2A and DRP2B, function coordinately in post-Golgi trafficking. *Biochemical and Biophysical Research Communications*, ***456*(1),** 238–244.

Ichikawa, M., Hirano, T., Enami, K., Fuselier, T., Kato, N., Kwon, C., and Sato, M. H. (2014) Syntaxin of plant proteins SYP123 and SYP132 mediate root hair tip growth in Arabidopsis thaliana. *Plant & Cell Physiology*, ***55*****(4),** 790–800.

Jha, S.G., Larson, E.R., Humble, J., Domozych, D. S., Barrington, D.S., and Tierney, M.L. (2018) Vacuolar Protein Sorting 26C encodes an evolutionarily conserved large retromer subunit in eukaryotes that is important for root hair growth in Arabidopsis thaliana. *Plant J,* **94 (4)**, 595-611

Konopka, C. A., and Bednarek, S. Y. (2008) Comparison of the dynamics and functional redundancy of the Arabidopsis dynamin-related isoforms DRP1A and DRP1C during plant development. *Plant Physiology*, ***147*****(4),** 1590–1602.

Larson, E. R., Zelm, E. V., Roux, C., Marion-Poll, A., and Blatt, M. R. (2017) Clathrin Heavy Chain Subunits Coordinate Endo- and Exocytic Traffic and Affect Stomatal Movement. *Plant Physiology*, ***175*****(2),** 708–720.

Matsushima, R., Hayashi, Y., Yamada, K., Shimada, T., Nishimura, M., and Hara-Nishimura, I. (2003a) The ER body, a novel endoplasmic reticulum derived structure in Arabidopsis. *Plant Cell Physiology,* **44,** 661-666

Matshisuma, R., Kondo, M., Nishimura, M., and Hara-Nishimura, I. (2003b) A novel ER-derived compartment, the ER body, selectively accumulates beta-glucosidase with an ER retention signal in Arabidopsis. *Plant J.,* **33,** 493-502.

Morita, M. T., Kato, T., Nagafusa, K., Saito, C., Ueda, T., Nakano, A., and Tasaka, M. (2002) Involvement of the Vacuoles of the Endodermis in the Early Process of Shoot Gravitropism in Arabidopsis. *The Plant Cell*, ***14*****(1),** 47–56.

Morita, M. T., and Shimada, T. (2014) The Plant Endomembrane System—A Complex Network Supporting Plant Development and Physiology. *Plant and Cell Physiology*, ***55*****(4),** 667–671.

Mravec, J., Petrášek, J., Li, N., Boeren, S., Karlova, R., Kitakura, S., and Friml, J. (2011) Cell plate restricted association of DRP1A and PIN proteins is required for cell polarity establishment in Arabidopsis. *Current Biology* ***21*****(12),** 1055–1060.

Mukadam Aamir S., and Seaman Matthew N.J. (2015) Retromer-mediated endosomal protein sorting: The role of unstructured domains. *FEBS Letters*, ***589*****,** 2620–2626.

Nagano, A.J., Fukao, Y., Fujiwara, M., Nishimura, M., and Hara-Nishimura, I. (2008) Antagonistic jacalin-related lectins regulate the size of ER body-type beta-glucosidase complexes in Arabidopsis thaliana. *Plant Cell Physiol.* **49,** 969-980

Nakano, R. T., Yamada, K., Bednarek, P., Nishimura, M., and Hara-Nishimura, I. (2014)

ER bodies in plants of the Brassicales order: biogenesis and association with innate immunity. *Frontiers in Plant Science*, ***5.***

Niihama, M., Uemura, T., Saito, C., Nakano, A., Sato, M. H., Tasaka, M., and Morita, M. T. (2005) Conversion of Functional Specificity in Qb-SNARE VTI1 Homologues of Arabidopsis. *Current Biology*, ***15*****(6),** 555–560.

Parsons, H. T., and Lilley, K. S. (2018) Mass spectrometry approaches to study plant endomembrane trafficking. *Seminars in Cell & Developmental Biology*, ***80*****,** 123–132.

Peterman, T. K., Ohol, Y. M., McReynolds, L. J., and Luna, E. J. (2004) Patellin1, a Novel Sec14-Like Protein, Localizes to the Cell Plate and Binds Phosphoinositides. *Plant Physiology*, ***136*****(2),** 3080–3094.

Sanderfoot, A. (2007) Increases in the Number of SNARE Genes Parallels the Rise of Multicellularity among the Green Plants. *Plant Physiology*, ***144*****(1),** 6–17.

Sawa, S., Koizumi, K., Naramoto, S., Demura, T., Ueda, T., Nakano, A., and Fukuda, H. (2005) DRP1A is responsible for vascular continuity synergistically working with VAN3 in Arabidopsis. *Plant Physiology*, ***138*****(2),** 819–826.

Shirakawa, M., Ueda, H., Shimada, T., Nishiyama, C., and Hara-Nishimura, I. (2009) Vacuolar SNAREs Function in the Formation of the Leaf Vascular Network by Regulating Auxin Distribution. *Plant and Cell Physiology*, ***50*****(7),** 1319–1328.

Smith, J. M., Leslie, M. E., Robinson, S. J., Korasick, D. A., Zhang, T., Backues, S. K., and Heese, A. (2014) Loss of Arabidopsis thaliana Dynamin-Related Protein 2B reveals separation of innate immune signaling pathways. *PLoS Pathogens*, ***10*****(12),** e1004578.

Steinmann, T., Geldner, N., Grebe, M., Mangold, S., Jackson, C. L., Paris, S., and Jürgens, G. (1999) Coordinated Polar Localization of Auxin Efflux Carrier PIN1 by GNOM ARF GEF. *Science*, ***286*****(5438),** 316–318.

Surpin, M., and Raikhel, N. (2004) Traffic jams affect plant development and signal transduction. *Nature Reviews Molecular Cell Biology*, ***5*****(2),** 100–109.

Surpin, M., Zheng, H., Morita, M. T., Saito, C., Avila, E., Blakeslee, J. J., and Raikhel, N. (2003) The VTI Family of SNARE Proteins Is Necessary for Plant Viability and Mediates Different Protein Transport Pathways. *The Plant Cell*, ***15*****(12),** 2885–2899.

Taylor, N. G. (2011) A role for Arabidopsis dynamin related proteins DRP2A/B in endocytosis; DRP2 function is essential for plant growth. *Plant Molecular Biology*, ***76*****,** 117–129.

Yamada, K., Hara-Nishimura, I., and Nishimura, M. (2011) Unique Defense Strategy by the Endoplasmic Reticulum Body in Plants. *Plant and Cell Physiology*, ***52*****(12),** 2039 -2049.

Yoshinari, A., Fujimoto, M., Ueda, T., Inada, N., Naito, S., and Takano, J. (2016) DRP1-Dependent Endocytosis is Essential for Polar Localization and Boron-Induced Degradation of the Borate Transporter BOR1 in Arabidopsis thaliana. *Plant & Cell Physiology*, ***57*****(9).**

Zeng, M.-H., Liu, S.-H., Yang, M.-X., Zhang, Y.-J., Liang, J.-Y., Wan, X.-R., and Liang, H. (2013) Characterization of a Gene Encoding Clathrin Heavy Chain in Maize Up-Regulated by Salicylic Acid, Abscisic Acid and High Boron Supply. *International Journal of Molecular Sciences*, ***14*****(7),** 15179–15198.

Zhang, M. (2008) Endocytic mechanisms and drug discovery in neurodegenerative diseases. *Frontiers in Bioscience: A Journal and Virtual Library*, ***13*****,** 6086–6105.

FIGURE LEGENDS

Figure 10.

Outline of the protein extraction procedure from wild type and 35S:GFP-VTI13 transgenic seedlings.

Figure 11.

Schematic representation of GFP-Trap immunoprecipitation of the protein fraction extracted from untransformed Col-0 seedlings (Control) and a transgenic line expressing 35S:GFP-VTI13 in a vti13 background.

Figure 12.

GFP-VTI13 was detected in the fraction used for proteomic analysis by Western Blot.

Five μL of the extracted protein sample was size separated by SDS-PAGE followed by Western blot to determine the presence of GFP-VTI13 in the sample. The primary antibody against GFP (Invitrogen – Molecular probes) was used at a dilution of 1:5000. The secondary antibody (Biorad) was used at a dilution of 1:20000. We detected a band for GFP-VTI13 with an expected size of 49 Kda**.**

Figure 13.

DRP2A and *DRP2B* are essential for root hair growth and are down regulated in the absence of *VTI13*.

(A) 5-day-old wild type seedlings and T-DNA insertion mutants of *drp2a* and *drp2b,* and wild type were grown on 1X MS medium, pH6 as well as on 1X MS, pH6 supplemented with 200 mM mannitol and were used to investigate root hair growth. *drp2a* and *drp2b* exhibited reduced root hair growth on both media when compared to wild type seedlings.

(B) Average root hair length (μm) of 5-day-old seedlings grown on 1X MS medium, pH 6 (blue bars) and on 1X MS medium, pH 6 supplemented with 200 mM mannitol (red bars). Twenty seedlings per genotype per treatment were scored and 10-15 root hairs per seedling were measured for each biological replicate. The graph shows an average of three biological replicates. Asterisks indicate statistical significance according to the Student's *t*-test, where wild type was compared in a pair-wise manner with each of the genotypes for each treatment ($P < 0.05$). Error bars represent the standard error of the mean of three biological replicates.

Table 1.

List of proteins enriched in the GFP-VTI13 fraction compared to the untransformed control.

The proteomic analysis resulted in a suite of proteins that are enriched in the GFP-VTI13 fraction when compared to the untransformed wild type fraction. The protein sequences that were enriched at least 1.5-fold in all of the three replicates tested are represented in bold, those enriched in only two of the three replicates are italicized. The rest of the proteins listed were enriched at least 1.5-fold in only one of the replicates tested.

Table 2.

Several genes from the study were differentially expressed in the *vti13* mutant when compared to wild type.

RNA was isolated from 7-day-old wild type and *vti13* seedlings for three independent biological replicates. qRT-PCR was used to determine expression of all of the genes

encoding the proteins enriched in the GFP-VTI13 fraction. Several of those genes' expression was dependent on the presence of *VTI13*. (A) List of genes down regulated in the *vti13,* and (B) List of genes up regulated in *vti13*.

SHORT LEGENDS FOR SUPPORTING INFORMATION

Table S3: Primer sequences used for qRT-PCR analysis of all the genes enriched in the GFP-VTI13 proteomic analysis.

Table S4: T-DNA insertion mutant lines investigated for root hair phenotype.

Figure S9: Differential expression of transcripts of proteins enriched in the GFP-VTI13 proteomic analysis.

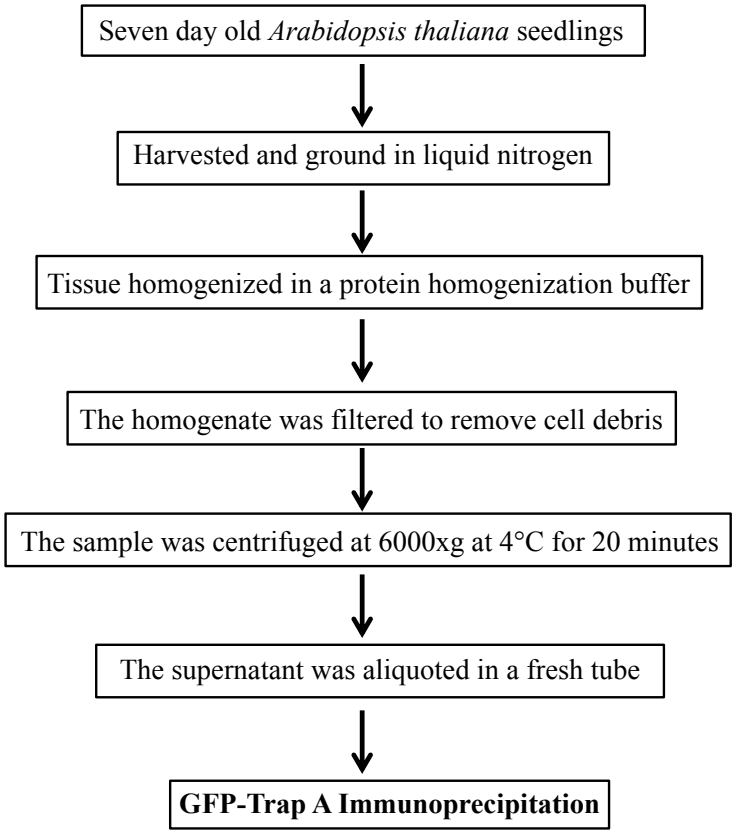

Figure 10: Outline of the protein extraction procedure from wild type and 35S:GFP-VTI13 transgenic seedlings.

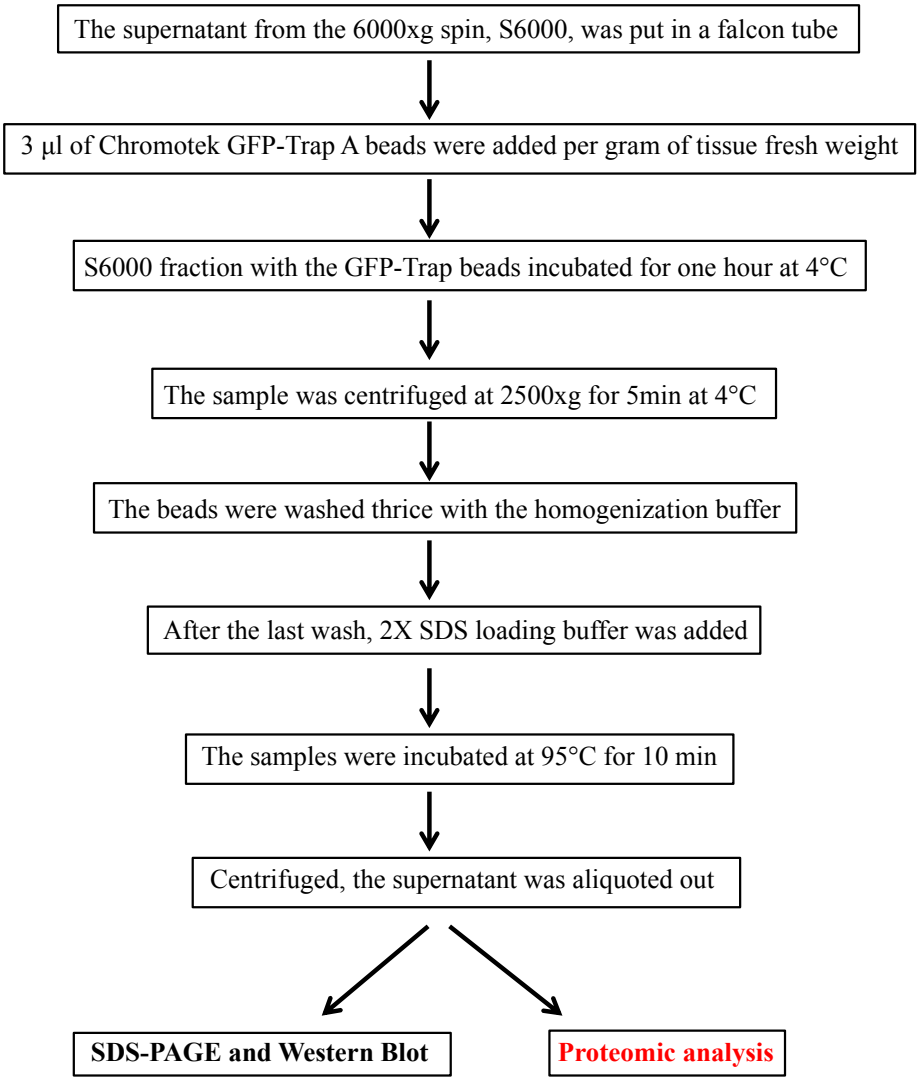

Figure 11: Schematic representation of GFP-Trap immunoprecipitation of the protein fraction extracted from untransformed Col-0 seedlings (Control) and a transgenic line expressing 35S:GFP-VTI13 in a *vti13* background.

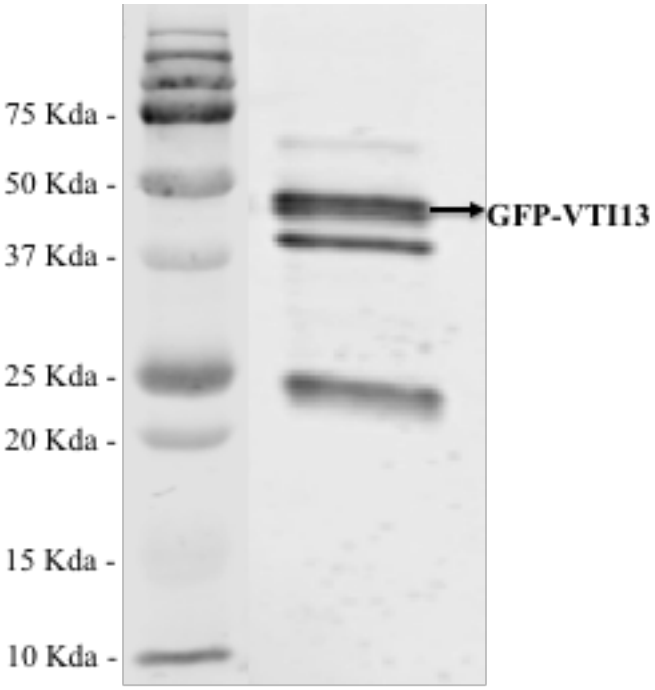

Figure 12: GFP-VTI13 was detected in the fraction used for proteomic analysis by Western Blot.

Five µL of the extracted protein sample was used to run on SDS-PAGE followed by Western blot to determine the presence of GFP-VTI13 in the sample. The primary antibody against GFP (Invitrogen – Molecular probes) was used at a dilution of 1:5000. The secondary antibody (Biorad) was used at a dilution of 1:20000. We detected a band for GFP-VTI13 with an expected size of 49 Kda.

Locus	Annotation	Predicted Subcellular Localization	References
AT3G29100	**VTI13**	**TGN, Vacuole membrane**	Larson et al., 2014.
DYNAMINS			
AT5G42080	*Dynamin-related protein 1A (DRP1A)*	Cell plate, CCVs	Kang et al., 2003; Konopka et al., 2008
AT1G14830	*Dynamin-related protein 1C (DRP1C)*	Cell Plate, Plasma membrane	Kang et al., 2003; Konopka et al., 2008
AT1G10290	**Dynamin-related protein 2A (DRP2A)**	**Golgi, CCVs, PM**	Jin et al., 2001; Taylor, 2011
AT1G59610	**Dynamin-related protein 2B (DRP2B)**	**Cell plate, CCVs, vacuole, PM**	Fujimoto et al., 2008; Backeus et al., 2010
CLATHRINs			
AT3G11130	Clatherin heavy chain 1 (CHC1)	Golgi, PM	Kitakura et al., 2011; Larson et al., 2017
AT3G08530	Clatherin heavy chain 2 (CHC2)	Golgi, PM	Wu et al., 2015; Larson et al., 2017
JACALINs			
AT1G52000	**Jacalin-related lectin 5 (JAL5)**	Extracellular region, cytosol	Theologis et al., 2010
AT2G36220	Jacalin-related lectin 22 (JAL 22)	Extracellular region	Lin et al., 1999
AT3G16420	Jacalin-related lectin 30 (JAL30)	Extracellular region, cytosol	Nagano et al., 2005
AT3G16440	*Jacalin-related lectin 32 (JAL32)*	Extracellular region	Salanoubat et al., 2000
AT3G16450	*Jacalin-related lectin 33 (JAL33)*	Extracellular region	Takeda et al., 2008
AT3G16460	*Jacalin-related lectin 34 (JAL34)*	Cytosol, Membrane compartments	Bae et al., 2003
GDSLs			
AT3G14780	*GDSL esterase/lipase*	Plasma membrane	Salanoubat et al., 2000
AT3G14210	**ESM1; GDSL-like**	**ER**	Zhang et al., 2006
AT1G54000	GDSL esterase/lipase 22, (GELP22)	Extracellular region (secreted); Vacuole	Minic et al., 2007
AT1G54030	MVP1; (GELP25)	vacuole/ER	Agee et al., 2010; Nakano et al., 2012
AT3G14220	*GDSL esterase/lipase 64, (GELP64)*	Extracellular region (secreted); Vacuole	Theologis et al., 2010
BGLUs			
AT1G52400	*Beta-glucosidase 18 (BGLU18)*	ER bodies	Ogasawara et al., 2009; Han et al., 2012
AT1G66270	*Beta-glucosidase 21(BGLU21)*	ER	Ahn et al., 2010
AT1G66280	*Beta-glucosidase 22 (BGLU22)*	ER	Ahn et al., 2010; Fujiwara et al., 2014
AT3G03640	**Beta-glucosidase 25 (BGLU25)**	**ER**	Salanoubat et al., 2000
PM ATPases			
AT2G18960	Plasma membrane ATPase 1 (AHA1)	Golgi, PM, Vacuole membrane	Merlot et al., 2007; Planes et al., 2015
AT4G30190	Plasma membrane ATPase 2 (AHA2)	Golgi, PM, Vacuole membrane	Mlodzinska et al., 2015
Others			
AT2G33370	**Ribosomal L14p/L23e family protein**	**Chloroplast, Ribosome, Cytoplasm**	Lin et al., 1999
AT2G40840	**Disproportinatiing Enzyme 2 (DPE2)**	**Chloroplast, Cytosol**	Malinova et al., 2014
AT2G43060	*IBH1*	Nucleus	Zhang et al., 2009
AT4G34450	Coatomer gamma-2 subunit	Golgi, COP1 vesicles	Mayer et al., 2009
AT1G72150	Patellin 1 (PATL1)	Cell plate, Golgi	Paterman et al., 2004
AT3G18820	Ras-related protein G3f (RABG3f)	vacuole, late endosome	Zelazny et al., 2013
AT1G52690	*Late embryogenesis 7 (LEA7)*	Cytosol	Popova et al., 2015
AT4G20850	*Tripeptidyl-peptidase 2 (TPP2)*	vacuole	Book et al., 2005
AT2G38000	*DNA J/Chaperone*	Cytoplasm	Lin et al., 1999
AT3G20370	*TRAF like*	Extracellular region; Membranes	Fujiwara et al., 2014

Table 1: List of proteins enriched in the GFP-VTI13 fraction compared to the untransformed control.

The proteomic analysis resulted in a suite of proteins that are enriched in the GFP-VTI13 fraction when compared to the untransformed wild type fraction. The protein sequences that were enriched at least 1.5-fold in all of the three replicates tested are represented in bold, those enriched in only two of the three replicates are italicized. The rest of the proteins listed were enriched at least 1.5-fold in only one of the replicates tested.

A

Genes down regulated in *vti13*
At5G42080 – Dynamin related protein 1A (DRP1A)
At1G10290 – Dynamin related protein 2A (DRP2A)
At1G59610 – Dynamin related protein 2B (DRP2B)
At3G11130 – Clathrin Heavy Chain 1 (CHC1)
At4G30190 – Plasma membrane ATPase 2 (AHA2)
At1G66270 – Beta Glucosidase 21 (BGLU21)
At1G54000 – GDSL Esterase/Lipase protein 22 (GELP22)

B

Genes up regulated in vti13
At3G03640 – Beta Glucosidase 25 (BGLU25)
At3G14780 – GDSL Esterase/Lipase
At2G36220 – Jacalin related Lectin 22 (JAL22)
At3G16460 – Jacalin related Lectin (JAL34)
At2G43060 – IBH1
At1G52690 – Late Embryogenesis 7 (LEA7)
At1G72150 – Patellin 1 (PATL1)
At3G20370 – TRAF-like Protein
At2G38000 – DNA-J/Chaperone

Table 2: Several genes from the study were differentially expressed in the *vti13* mutant when compared to wild type.

RNA was isolated from 7-day-old wild type and *vti13* seedlings for three independent biological replicates. qRT-PCR was used to determine expression of all of the genes encoding the proteins enriched in the GFP-VTI13 fraction. Several of those genes' expression was dependent on the presence of *VTI13*. **(A)** List of genes down regulated in the *vti13,* and **(B)** List of genes up regulated in *vti13.*

A

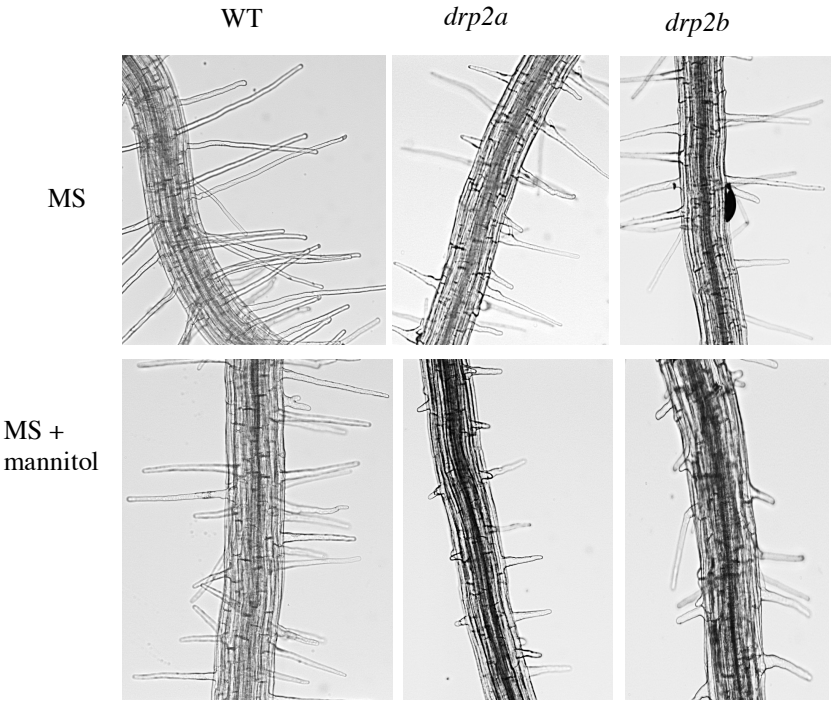
WT
drp2a
drp2b
MS
MS +
mannitol

B

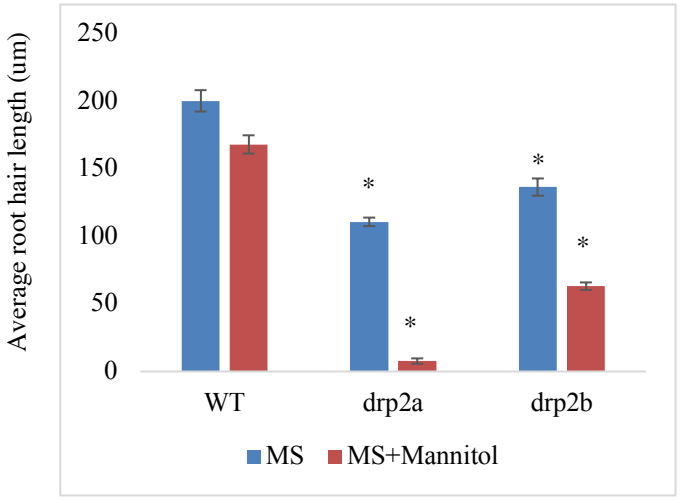
Average root hair length (um)
250
200
150
100
50
0
*
*
*
*
WT
drp2a
drp2b
MS
MS+Mannitol

Figure 13: *DRP2A* and *DRP2B* are essential for root hair growth and are down regulated in the absence of *VTI13*.

(A) 5-day-old wild type seedlings and T-DNA insertion mutants of *drp2a* and *drp2b* were grown on 1X MS medium, pH6 as well as on 1X MS, pH6 supplemented with 200 mM mannitol and were used to investigate root hair growth. *drp2a* and *drp2b* exhibited reduced root hair growth on both media when compared to wild type seedlings.

(B) Average root hair length (μm) of 5-day-old seedlings grown on 1X MS medium, pH 6 (blue bars) and on 1X MS medium, pH 6 supplemented with 200 mM mannitol (red bars). Twenty seedlings per genotype per treatment were scored and 10-15 root hairs per seedling were measured for each biological replicate. The graph shows an average of three biological replicates. Asterisks indicate statistical significance according to the Student's *t*-test, where wild type was compared in a pair-wise manner with each of the genotypes for each treatment ($P < 0.05$). Error bars represent the standard error of the mean of three biological replicates.

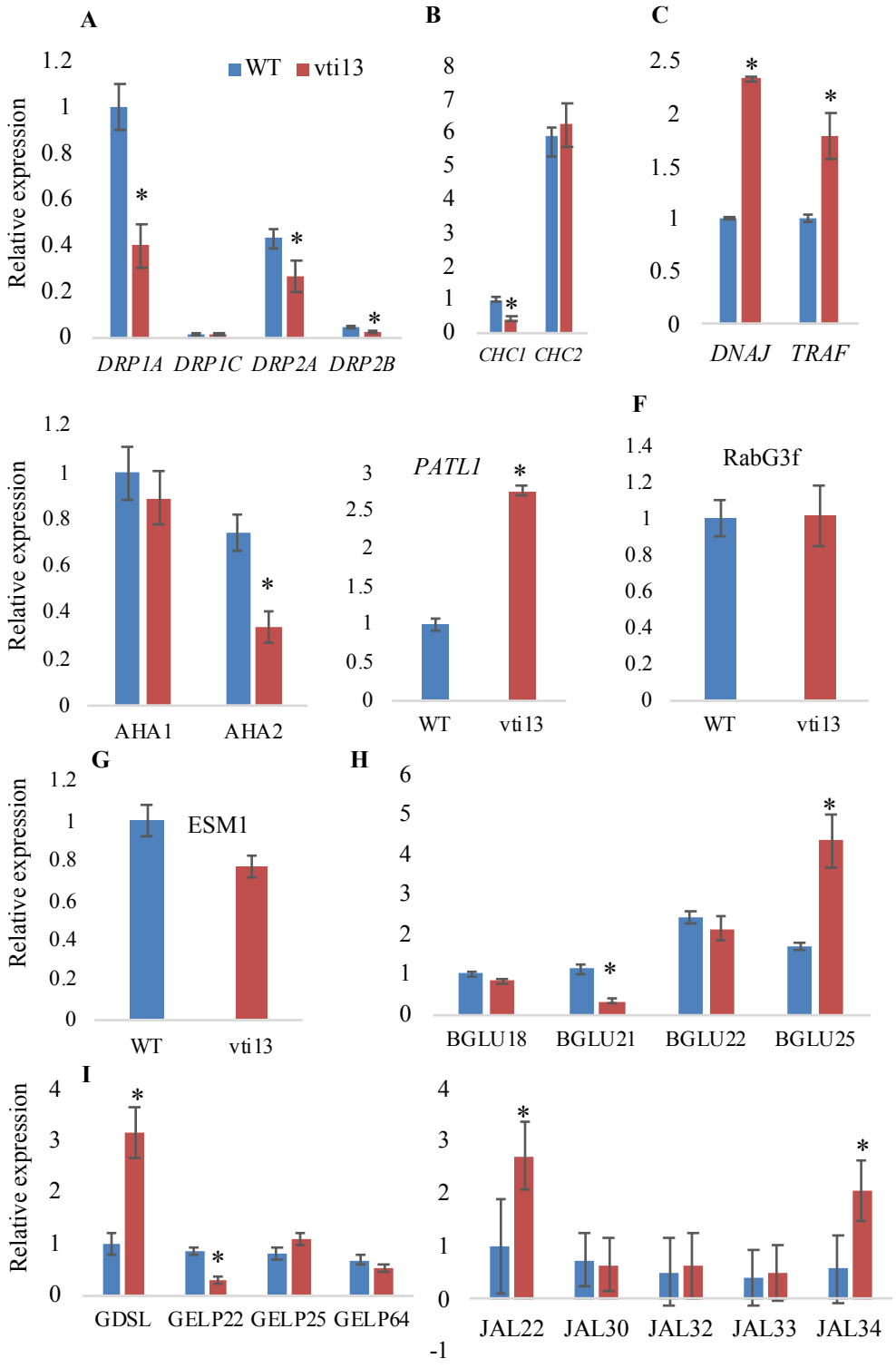
A
B
C
WT
vti13
Relative expression
DRP1A
DRP1C
DRP2A
DRP2B
CHC1
CHC2
DNAJ
TRAF
F
PATL1
RabG3f
AHA1
AHA2
G
ESM1
H
BGLU18
BGLU21
BGLU22
BGLU25
I
GDSL
GELP22
GELP25
GELP64
JAL22
JAL30
JAL32
JAL33
JAL34

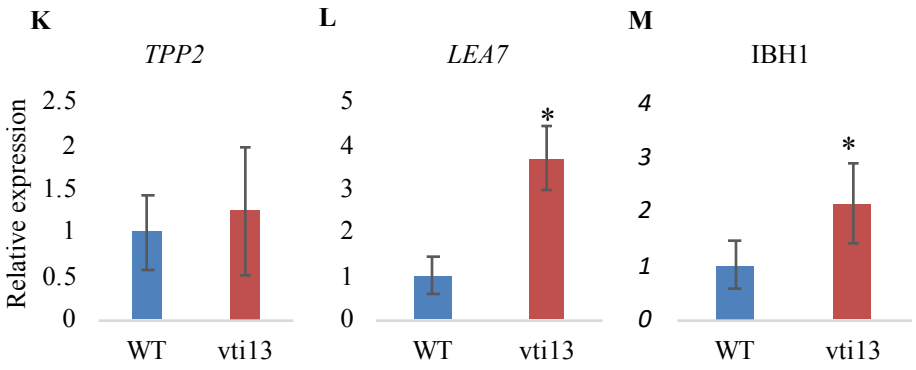

Figure S9: Differential expression of transcripts of proteins enriched in the GFP-VTI13 proteomic analysis.

qRT-PCR was used to determine the transcript level of proteins that were enriched in the GFP-VTI13 fraction. RNA was isolated from wild type and *vti13* seedlings and cDNA synthesized from this RNA was used as a template to investigate whether the transcript levels of these proteins were differentially regulated in the *vti13* mutant. Error bars represent standard error of mean, and asterisks represent statistical significance ($P<0.05$)

AT3G14220	GDSL esterase/lipase 64 (GELP64)	Forward: AGGTGGAGCGAGGAAGTTTG
		Reverse: AAAGAGGCTGTACCGGAAGC
AT1G54000	GDSL esterase/lipase 22 (GELP22)	Forward: TGGTGACTCCAACTTCGACG
		Reverse: ATCGCGAGCGGAATCTTCAT
AT1G54030	GDSL esterase/lipase-like protein 25 (GELP25)	Forward: CGTGAAACAAGCAAGCGGAA
		Reverse: CCAGTTCCACAACAAGCAGC
AT3G14210	ESM1; GDSL esterase/lipase	Forward: AAGGGAAACGTGCACTCGAA
		Reverse: GGGTTCCCAATACTCACGCA
AT1G52400	Beta-glucosidase 18 (BGLU18)	Forward: CTCTTGTCGCATGCTTACGC
		Reverse: TTGGAGCCAAATGCCATCCT
AT1G66270	Beta-glucosidase 21(BGLU21)	Forward: TTCCAAGCTAAGCCGAGCAA
		Reverse: GAAATCAACGGCCACATCGG
AT1G66280	Beta-glucosidase 22 (BGLU22)	Forward: TCACAACCTCCTCAACGCTC
		Reverse: TGGGTCTAGATGCCATCCCA
AT3G03640	Beta-gluosidase 25 (BGLU25)	Forward: CAGTCTGCGAGGACAAGGTT
		Reverse: CGTGTCCGGGACTTTCTCAA
At2g43060	IBH1	Forward: ACAATGGCCTCTGCAGACAA
		Reverse: AACGTACGCAGCCTTCTTGA
AT1G72150	Patellin 1 (PATL1)	Forward: AAACAGCTCCGACCAGTCTG
		Reverse: CTCTTTCTCTGCCACAGGGG
AT3G18820	Ras-related protein G3f (RABG3f)	Forward: GCTTGGTGTGCTTCAAAGGG
		Reverse: GCCTCGTTTCCTTCTGGTGA
At1G52690	Late embryogenesis 7 (LEA7)	Forward: AGACGTCTCAAGCTGCACAA
		Reverse: TTCACCGCATCAGTAGCTCC
At4G20850	Tripeptidyl-peptidase 2 (TPP2)	Forward: GCAACAGTGGTCCAGCTTTG
		Reverse: CCCGGCTTGACCAAGTGTAT

Table S3: Primer sequences used for qRT-PCR analysis of all the genes enriched in the GFP-VTI13 proteomic analysis.

Locus	Annotation	Accession No.	Root hair phenotype
At5G42080	Dynamin related protein 1A (*DRP1A*)	CS835032	Present
At1G14830	Dynamin related protein 1C (*DRP1C*)	SALK_080307 SALK_088722	Present
At1G10290	Dynamin related protein 2A (*DRP2A*)	SALK_018859C	Present
At1G59610	Dynamin related protein 2B (*DRP2B*)	SALK_003049	Present
At3G11130	Clathrin Heavy Chain 1 (*CHC1*)	SALK_112213 SALK_103252	Present
At3G08530	Clathrin Heavy Chain 2 (*CHC2*)	SALK_151638	Present
At2G18960	Plasma membrane ATPase 1 (*AHA1*)	SALK_065288C	Present
At3G14780	GDSL esterase lipase	SALK_039970C	Absent
At4G34450	Coatomer gamma 2 subunit	SALK_103820 SALK_103822	Present
At1G72150	Patellin 1 (*PATL1*)	SALK_080204	Present
At2G38000	DNA J Chaperone	SALK_038497	Absent
At3G20370	TRAF-like protein	SALK_030953	Absent

Table S4: T-DNA insertion mutant lines investigated for root hair phenotype.

CHAPTER 4

Synthesis and Future Directions

Introduction

Polarized growth occurs when cells synthesize and secrete new cell wall and plasma membrane components at their tip, resulting in highly elongated cells (Bedinger et al., 1994; Hepler et al., 2001). This is one of two primary ways in which plant cells expand and is important in the development of evolutionarily diverse organisms (Jones and Dolan, 2012; Rensing et al., 2016). Such growth was first reported in fungal hyphae (Levina et al., 1994; Robson et al., 1996), and later in algal cells and moss protonema (Braun and Limbach, 2006; Vidali et al., 2007; Augustine et al., 2008; Eklund et al., 2010). In angiosperms and gymnosperms, polarized growth functions in two cell types: pollen tubes and root hairs.

Root hairs in the model angiosperm *Arabidopsis thaliana* (Arabidopsis) are specialized extensions of particular root epidermal cells, known as trichoblasts, and are a great model for understanding polarized growth (Dolan, 2001). They function to increase root surface area, absorb water and nutrients, anchor plants in their environment, and participate in plant-soil microbe interactions, and are thus a highly tractable system for detecting growth phenotypes in different genetic and environmental contexts. Tip growth in root hairs is brought about by coordinated vesicular trafficking processes (Richter et al., 2011; Yao et al., 2011; Ichikawa et al., 2014; Larson et al., 2014; Jha et al., 2018) resulting in the secretion of new cell wall polymers at the growing tip (Park et al., 2011; Velasquez et al., 2011). Polarized growth of root hairs is also controlled by a calcium gradient at the tip, by

modulations in extracellular pH (Halperin et al., 2003), adjustment of turgor pressure in the interior of the cell to control cell expansion (Mendrina and Persson, 2015; Mangano et al., 2016), and the coordinated assembly of cytoskeletal components (Bibikova et al., 1999; Ketelaar et al., 2013).

To dissect the mechanism of polarized growth, I am primarily interested in understanding the endosomal trafficking pathways which are important for this developmental process in Arabidopsis. In this dissertation, I have described a novel protein complex important for root hair growth and its interaction with a pathway involving VTI13, a SNARE protein that maintains polarized growth and cell wall organization. I also initiated the mechanistic dissection of these pathways by investigating other components that are involved in the process of tip growth in root hairs. In this final chapter, I will summarize my findings and present current outstanding questions to generate hypotheses that should allow us to build upon our knowledge of the cell biology of polarized growth in root hairs.

VPS26C is a retromer/retriever complex essential for root hair growth in Arabidopsis

Retromers are multi-protein complexes that were initially described in yeast to function in recycling receptors and other cargo from endosomal compartments back to Golgi or TGN, but recently have also been shown to function in trafficking receptors between endosomes and the plasma membrane (REFS). Vacuolar Protein Sorting (VPS) 26C is a novel, evolutionarily conserved, large retromer complex protein. VPS26C interacts with VPS35A and colocalizes with VPS29 in Arabidopsis to form a large retromer/retriever complex that is essential for proper root hair growth under specific environmental conditions and

localizes to endosomal membranes in root epidermal cells (Jha et al., 2018). Koumandou et al. (2010) described the phylogeny of core retromer subunits in eukaryotes and showed that the VPS26C/DSCR3 sequences in plant and animal systems, including Arabidopsis and human, belong to a monophyletic clade distinct from the VPS26A/B sequences. Sequences within this clade may also share a conserved biochemical function as the human VPS26C/DSCR3 ortholog can complement the root hair phenotype of the *vps26c* mutant in Arabidopsis (Jha et al., 2018). A recent study using human cell lines (McNally et al., 2017) has demonstrated the human VPS26C/DSCR3 ortholog forms of a retromer-like 'retriever' complex with VPS29 and a VPS35-like (C16orf62) protein, similar to the VPS26C complex identified in Arabidopsis (Jha et al., 2018).

An investigation into proteins that form a complex with DSCR3 in humans has led to some other major conclusions about the retriever complex (McNally et al., 2017). Firstly, this complex localizes to endosomal membranes, and the Copper Metabolism MURR1 Domain (COMMD)/Coiled-Coil Domain Containing CCDC22/CCDC93 (CCC) complex mediates this recruitment. The CCC complex functions in association with the WASH (Wiscott – Aldrich syndrome and SCAR Homolog) complex in humans, a group of proteins involved in actin nucleation to control endosomal sorting of transmembrane receptors (Bartuzi et al., 2016). Secondly, the retriever complex in humans interacts with the cargo adaptor Sorting Nexin (SNX)17, through a direct interaction with VPS26C/DSCR3. to mediate the retrograde trafficking of a subset of proteins from endosomes to the plasma membrane (REF). Lastly, suppression of CCDC22 and CCDC93, using siRNA, interrupts the

endosomal association of the retriever complex with SNX17, and therefore leads to the mis-sorting of the $\alpha_5\beta_1$ integrin, one of the VPS26C/SNX17 cargo proteins.

Based on our identification and functional characterization of the Arabidopsis VPS26C-complex, as well as our recent knowledge of this complex in humans, several key questions arise that need to be addressed:

1) **Is the VPS26C-complex in Arabidopsis recruited to endosomes in the same way as the human VPS26C-retriever complex?**

The mechanism of retromer recruitment in plants, unlike animals, is largely unknown. We have recently found that only two of the human CCC complex members, CCDC22 and CCDC93, have homologs in Arabidopsis. Preliminary studies show that the Arabidopsis orthologs share about 65% amino acid sequence similarity with their human counterparts, and both CCDC22 and CCDC93 are essential in root hair growth (Appendix; Figure 18). Moreover, *CCDC22* and *CCDC93* are expressed in a *VPS26C*-dependent manner (Appendix; Figure 19). To address whether these proteins are responsible for the recruitment of the VPS26C-complex to membranes, as they are in humans, it will be important to establish that CCDC22 and/or CCDC93 co-localize with VPS26C in the same endosomal membrane. This could be addressed by either transient expression of GFP-VPS26C and YFP-CCDC22 and YFP-CCDC93 in tobacco leaves or by co-expressing GFP-VPS26C and YFP-fusions for CCDC22 or CCDC93 stably in Arabidopsis.

siRNA-mediated down-regulation of CCDCs in human cell lines results in a lack of recruitment of the VPS26C-complex to the endosomes. This is very direct evidence of the

role that the CCDC proteins play in the localization of the retriever complex to the endosomal membranes. In Arabidopsis, we know that VPS26C localizes to endosomal membranes in root epidermal cells. Is this localization dependent upon CCDC22/93? If we express 35S:GFP-VPS26C in the loss-of-function mutants, *ccdc22* and *ccdc93,* and compare the localization of this retromer protein with that observed in wild type seedlings expressing GFP-VPS26C, we will get a clearer picture of whether the CCDC proteins play a role in mediating VPS26C localization to the endosomal membranes.

CCDC93 in humans physically interacts with a VPS35-like protein during localization of the retriever complex to endosomes. In Arabidopsis, another vital question is then whether CCDC93 interacts with VPS35A or any other member of the retromer complex. Jha et al. (2018) used bimolecular fluorescence complementation to detect the physical interaction of VPS26C with VPS35A. Similar methods can be used to detect a possible interaction between any member of the VPS26C-VPS35A-VPS29 complex and CCDC93. Other assays include directed yeast two-hybrid interactions or co-immunoprecipitation of a member of the VPS26C protein complex with CCDC93.

Retromer complexes, and now the retriever in animal systems, are dependent on the WASH complex (Helfer et al., 2013; Reviewed in Seaman et al., 2013; McNally et al., 2017), traditionally defined as ARP2/3 activators. In Arabidopsis, the SCAR/WAVE complex has been shown to function as an ARP2/3 activator (Frank et al., 2004) involved in actin polymerization related to root elongation (Dyachok et al., 2011), root hair growth, and tissue morphogenesis (Zhang et al., 2008). The SCAR/WAVE complex in Arabidopsis is

a multi-domain, multi-protein subunit that regulates ARP2/3 activation, and hence brings about actin polymerization (reviewed in Yanagisawa et al., 2013). Several proteins within the SCAR complex in Arabidopsis have been reported to function in coordinating distinct processes in plants through ARP2/3 activation and actin polymerization. For example, NAP1 regulates the formation of autophagosomes under conditions of nitrogen starvation and salt stress, by associating with ER membranes and sequentially colocalizing with the autophagy-related protein, ATG8 (Wang et al., 2016). SRA1, another member of the SCAR/WAVE complex, mediates stomatal response to darkness by controlling the actin reorganization in guard cells (Isner et al., 2017). *sra1/pir1* mutants show defective actin organization in guard cells and leaf epidermal cells, leading to defects in stomatal closing in darkness and trichome morphology, respectively. However, there is currently no evidence that the SCAR complex recruits retromers to endosomes.

A valid question is whether a SCAR complex member, similar to the WASH protein FAM21 in humans, that is responsible for interacting with either a retromer subunit or a CCDC complex member to mediate the recruitment of a VPS26C-containing retromer/retriever complex to endosomes in plants. There are a couple of ways to address this question. The Arabidopsis SCAR/WAVE complex consists of *NAP1, SRA1, BRK1, ABIL1/2* and four *SCARs (SCAR 1-4).* It will be important to determine if the whole complex together or individual subunits within the complex function in retromer recruitment in Arabidopsis, if at all. *nap1* and *scar2* (Basu et al., 2005; Zhang et al., 2005; Wang et al., 2016)*, sra1* (Isner et al., 2017)*,* and *brk1* (Le et al., 2006) have been implicated in autophagy vesicle formation and trichome morphology. BRK1 is important for

stabilizing the SCARs in plants (Le et al., 2006), in contrast to non-plant systems where stability of each of the proteins in the WASH complex is interdependent (Derivery and Gautreau, 2010). Based on this information, we can use *brk1* and *scar2* mutants to analyze if there are defects in VPS26C or CCDC localization to endosomal membranes. Another approach would be to affinity purify GFP-VPS26C-endosomes and use proteomics to determine if any of the SCAR complex proteins are pulled down. Overall, these approaches would begin to address a cellular mechanism describing how VPS26C localizes to the endosomes in plants.

2) Is the VPS26C-complex in Arabidopsis a retromer or a retriever?

The VPS26C-complex in humans is termed a 'retriever' because of several distinctions with human VPS35-retromer function: 1) the sorting nexin SNX17 binds to the VPS26C complex while SNX27 binds to the VPS35-retromer complex; 2) the mechanism used to recruit the retromer and retriever complexes to endosomal membranes; and 3) the trafficking pathway that each complex functions in. Whether the VPS26C complex in plants also functions as a 'retriever' needs further investigation.

First, we need to determine whether VPS26C in Arabidopsis interacts with an integral membrane protein on endosomes. VPS26C in humans physically interacts with the membrane-associated cargo adapter, SNX17, which is distinct from the sorting nexins that make up the small subunit of the retromers. Whether VPS26C in Arabidopsis, similar to humans, physically binds with a membrane-associated cargo adaptor remains to be addressed. While there are no known orthologs of SNX17 in Arabidopsis, however, in an

earlier study the Rab7 homolog, RabG3f, has been shown to physically interact with VPS35A to bring about VPS35 association with late endosomal membranes (Zelazny et al., 2013). However, in the study of subcellular localization of VPS26C, I observed that the membrane compartment that VPS26C associated with is not a late endosome, as the localization was insensitive to Wortmannin treatment (Jha et al., 2018). Second, we need to identify cargo that binds to the VPS26C-complex in Arabidopsis. To investigate both of these aspects of VPS26C function, affinity purification-based proteomic analysis will help us identify potential candidates for cargo, as well as potential adaptor proteins that may interact with the endosomal membrane and bind to VPS26C.

In Arabidopsis, retromer complexes have been defined to play a role in development. For example, VPS35 plays a role in immunity-associated cell death and associates with VPS29 and VPS35B in a large retromer complex (Munch et al., 2015). VPS26A and VPS35A are important in maintaining shoot gravitropism as part of a VPS35A-VPS29-VPS26A complex. To define whether the VPS26C-VPS35A-VPS29 is a classic retromer, or a distinct 'retriever' complex is an important question. One of the differences between the retromer and retriever complexes in human cells is that the latter is involved in recycling plasma membrane proteins from endosomal membranes. In Arabidopsis, Oliviusson et al. (2006) showed an interaction between core retromer subunits VPS35 and VPS26 with the Vacuolar Sorting Receptor, VSR1, by colocalization experiments using antibodies against the core retromer subunits and suggested that the retromer complex is involved in recycling of the VSRs. There is no other report of retromer cargo in plants. Investigating the VPS26C-endosomes using affinity purification-based MS/MS analysis from the GFP-

VPS26C expressing line can be useful in identifying cargo for the VPS26C-complex. Experiments to detect whether the candidate proteins co-localize with VPS26C, as well as to see if some of those would physically interact to function as a complex with VPS26C will be subsequently necessary to find out if VPS26C or VPS35A interacts with the cargo, and hence to distinguish this complex from a traditional retromer. If several major distinctions are found regarding the trafficking pathway markers, cargo or the interacting proteins, we can possibly conclude that the VPS26C complex is distinct from other retromer complexes characterized in Arabidopsis. All of these results taken together would be useful in illuminating the functioning of this complex in controlling polarized growth.

3) How would an understanding of VPS26C biochemical function inform us about evolution of the ancient VPS26C progenitor in plant and animal kingdoms?

VPS26C is an ancient gene having a conserved sequence across not only plants, but also animals and other eukaryotes (Koumandou et al., 2010). I have shown that *VPS26C* in Arabidopsis and humans are similar enough that the human VPS26C can substitute for the loss of VPS26C in Arabidopsis. This result is exciting, but more importantly, it is also thought provoking: does that mean they have the same cellular localization? Do they interact with the same set of proteins in both kingdoms? What function does VPS26C play in humans? On the other hand, if they are not similar in localization and interaction with other proteins, what does that mean for the evolution of VPS26C?

Plants and animals are complex and have evolved to perform specialized functions. Although they share certain conserved proteins and pathways, there are many

developmental processes that are distinct between the two kingdoms. The difference therefore lies in how conserved a particular protein's role is in cells, where these proteins are expressed in the organism, and whether they have evolved to have a specialized function in addition to their basic function. I have built upon the information we obtained from the monophyletic VPS26C clade that Koumandou et al. (2011) described by identifying additional VPS26C orthologs and, these sequences (Figure 14). This alignment is useful for identifying conserved residues within VPS26C and may lead us to a model for conserved regions within VPS26C that are necessary for function and would explain the complementation of the Arabidopsis *vps26c* root hair phenotype by the human ortholog. A recent study of the structural mechanism of VPS26-VPS35-VPS29 retromer complex has used crystal structures of VPS26 and VPS35 to describe the interaction between the retromer subunit proteins (Lucas et al., 2016). The authors showed that the C-terminal end of the VPS26 interacts with the N-terminal α-helices of VPS35 through a hydrophobic core defined by a proline residue at 247 (P247). Mutation studies have also revealed that the VPS26 binding site on VPS35 is defined by a conserved ^{106}PRLYL^{110} sequence (Gokool et al., 2007). Similar investigations with VPS26C will to define sequences necessary for its binding to VPS35A in the Arabidopsis retromer/retriever complex. This alignment also identifies conserved amino acids within VPS26C proteins across organisms. We can use this information to change specific amino acid residues through mutagenesis and then investigate the ability of mutant VPS26C orthologs to complement the *vps26c* root hair phenotype is lost. In summary, identification of conserved sequences within VPS26C orthologs will be helpful in building models to delineate their functional similarities and differences and define how these properties may have evolved.

VPS26C function in a shared pathway with the SNARE VTI13

One of the VTI SNARE family members, *VTI11*, traffics cargo to the lytic vacuole and is required for shoot gravitropism in Arabidopsis (REF). Genetic suppressor analysis has been shown the VTI11 trafficking pathway interacts with a pathway involving the core retromer subunits *VPS26A* and *VPS35A* (Hashiguchi et al., 2010). In this case, the shoot gravitropic phenotype of the *VTI11* mutant 'zig' is suppressed by the retromer *vps26a* and *vps35a* mutations. Another family member of the VTI-SNAREs, VTI13, localizes to early endosomes and the vacuole membrane and is essential for proper root hair growth and cell wall organization (Larson et al., 2014). Similar to the genetic interaction described above, we also see a suppression of the *vti13* root hair growth and cell wall organization phenotypes of *vti13* in a *vti13 vps26c* double mutant. In both instances, the suppression is very clear, but the mechanism of this suppression is not known yet.

I have identified a number of proteins in the VTI13-proteome that may help us generate hypotheses stating how a VTI13 pathway interacts with those pathways controlled by the VPS26C complex control root hair growth. Based on my proteomic data, questions that I would like to address are as follows:

1) **In what endosomal pathways do both VPS26C and VTI13 function?**

Analysis of the VTI13 proteome identified a number of proteins, including the dynamin-related proteins (DRPs) and clathrin heavy chain proteins (CHCs), that are involved in endocytosis and are localized in the tip of growing root hairs as well as to the site of cell plate formation. Of these, *DRP2A, DRP2B,* and *CHC1* are mis-expressed in the *vti13*

mutant. One possible explanation for the *vps26c* suppression of the *vti13* mutant phenotypes is that VTI13 is responsible for trafficking of the DRPs once they are endocytosed to the vacuole. This would explain the localization of VTI13 between early endosomes and vacuole membranes. To test this, co-localization experiments involving fluorescent fusion proteins of VTI13 and the DRPs can be performed. The localization pattern of the two proteins will confirm whether they are part of the same cellular compartment and further experiments can delineate whether they associate with VTI13 as part of endocytosis from the cell plate.

Dissection of the pathway that VTI13 functions in, and the cargo associated with the VTI13-endosomes, would lead us to understand the phenotypes that *vti13* exhibits. *DRP2A* and *DRP2B* mutants show defective root hair growth. This defect might be the result of aberrant endocytosis in the absence of the DRPs at the growing root tip. It will be worthwhile to understand whether DRPs also have defective cell wall organization. Surface labeling of root hairs with monoclonal antibodies (Larson et al., 2014) can be used to detect cell wall components on the cell surface.

Another pertinent question is where does VPS26C fit in to this pathway? We have genetic evidence suggesting that VPS26C has a shared pathway with VTI13, but further details regarding this pathway remain elusive. One way to approach this question would be to use an affinity purification-based proteomic analysis, using the GFP-VPS26C expressing line and determine if there are any common proteins between the VTI13- and VPS26C-dependent pathways that can be immunoprecipitated with both GFP-VTI13 and GFP-

VPS2C. So far, in the lab, I have not been able to detect the GFP-VPS26C fusion protein by a Western blot. This is surprising as I could detect the GFP-fusion both driven by the 35S and the VPS26C endogenous promoters in the root epidermal cells and root hairs using confocal microscopy. One possible reason for this is that GFP-VPS26C is being degraded in the extraction buffers that I use such that I am unable to detect this protein on western blots. Further steps towards optimizing the homogenization buffer as well as troubleshooting the tissue harvest procedure might be helpful to extract this protein from the cells.

2) **How is the suppression of phenotypes happening?**

Jha et al. (2018) and Hashiguchi et al. (2010) report a genetic interaction between a VTI SNARE member and a retromer subunit. In both cases, this involves suppression of the SNARE mutant phenotype by mutations in large retromer subunit genes. The question I have been asked several times when I presented my work is how do we explain the suppression that we observe? I do not have a clear answer for this yet. One possibility is that other family members are having a compensatory effect. For example, *VPS26A* is significantly upregulated in the *vps26c* mutant compared to wild type. So, in the *vti13 vps26c* double mutant, *VPS26A,* and one of the other VTI SNARE family members, *VTI11* or *VTI12* might be able to compensate for the pathways that VPS26C and VTI13 function in, to display a more normal root hair growth. This hypothesis is aligned to the multiple examples of compensatory roles that gene family members play in regulation of plant development. However, the fact that the single mutants still display quite severe phenotypes does not support a compensatory mechanism by other gene family members.

The current model describing the functioning of VTI13- and VPS26C- pathways, based on my work and what we know so far from the literature is shown in Figure 15. In this model we show that VTI13 is involved in trafficking between early endosomes and lytic vacuole, and that VPS26C is trafficking from endosomes to either the Golgi/TGN or to the plasma membrane. The common component of these two pathways, whether it is an interacting protein or a membrane compartment that both are part of, will require further investigation. The proteomic analysis described in chapter 3 of this dissertation will be helpful in identifying candidates that are functioning in these pathways and will be helpful in dissecting this question. If VTI13 is involved in trafficking of plasma membrane cargo between endosomes and the vacuole, the interaction of VTI13 and VPS26C endosomal trafficking pathways can possibly occur on the endosomes where the cargo not destined for the lytic vacuole but is recycled by the VPS26C-complex to the plasma membrane. This will predict a similar function to the VPS26C-retriever complex in humans where the latter recycles plasma membrane integrins. Common partners of these two pathways identified through proteomics will determine how these proteins are connected to each other.

I hypothesize that in a common endosomal pathway, one half of the pathway has VTI13 trafficking cargo from the early endosome to the vacuole, and the other half has VPS26C trafficking cargo from endosomes to the plasma membrane or Golgi. Loss of function of one of these partners exhibits a more severe phenotype than losing both. Therefore, the double mutant shows a more 'normal' root hair growth and cell wall organization. One question that has not been addressed is the level of similarity of cell wall organization in the double mutant when compared to wild type seedlings. An approach that can answer

this is a glycome profiling of cell walls (Patthathil et al., 2012) of wild type, single *vps26c* and *vti13* mutants, and *vti13 vps26c* to characterize the contents of the walls, beyond the surface organization that has previous been performed.

In summary, this dissertation characterizes a novel retromer complex and its function in controlling root hair growth, and also is a second report of a SNARE-retromer interaction to maintain a common developmental pathway important for cell wall organization in root epidermal cells of Arabidopsis seedlings. This work leads to further hypotheses about how these two pathways are delineated and how they the each coordinate the endosomal trafficking pathway that regulates polarized growth and cell wall organization in Arabidopsis.

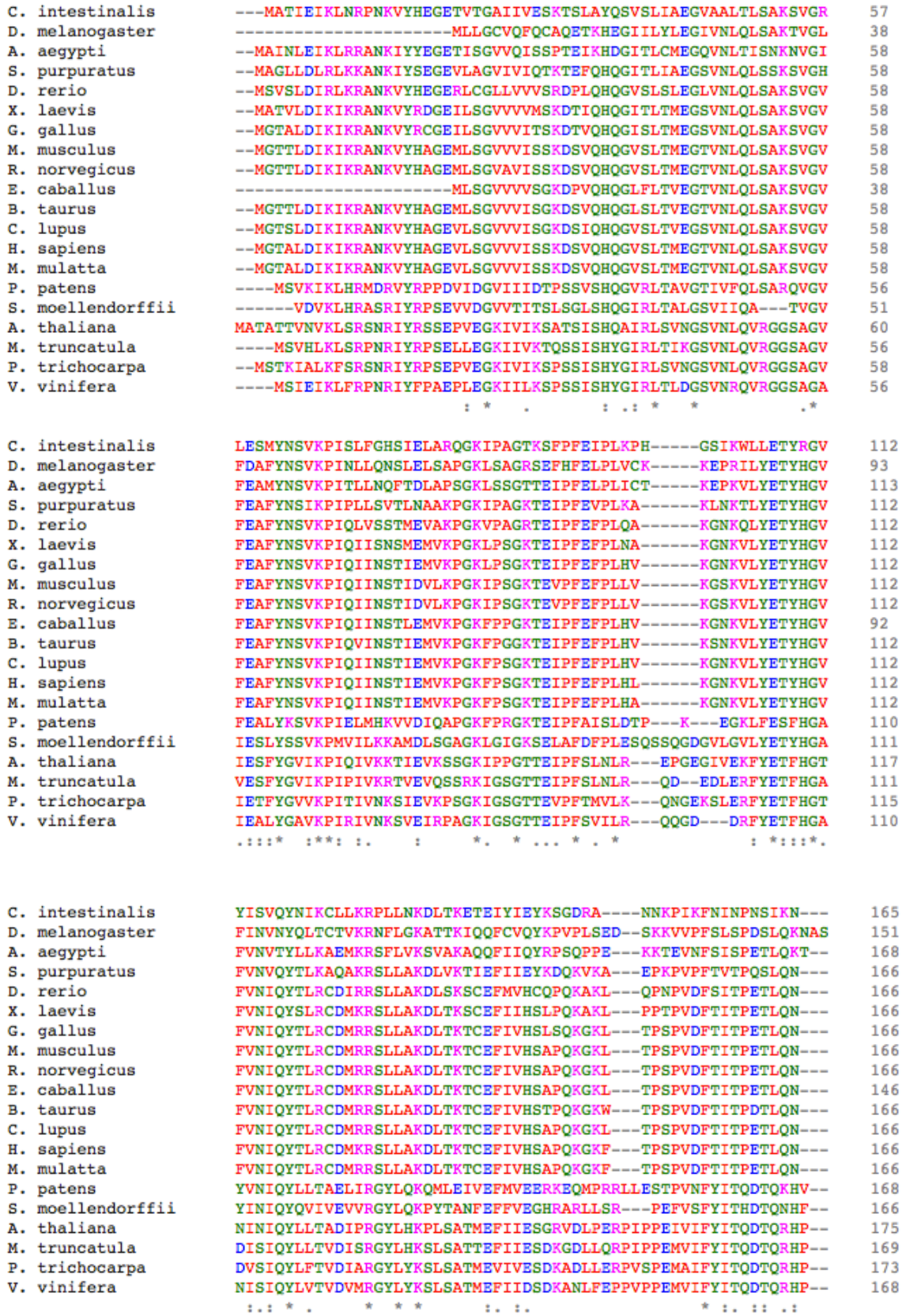
C. intestinalis ---MATIEIKLNRPNKVYHEGETVTGAIIVESKTSLAYQSVSLIAEGVAALTLSAKSVGR 57
D. melanogaster ----------MLLGCVQFQCAQETKHEGIILYLEGIVNLQLSAKTVGL 38
A. aegypti --MAINLEIKLRRANKIYYEGETISGVVQISSPTEIKHDGITLCMEGQVNLTISNKNVGI 58
S. purpuratus --MAGLLDLRLKKANKIYSEGEVLAGVIVIQTKTEFQHQGITLIAEGSVNLQLSSKSVGH 58
D. rerio --MSVSLDIRLKRANKVYHEGERLCGLLVVVSRDPLQHQGVSLSLEGLVNLQLSAKSVGV 58
X. laevis --MATVLDIKIKRANKVYRDGEILSGVVVVMSKDTIQHQGITLTMEGSVNLQLSAKSVGV 58
G. gallus --MGTALDIKIKRANKVYRCGEILSGVVVITSKDTVQHQGISLTMEGSVNLQLSAKSVGV 58
M. musculus --MGTTLDIKIKRANKVYHAGEMLSGVVVISSKDSVQHQGVSLTMEGTVNLQLSAKSVGV 58
R. norvegicus --MGTTLDIKIKRANKVYHAGEMLSGVAVISSKDSVQHQGVSLTMEGTVNLQLSAKSVGV 58
E. caballus ----------MLSGVVVVSGKDPVQHQGLFLTVEGTVNLQLSAKSVGV 38
B. taurus --MGTTLDIKIKRANKVYHAGEMLSGVVVISGKDSVQHQGLSLTVEGTVNLQLSAKSVGV 58
C. lupus --MGTSLDIKIKRANKVYHAGEVLSGVVVISGKDSIQHQGVSLTVEGSVNLQLSAKSVGV 58
H. sapiens --MGTALDIKIKRANKVYHAGEVLSGVVVISSKDSVQHQGVSLTMEGTVNLQLSAKSVGV 58
M. mulatta --MGTALDIKIKRANKVYHAGEVLSGVVVISSKDSVQHQGVSLTMEGTVNLQLSAKSVGV 58
P. patens ----MSVKIKLHRMDRVYRPPDVIDGVIIIDTPSSVSHQGVRLTAVGTIVFQLSARQVGV 56
S. moellendorffii ------VDVKLHRASRIYRPSEVVDGVVTITSLSGLSHQGIRLTALGSVIIQA---TVGV 51
A. thaliana MATATTVNVKLSRSNRIYRSSEPVEGKIVIKSATSISHQAIRLSVNGSVNLQVRGGSAGV 60
M. truncatula ----MSVHLKLSRPNRIYRPSELLEGKIIVKTQSSISHYGIRLTIKGSVNLQVRGGSAGV 56
P. trichocarpa --MSTKIALKFSRSNRIYRPSEPVEGKIVIKSPSSISHYGIRLSVNGSVNLQVRGGSAGV 58
V. vinifera ----MSIEIKLFRPNRIYFPAEPLEGKIILKSPSSISHYGIRLTLDGSVNRQVRGGSAGA 56
LESMYNSVKPISLFGHSIELARQGKIPAGTKSFPFEIPLKPH-----GSIKWLLETYRGV 112
FDAFYNSVKPINLLQNSLELSAPGKLSAGRSEFHFELPLVCK-----KEPRILYETYHGV 93
FEAMYNSVKPITLLNQFTDLAPSGKLSSGTTEIPFELPLICT-----KEPKVLYETYHGV 113
FEAFYNSIKPIPLLSVTLNAAKPGKIPAGKTEIPFEVPLKA------KLNKTLYETYHGV 112
FEAFYNSVKPIQLVSSTMEVAKPGKVPAGRTEIPFEFPLQA------KGNKQLYETYHGV 112
FEAFYNSVKPIQIISNSMEMVKPGKLPSGKTEIPFEFPLNA------KGNKVLYETYHGV 112
FEAFYNSVKPIQIINSTIEMVKPGKLPSGKTEIPFEFPLHV------KGNKVLYETYHGV 112
FEAFYNSVKPIQIINSTIDVLKPGKIPSGKTEVPFEFPLLV------KGSKVLYETYHGV 112
FEAFYNSVKPIQIINSTIDVLKPGKIPSGKTEVPFEFPLLV------KGSKVLYETYHGV 112
FEAFYNSVKPIQIINSTLEMVKPGKFPPGKTEIPFEFPLHV------KGNKVLYETYHGV 92
FEAFYNSVKPIQVINSTIEMVKPGKFPGGKTEIPFEFPLHV------KSNKVLYETYHGV 112
FEAFYNSVKPIQIINSTIEMVKPGKFPSGKTEIPFEFPLHV------KGNKVLYETYHGV 112
FEAFYNSVKPIQIINSTIEMVKPGKFPSGKTEIPFEFPLHL------KGNKVLYETYHGV 112
FEAFYNSVKPIQIINSTIEMVKPGKFPSGKTEIPFEFPLHA------KGNKVLYETYHGV 112
FEALYKSVKPIELMHKVVDIQAPGKFPRGKTEIPFAISLDTP---K---EGKLFESFHGA 110
IESLYSSVKPMVILKKAMDLSGAGKLGIGKSELAFDFPLESQSSQGDGVLGVLYETYHGA 111
IESFYGVIKPIQIVKKTIEVKSSGKIPPGTTEIPFSLNLR---EPGEGIVEKFYETFHGT 117
VESFYGVIKPIPIVKRTVEVQSSRKIGSGTTEIPFSLNLR---QD--EDLERFYETFHGA 111
IETFYGVVKPITIVNKSIEVKPSGKIGSGTTEVPFTMVLK---QNGEKSLERFYETFHGT 115
IEALYGAVKPIRIVNKSVEIRPAGKIGSGTTEIPFSVILR---QQGD---DRFYETFHGA 110
YISVQYNIKCLLKRPLLNKDLTKETEIYIEYKSGDRA----NNKPIKFNINPNSIKN--- 165
FINVNYQLTCTVKRNFLGKATTKIQQFCVQYKPVPLSED--SKKVVPFSLSPDSLQKNAS 151
FVNVTYLLKAEMKRSFLVKSVAKAQQFIIQYRPSQPPE---KKTEVNFSISPETLQKT-- 168
FVNVQYTLKAQAKRSLLAKDLVKTIEFIIEYKDQKVKA---EPKPVPFTVTPQSLQN--- 166
FVNIQYTLRCDIRRSLLAKDLSKSCEFMVHCQPQKAKL---QPNPVDFSITPETLQN--- 166
FVNIQYSLRCDMKRSLLAKDLTKSCEFIIHSLPQKAKL---PPTPVDFTITPETLQN--- 166
FVNIQYTLRCDMRRSLLAKDLTKTCEFIVHSLSQKGKL---TPSPVDFTITPETLQN--- 166
FVNIQYTLRCDMRRSLLAKDLTKTCEFIVHSAPQKGKL---TPSPVDFTITPETLQN--- 166
FVNIQYTLRCDMRRSLLAKDLTKTCEFIVHSAPQKGKL---TPSPVDFTITPETLQN--- 166
FVNIQYTLRCDMKRSLLAKDLTKTCEFIVHSAPQKGKL---TPSPVDFTITPETLQN--- 146
FVNIQYTLRCDMRRSLLAKDLTKTCEFIVHSTPQKGKW---TPSPVDFTITPDTLQN--- 166
FVNIQYTLRCDMRRSLLAKDLTKTCEFIVHSAPQKGKL---TPSPVDFTITPETLQN--- 166
FVNIQYTLRCDMKRSLLAKDLTKTCEFIVHSAPQKGKF---TPSPVDFTITPETLQN--- 166
FVNIQYTLRCDMRRSLLAKDLTKTCEFIVHSAPQKGKF---TPSPVDFTITPETLQN--- 166
YVNIQYLLTAELIRGYLQKQMLEIVEFMVEERKEQMPRRLLESTPVNFYITQDTQKHV-- 168
YINIQYQVIVEVVRGYLQKPYTANFEFFVEGHRARLLSR---PEFVSFYITHDTQNHF-- 166
NINIQYLLTADIPRGYLHKPLSATMEFIIESGRVDLPERPIPPEIVIFYITQDTQRHP-- 175
DISIQYLLTVDISRGYLHKSLSATTEFIIESDKGDLLQRPIPPEMVIFYITQDTQRHP-- 169
DVSIQYLFTVDIARGYLYKSLSATMEVIVESDKADLLERPVSPEMAIFYITQDTQRHP-- 173
NISIQYLVTVDVMRGYLYKSLSATMEFIIDSDKANLFEPPVPPEMVIFYITQDTQRHP-- 168

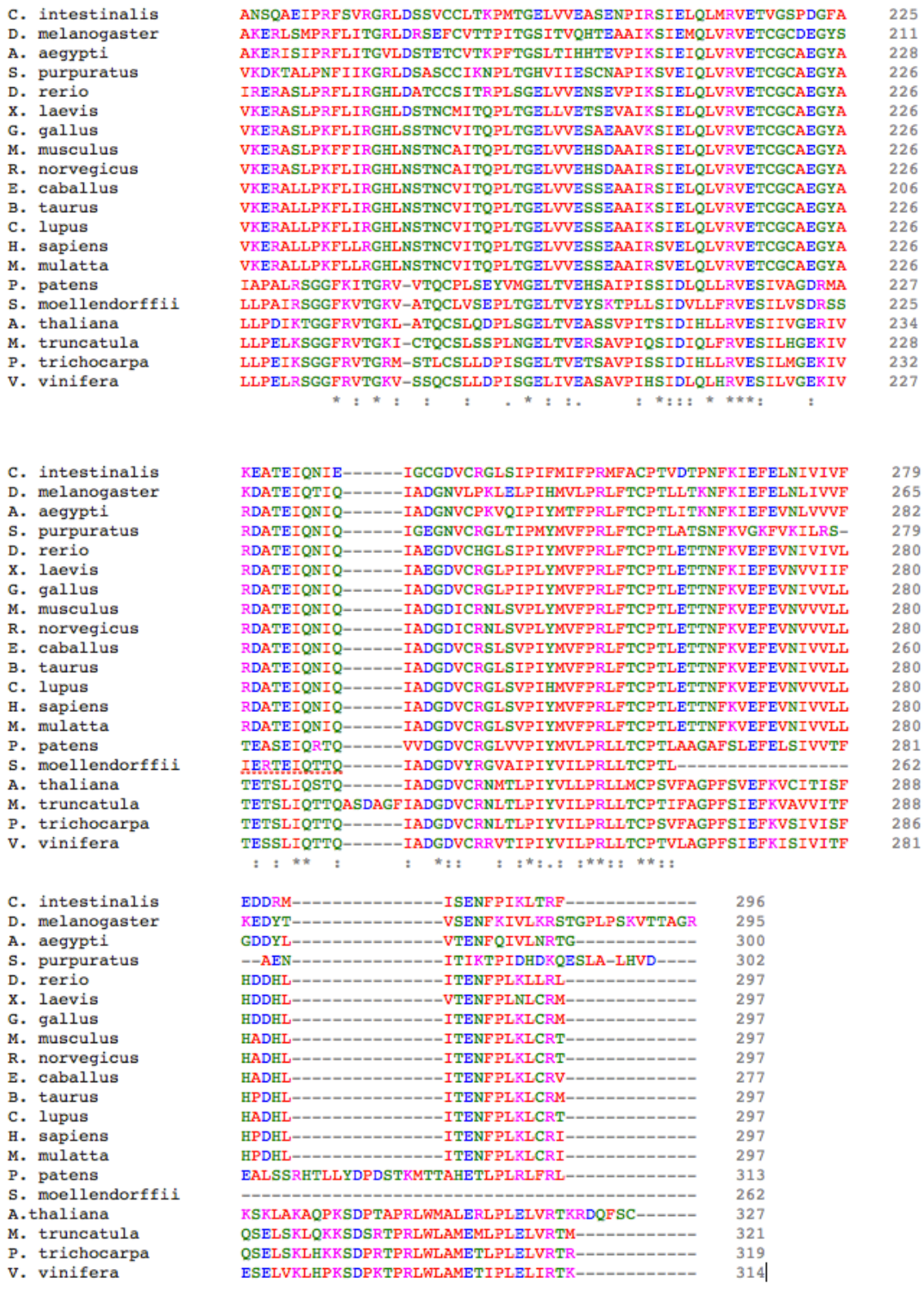

Figure 14: Alignment of VPS26C amino acid sequences in plant and animal systems

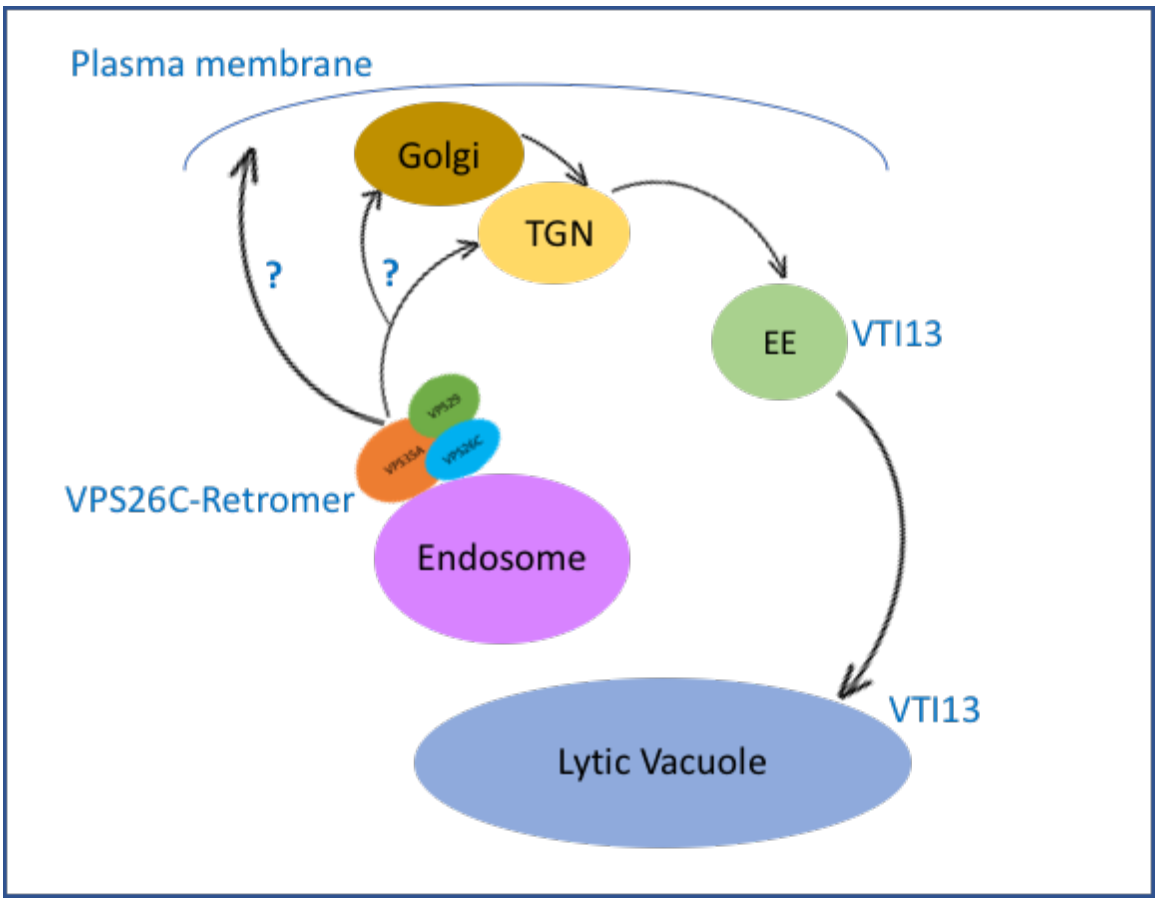

Figure 15: Current model representing VTI13 and VPS26C dependent endosomal trafficking pathways

REFERENCES

Augustine, R. C., Vidali, L., Kleinman, K. P., and Bezanilla, M. (2008) Actin depolymerizing factor is essential for viability in plants, and its phosphoregulation is important for tip growth. *The Plant Journal: For Cell and Molecular Biology*, ***54*(5),** 863–875.

Bedinger, P. A., Hardeman, K. J., and Loukides, C. A. (1994) Travelling in style: the cell biology of pollen. *Trends in Cell Biology*, ***4*(4),** 132–138.

Bibikova, T. N., Blancaflor, E. B., and Gilroy, S. (1999) Microtubules regulate tip growth and orientation in root hairs of *Arabidopsis thaliana*. *The Plant Journal: For Cell and Molecular Biology*, ***17*(6),** 657–665.

Braun, M., and Limbach, C. (2006) Rhizoids and protonemata of characean algae: model cells for research on polarized growth and plant gravity sensing. *Protoplasma*, ***229*,** 133–142.

Deeks, M. J., Kaloriti, D., Davies, B., Malhó, R., and Hussey, P. J. (2004) Arabidopsis NAP1 is essential for Arp2/3-dependent trichome morphogenesis. *Current Biology,* ***14*(15),** 1410–1414.

Dolan, L. (2001) How and where to build a root hair. *Current Opinion in Plant Biology*, ***4*(6),** 550–554.

Eklund, D. M., Svensson, E. M., and Kost, B. (2010) Physcomitrella patens: a model to investigate the role of RAC/ROP GTPase signaling in tip growth. *Journal of Experimental Botany*, ***61*(7),** 1917–1937.

Frank, M., Egile, C., Dyachok, J., Djakovic, S., Nolasco, M., Li, R., and Smith, L. G. (2004) Activation of Arp2/3 complex-dependent actin polymerization by plant proteins distantly related to Scar/WAVE. *Proceedings of the National Academy of Sciences of the United States of America*, ***101*(46),** 16379–16384.

Hepler, P. K., Vidali, L., and Cheung, A. Y. (2001) Polarized cell growth in higher plants. *Annual Review of Cell and Developmental Biology*, ***17*,** 159–187.

Ichikawa, M., Hirano, T., Enami, K., Fuselier, T., Kato, N., Kwon, C., and Sato, M. H. (2014) Syntaxin of plant proteins SYP123 and SYP132 mediate root hair tip growth in Arabidopsis thaliana. *Plant & Cell Physiology*, ***55*(4),** 790–800.

Isner, J.-C., Xu, Z., Costa, J. M., Monnet, F., Batstone, T., Ou, X., and Hetherington, A. M. (2017) Actin filament reorganisation controlled by the SCAR/WAVE complex mediates stomatal response to darkness. *The New Phytologist*, ***215*(3),** 1059–1067.

Jones, V. A. S., and Dolan, L. (2012) The evolution of root hairs and rhizoids. *Annals of*

Botany, ***110*****(2),** 205–212.

Ketelaar, T. (2013) The actin cytoskeleton in root hairs: all is fine at the tip. *Current Opinion in Plant Biology*, ***16*****(6),** 749–756.

Krichevsky, A., Kozlovsky, S. V., Tian, G.-W., Chen, M.-H., Zaltsman, A., and Citovsky, V. (2007) How pollen tubes grow. *Developmental Biology*, ***303*****(2),** 405–420.

Larson, E. R., Domozych, D. S., and Tierney, M. L. (2014) SNARE VTI13 plays a unique role in endosomal trafficking pathways associated with the vacuole and is essential for cell wall organization and root hair growth in arabidopsis. *Annals of Botany*, ***114*****(6),** 1147–1159.

Levina, N. N., Lew, R. R., and Heath, I. B. (1994) Cytoskeletal regulation of ion channel distribution in the tip-growing organism Saprolegnia ferax. *Journal of Cell Science*, 127–134.

Mangano, S., Juárez, S. P. D., and Estevez, J. M. (2016) ROS Regulation of Polar Growth in Plant Cells. *Plant Physiology*, ***171*****(3),** 1593–1605.

Mendrinna, A., and Persson, S. (2015) Root hair growth: it's a one-way street. *F1000prime Reports*, ***7*****,** 23-27.

Park, S., Szumlanski, A. L., Gu, F., Guo, F., and Nielsen, E. (2011) A role for CSLD3 during cell-wall synthesis in apical plasma membranes of tip-growing root-hair cells. *Nature Cell Biology*, ***13*****(8),** 973–980.

Pattathil, S., Avci, U., Miller, J. S., and Hahn, M. G. (2012) Immunological approaches to plant cell wall and biomass characterization: Glycome Profiling. *Methods in Molecular Biology*, ***908***, 61–72.

Pourcher, M., Santambrogio, M., Thazar, N., Thierry, A.-M., Fobis-Loisy, I., Miège, C., and Gaude, T. (2010) Analyses of sorting nexins reveal distinct retromer-subcomplex functions in development and protein sorting in Arabidopsis thaliana. *The Plant Cell*, ***22*****(12),** 3980–3991.

Rensing, S. A. (2016) Plant Evo-Devo: How Tip Growth Evolved. *Current Biology,* ***26*****(23),** R1228–R1230.

Richter, S., Müller, L. M., Stierhof, Y.-D., Mayer, U., Takada, N., Kost, B., and Jürgens, G. (2011) Polarized cell growth in Arabidopsis requires endosomal recycling mediated by GBF1-related ARF exchange factors. *Nature Cell Biology*, ***14*****(1),** 80–86.

Seaman, M. N. J., Gautreau, A., and Billadeau, D. D. (2013) Retromer-mediated endosomal protein sorting: all WASHed up! *Trends in Cell Biology*, ***23*****(11),** 522–528.

Velasquez, S. M., Ricardi, M. M., Dorosz, J. G., Fernandez, P. V., Nadra, A. D., Pol-Fachin, L., and Estevez, J. M. (2011) O-glycosylated cell wall proteins are essential in root hair growth. *Science, **332*(6036),** 1401–1403.

Vidali, L., Augustine, R. C., Kleinman, K. P., and Bezanilla, M. (2007) Profilin is essential for tip growth in the moss Physcomitrella patens. *The Plant Cell*, ***19*(11),** 3705–3722.

Wang, J., Fedoseienko, A., Chen, B., Burstein, E., Jia, D., and Billadeau, D. D. (2018) Endosomal receptor trafficking: Retromer and beyond. *Traffic*.

Wang, P., Richardson, C., Hawes, C., and Hussey, P. J. (2016) Arabidopsis NAP1 Regulates the Formation of Autophagosomes. *Current Biology, **26*(15),** 2060–2069.

Yanagisawa, M., Zhang, C., and Szymanski, D. B. (2013) ARP2/3-dependent growth in the plant kingdom: SCARs for life. *Frontiers in Plant Science*, ***4*,** 166.

Yao, H.-Y., and Xue, H.-W. (2011) Signals and mechanisms affecting vesicular trafficking during root growth. *Current Opinion in Plant Biology*, ***14*(5),** 571–579.

Zhang, C., Mallery, E. L., Schlueter, J., Huang, S., Fan, Y., Brankle, S., and Szymanski, D. B. (2008) Arabidopsis SCARs function interchangeably to meet actin-related protein 2/3 activation thresholds during morphogenesis. *The Plant Cell*, ***20*(4),** 995–1011.

COMPLETE BIBLIOGRAPHY

Appel, J. R., Ye, S., Tang, F., Sun, D., Zhang, H., Mei, L., and Xiong, W.-C. (2018) Increased Microglial Activity, Impaired Adult Hippocampal Neurogenesis, and Depressive-like Behavior in Microglial VPS35-Depleted Mice. *The Journal of Neuroscience: The Official Journal of the Society for Neuroscience*, ***38*(26),** 5949–5968.

Augustine, R. C., Vidali, L., Kleinman, K. P., and Bezanilla, M. (2008) Actin depolymerizing factor is essential for viability in plants, and its phosphoregulation is important for tip growth. *The Plant Journal: For Cell and Molecular Biology*, ***54*(5),** 863–875.

Backues, S. K., Korasick, D. A., Heese, A., and Bednarek, S. Y. (2010) The Arabidopsis dynamin-related protein2 family is essential for gametophyte development. *The Plant Cell*, ***22*(10),** 3218–3231.

Bai, Z., and Grant, B. D. (2015) A TOCA/CDC-42/PAR/WAVE functional module required for retrograde endocytic recycling. *Proceedings of the National Academy of Sciences of the United States of America*, ***112*(12),** E1443-1452.

Bedinger, P. A., Hardeman, K. J., and Loukides, C. A. (1994) Travelling in style: the cell biology of pollen. *Trends in Cell Biology*, ***4*(4),** 132–138.

Bercusson, A., de Boer, L., and Armstrong-James, D. (2017) Endosomal sensing of fungi: current understanding and emerging concepts. *Medical Mycology*, ***55*(1),** 10–15.

Bibikova, T. N., Blancaflor, E. B., and Gilroy, S. (1999) Microtubules regulate tip growth and orientation in root hairs of *Arabidopsis thaliana*. *The Plant Journal: For Cell and Molecular Biology*, ***17*(6),** 657–665.

Bonifacino, J. S., and Hurley, J. H. (2008) Retromer. *Current Opinion in Cell Biology*, ***20*(4),** 427–436.

Braschi, E., Goyon, V., Zunino, R., Mohanty, A., Xu, L., and McBride, H. M. (2010) Vps35 mediates vesicle transport between the mitochondria and peroxisomes. *Current Biology,* ***20*(14),** 1310–1315.

Braun, M., and Limbach, C. (2006) Rhizoids and protonemata of characean algae: model cells for research on polarized growth and plant gravity sensing. *Protoplasma*, ***229*,** 133–142.

Bugarcic, A., Zhe, Y., Kerr, M. C., Griffin, J., Collins, B. M., and Teasdale, R. D. (2011) Vps26A and Vps26B Subunits Define Distinct Retromer Complexes. *Traffic*, ***12*(12),** 1759–1773.

Burd, C. G. (2011) Physiology and pathology of endosome-to-Golgi retrograde sorting. *Traffic,* ***12*****(8),** 948–955.

Burda, P., Padilla, S. M., Sarkar, S., and Emr, S. D. (2002) Retromer function in endosome-to-Golgi retrograde transport is regulated by the yeast Vps34 PtdIns 3-kinase. *Journal of Cell Science*, ***115*****(20),** 3889–3900.

Chen, D., Xiao, H., Zhang, K., Wang, B., Gao, Z., Jian, Y., andYang, C. (2010) Retromer is required for apoptotic cell clearance by phagocytic receptor recycling. *Science*, ***327*****(5970),** 1261–1264.

Clough, S.J. and Bent, A.F. (1998) Floral dip: a simplified method for Agrobacterium-mediated transformation of *Arabidopsis thaliana*. *Plant J.* **16**, 735–743.

Collins, B.M. (2008) The structure and function of the retromer protein complex. *Traffic*, **9**, 1811-1822

Collings, D. A., Gebbie, L. K., Howles, P. A., Hurley, U. A., Birch, R. J., Cork, A. H., and Williamson, R. E. (2008) Arabidopsis dynamin-like protein DRP1A: a null mutant with widespread defects in endocytosis, cellulose synthesis, cytokinesis, and cell expansion. *Journal of Experimental Botany*, ***59*****(2),** 361–376.

Deeks, M. J., Kaloriti, D., Davies, B., Malhó, R., and Hussey, P. J. (2004) Arabidopsis NAP1 is essential for Arp2/3-dependent trichome morphogenesis. *Current Biology,* ***14*****(15),** 1410–1414.

Dolan, L. (2001) How and where to build a root hair. *Current Opinion in Plant Biology*, ***4*****(6),** 550–554.

Ebine, K., and Ueda, T. (2015) Roles of membrane trafficking in plant cell wall dynamics. *Frontiers in Plant Science*, ***6***.

Edgar, A.J. and Polak, J.M. (2000) Human homologues of yeast vacuolar protein sorting 29 and 35. *Biochem. Biophys. Res. Comm.* **277**, 622–630.

Eklund, D. M., Svensson, E. M., and Kost, B. (2010) Physcomitrella patens: a model to investigate the role of RAC/ROP GTPase signaling in tip growth. *Journal of Experimental Botany*, ***61*****(7),** 1917–1937.

Esch, L., and Schaffrath, U. (2017) An Update on Jacalin-Like Lectins and Their Role in Plant Defense. *International Journal of Molecular Sciences*, ***18*****(7).**

Frank, M., Egile, C., Dyachok, J., Djakovic, S., Nolasco, M., Li, R., and Smith, L. G. (2004) Activation of Arp2/3 complex-dependent actin polymerization by plant proteins distantly related to Scar/WAVE. *Proceedings of the National Academy of Sciences of the United States of America*, ***101*****(46),** 16379–16384.

Früholz, S. and Pimpl, P. (2017) Analysis of Nanobody-Epitope Interactions in Living Cells via Quantitative Protein Transport Assays. *Methods Mol. Biol.* **1662**,171-182.

Fujimoto, M., Arimura, S., Nakazono, M., and Tsutsumi, N. (2008) Arabidopsis dynamin-related protein DRP2B is co-localized with DRP1A on the leading edge of the forming cell plate. *Plant Cell Reports*, ***27*(10),** 1581–1586.

Gallon, M., Clairfeuille, T., Steinberg, F., Mas, C., Ghai, R., Sessions, R. B., and Cullen, P. J. (2014). A unique PDZ domain and arrestin-like fold interaction reveals mechanistic details of endocytic recycling by SNX27-retromer. *Proceedings of the National Academy of Sciences of the United States of America*, ***111*(35),** E3604-3613.

Gallon, M. and Cullen, P.J. (2015) Retromer and sorting nexins in endosomal sorting. *Biochem. Soc. Trans.* **43**, 33–47.

Gambardella, S., Biagioni, F., Ferese, R., Busceti, C. L., Frati, A., Novelli, G., Rugierri, S., and Fornai, F. (2016) Vacuolar Protein Sorting Genes in Parkinson's Disease: A Re-appraisal of Mutations Detection Rate and Neurobiology of Disease. *Frontiers in Neuroscience*. **10**, 532-542.

Geldner, N., Friml, J., Stierhof, Y.-D., Jürgens, G. and Palme, K. (2001) Auxin transport inhibitors block PIN1 cycling and vesicle trafficking. *Nature*, **413**, 425-428.

Geldner, N. (2004) The plant endosomal system--its structure and role in signal transduction and plant development. *Planta*, ***219*(4),** 547–560.

Haft, C.R., de la Luz Sierra, M., Bafford, R., Lesniak, M.A., Barr, V.A. and Taylor, S.I. (2000) Human orthologs of yeast vacuolar protein sorting proteins Vps26, 29, and 35: assembly into multimeric complexes. *Mol. Biol. Cell*, **11**, 4105–4116.

Halperin, S.J., Gilroy, S. and Lynch, J.P. (2003) Sodium chloride reduces growth and cytosolic calcium, but does not affect cytosolic pH, in root hairs of *Arabidopsis thaliana* L. *J. Exp. Bot.* **54**, 1269–1280.

Hara-Nishimura, I., and Matsushima, R. (2003) A wound-inducible organelle derived from endoplasmic reticulum: a plant strategy against environmental stresses? *Current Opinion in Plant Biology*, ***6*(6),** 583–588.

Harbour, M. E., and Seaman, M. N. J. (2011) Evolutionary variations of VPS29, and their implications for the heteropentameric model of retromer. *Communicative & Integrative Biology*, ***4*(5),** 619–622.

Harterink, M., Port, F., Lorenowicz, M. J., McGough, I. J., Silhankova, M., Betist, M. C., and Korswagen, H. C. (2011) A SNX3-dependent retromer pathway mediates retrograde transport of the Wnt sorting receptor Wntless and is required for Wnt secretion. *Nature*

Cell Biology, ***13*****(8),** 914–923.

Hashiguchi, Y., Niihama, M., Takahashi, T., Saito, C., Nakano, A., Tasaka, M. and Morita, M.T. (2010) Loss-of-function mutations of retromer large subunit genes suppress the phenotype of an Arabidopsis *zig* mutant that lacks Qb-SNARE VTI11. *Plant Cell,* **22**, 159–172.

Heard, W., Sklenář, J., Tomé, D.F., Robatzek, S. and Jones, A.M. (2015) Identification of Regulatory and Cargo Proteins of Endosomal and Secretory Pathways in Arabidopsis thaliana by Proteomic Dissection. *Mol Cell Proteomics*, **14**, 1796-1813.

Hepler, P. K., Vidali, L., and Cheung, A. Y. (2001) Polarized cell growth in higher plants. *Annual Review of Cell and Developmental Biology*, ***17*****,** 159–187.

Hong, Z., Geisler-Lee, C. J., Zhang, Z., and Verma, D. P. S. (2003). Phragmoplastin dynamics: multiple forms, microtubule association and their roles in cell plate formation in plants. *Plant Molecular Biology*, ***53*****(3),** 297–312.

Huang, J., Fujimoto, M., Fujiwara, M., Fukao, Y., Arimura, S.-I., and Tsutsumi, N. (2015) Arabidopsis dynamin-related proteins, DRP2A and DRP2B, function coordinately in post-Golgi trafficking. *Biochemical and Biophysical Research Communications*, ***456*****(1),** 238–244.

Horazdovsky, B.F., Davies, B.A., Seaman, M.N., McLaughlin, S.A., Yoon, S. and Emr, S.D. (1997) A sorting nexin-1 homologue, Vps5p, forms a complex with Vps17p and is required for recycling the vacuolar protein-sorting receptor. *Mol. Biol. Cell*, **8**, 1529–1541.

Ichikawa, M., Hirano, T., Enami, K., Fuselier, T., Kato, N., Kwon, C., and Sato, M. H. (2014) Syntaxin of plant proteins SYP123 and SYP132 mediate root hair tip growth in Arabidopsis thaliana. *Plant & Cell Physiology*, ***55*****(4),** 790–800.

Isner, J.-C., Xu, Z., Costa, J. M., Monnet, F., Batstone, T., Ou, X., and Hetherington, A. M. (2017) Actin filament reorganisation controlled by the SCAR/WAVE complex mediates stomatal response to darkness. *The New Phytologist*, ***215*****(3),** 1059–1067.

Ivanov, R., Brumbarova, T., Blum, A., Jantke, A.-M., Fink-Straube, C., and Bauer, P. (2014) SORTING NEXIN1 is required for modulating the trafficking and stability of the Arabidopsis IRON-REGULATED TRANSPORTER1. *The Plant Cell*, ***26*****(3),** 1294–1307.

Jaillais, Y., Fobis-Loisy, I., Miege, C., Rollin, C. and Gaude, T. (2006) AtSNX1 defines an endosome for auxin-carrier trafficking in Arabidopsis. *Nature*, **443**, 106–109.

Jaillais, Y., Santambrogio, M., Rozier, F., Fobis-Loisy, I., Miège, C. and Gaude, T. (2007) The retromer protein VPS29 links cell polarity and organ initiation in plants. *Cell,* **130**, 1057–1070.

Jaillais, Y., Fobis-Loisy, I., Miège, C. and Gaude, T. (2008) Evidence for a sorting endosome in Arabidopsis root cells. *Plant J.* **53**, 237-47.

Jha, S.G., Larson, E.R., Humble, J., Domozych, D. S., Barrington, D.S., and Tierney, M.L. (2018) Vacuolar Protein Sorting 26C encodes an evolutionarily conserved large retromer subunit in eukaryotes that is important for root hair growth in Arabidopsis thaliana. *Plant J,* **94 (4)**, 595-611

Jones, V. A. S., and Dolan, L. (2012) The evolution of root hairs and rhizoids. *Annals of Botany*, ***110*****(2),** 205–212.

Kang, H., Kim, S.Y., Song, K., Sohn, E.J., Lee, Y., Lee, D.W., Hara-Nishimura, I. and Hwang, I. (2012) Trafficking of vacuolar proteins: the crucial role of Arabidopsis vacuolar protein sorting 29 in recycling vacuolar sorting receptor. *Plant Cell*, **24**, 5058–5073.

Kearse, M., Moir, R., Wilson, A., Stones-Havas, S., Cheung, M., Sturrock, S., Buxton, S., Cooper, A., Markowitz, S., Duran, C., Thierer, T., Ashton, B., Mentjies, P. and Drummond, A. (2012) Geneious Basic: an integrated and extendable desktop software platform for the organization and analysis of sequence data. *Bioinformatics,* **28**, 1647–1649. https://www.geneious.com

Ketelaar, T. (2013) The actin cytoskeleton in root hairs: all is fine at the tip. *Current Opinion in Plant Biology*, ***16*****(6),** 749–756.

Kerr, M.C., Bennetts, J.S., Simpson, F., Thomas, E.C., Flegg, C., Gleeson, P.A., Wicking, C. and Teasdale, R.D. (2005) A novel mammalian retromer component, Vps26B. *Traffic*, **6**, 991–1001.

Kim, E., Lee, Y., Lee, H.J., Kim, J.S., Song, B.S., Huh, J.W., Lee, S.R., Kim, S.U., Kim, S.H., Hong, Y., Shim, I. and Chang, K.T. (2010) Implication of mouse Vps26b-Vps29-Vps35 retromer complex in sortilin trafficking. *Biochem. Biophys. Res. Comm.* **403**, 167–171.

Krichevsky, A., Kozlovsky, S. V., Tian, G.-W., Chen, M.-H., Zaltsman, A., and Citovsky, V. (2007) How pollen tubes grow. *Developmental Biology*, ***303*****(2),** 405–420.

Kleine-Vehn, J., Dhonukshe, P., Sauer, M., Brewer, P.B., Wiśniewska. J., Paciorek, T., Benková, E. and Friml, J. (2008a) ARF GEF-dependent transcytosis and polar delivery of PIN auxin carriers in Arabidopsis. *Curr. Biol.* **8**, 526-31.

Kleine-Vehn, J., Langowski, L., Wisniewska, J., Dhonukshe, P., Brewer, P.B. and Friml, J. (2008b) Cellular and molecular requirements for polar PIN targeting and transcytosis in plants. *Mol. Plant*, **1**, 1056-66.

Konopka, C. A., and Bednarek, S. Y. (2008) Comparison of the dynamics and functional redundancy of the Arabidopsis dynamin-related isoforms DRP1A and DRP1C during plant development. *Plant Physiology*, ***147*****(4),** 1590–1602.

Koumandou, V.L., Klute, M.J., Herman, E.K., Nunez-Miguel, R., Dacks, J.B. and Field, M.C. (2011) Evolutionary reconstruction of the retromer complex and its function in *Trypanosoma brucei*. *J. Cell Sci*. **124**, 1496–1509.

Künzl, F., Früholz, S., Fäßler, F., Li, B. and Pimpl, P. (2016) Receptor-mediated sorting of soluble vacuolar proteins ends at the trans-Golgi network/early endosome. *Nature Plants* **2,** 16017.

Kvainickas, A., Jimenez-Orgaz, A., Nägele, H., Hu, Z., Dengjel, J. and Steinberg, F. 2017 Cargo-selective SNX-BAR proteins mediate retromer trimer independent retrograde transport. *J Cell Biol.* **216**, 3677-3693.

Larson, E.R., Domozych, D.S. and Tierney, M.L. (2014a) SNARE VTI13 plays a unique role in endosomal trafficking pathways associated with the vacuole and is essential for cell wall organization and root hair growth in arabidopsis. *Annals of Botany,* **114**, 1147–1159.

Larson, E.R., Tierney, M.L., Tinaz, B. and Domozych, D.S. (2014b) Using monoclonal antibodies to label living root hairs: a novel tool for studying cell wall microarchitecture and dynamics in Arabidopsis. *Plant Methods,* **10**, 30.

Larson, E. R., Zelm, E. V., Roux, C., Marion-Poll, A., and Blatt, M. R. (2017) Clathrin Heavy Chain Subunits Coordinate Endo- and Exocytic Traffic and Affect Stomatal Movement. *Plant Physiology*, ***175*(2),** 708–720.

Levina, N. N., Lew, R. R., and Heath, I. B. (1994) Cytoskeletal regulation of ion channel distribution in the tip-growing organism Saprolegnia ferax. *Journal of Cell Science*, 127–134.

Mangano, S., Juárez, S. P. D., and Estevez, J. M. (2016) ROS Regulation of Polar Growth in Plant Cells. *Plant Physiology*, ***171*(3),** 1593–1605.

Matsushima, R., Hayashi, Y., Yamada, K., Shimada, T., Nishimura, M., and Hara-Nishimura, I. (2003a) The ER body, a novel endoplasmic reticulum derived structure in Arabidopsis. *Plant Cell Physiology,* **44,** 661-666

Matshisuma, R., Kondo, M., Nishimura, M., and Hara-Nishimura, I. (2003b) A novel ER-derived compartment, the ER body, selectively accumulates beta-glucosidase with an ER retention signal in Arabidopsis. *Plant J.,* **33,** 493-502.

Mendrinna, A., and Persson, S. (2015) Root hair growth: it's a one-way street. *F1000prime Reports*, ***7*,** 23-27.

McNally, K. E., Faulkner, R., Steinberg, F., Gallon, M., Ghai, R., Pim, D., Langton, P., Pearson, N., Danson, C. M., Nagelle, H., Morris, L. L., Singla, A., Overlee, B. L., Heesom, K. J., Sessions, R., Banks, L., Collins, B. M., Berger, I., Billadeau, D. D., Burstein, E., and Cullen, P. J. (2017) Retriever is a Multiprotein Complex for Retromer- independent

Endosomal Cargo Recycling. *Nat. Cell Biol.* **19**, 1214-1225.

Miller, M.A., Pfeiffer, W. and Schwartz, T. (2010) Creating the CIPRES Science Gateway for inference of large phylogenetic trees. pp 1-8 in Proceedings of the Gateway Computing Environments Workshop (GCE), 14 Nov. 2010, New Orleans, LA.

Morita, M. T., Kato, T., Nagafusa, K., Saito, C., Ueda, T., Nakano, A., and Tasaka, M. (2002) Involvement of the Vacuoles of the Endodermis in the Early Process of Shoot Gravitropism in Arabidopsis. *The Plant Cell*. **14**, 47–56.

Morita, M. T., and Shimada, T. (2014) The Plant Endomembrane System—A Complex Network Supporting Plant Development and Physiology. *Plant and Cell Physiology*, ***55*(4),** 667–671.

Mravec, J., Petrášek, J., Li, N., Boeren, S., Karlova, R., Kitakura, S., and Friml, J. (2011) Cell plate restricted association of DRP1A and PIN proteins is required for cell polarity establishment in Arabidopsis. *Current Biology* ***21*(12),** 1055–1060.

Mukadam Aamir S., and Seaman Matthew N.J. (2015) Retromer-mediated endosomal protein sorting: The role of unstructured domains. *FEBS Letters*, ***589*,** 2620–2626.

Munch, D., Teh, O.-K., Malinovsky, F.G., Liu, Q., Vetukuri, R.R., El Kasmi, F., Brodersen, P., Hara-Nishimura, I., Dangl, J.L., Petersen, M., Mundy, J. and Hofius, D. (2015) Retromer contributes to immunity-associated cell death in Arabidopsis. *Plant Cell,* **27**, 463–479.

Murashige, T. and Skoog, F. (1962) A revised medium for rapid growth and bio assays with tobacco tissue cultures. *Physiol. Plant.* **15**, 473-497.

Nagano, A.J., Fukao, Y., Fujiwara, M., Nishimura, M., and Hara-Nishimura, I. (2008) Antagonistic jacalin-related lectins regulate the size of ER body-type beta-glucosidase complexes in Arabidopsis thaliana. *Plant Cell Physiol.* **49,** 969-980

Nakano, R. T., Yamada, K., Bednarek, P., Nishimura, M., and Hara-Nishimura, I. (2014) ER bodies in plants of the Brassicales order: biogenesis and association with innate immunity. *Frontiers in Plant Science*, ***5*.**

Niemes, S., Langhans, M., Viotti, C., Scheuring, D., San Wan Yan, M., Jiang, L., Hillmer, S., Robinson, D.G. and Pimpl, P. (2010) Retromer recycles vacuolar sorting receptors from the trans-Golgi network. *Plant J.* **61**, 107-121.

Niihama, M., Uemura, T., Saito, C., Nakano, A., Sato, M. H., Tasaka, M., and Morita, M. T. (2005) Conversion of Functional Specificity in Qb-SNARE VTI1 Homologues of Arabidopsis. *Current Biology*. **15**, 555–560.

Nodzyński, T., Feraru, M.I., Hirsch, S., De Rycke, R., Niculaes, C., Boerjan, W., Van Leene, J., De Jaeger, G., Vanneste, S. and Friml, J. (2013) Retromer Subunits VPS35A and

VPS29 Mediate Prevacuolar Compartment (PVC) Function in Arabidopsis. *Mol. Plant*, **6**, 1849–1862.

Nothwehr, S.F. and Hindes, A.E. (1997) The yeast VPS5/GRD2 gene encodes a sorting nexin-1-like protein required for localizing membrane proteins to the late Golgi. *J. Cell Sci.* **110**, 1063–1072.

Oliviusson, P., Heinzerling, O., Hillmer, S., Hinz, G., Tse, Y.C., Jiang, L. and Robinson, D.G. (2006) Plant retromer, localized to the prevacuolar compartment and microvesicles in Arabidopsis, may interact with vacuolar sorting receptors. *Plant Cell*, **18**, 1239-1252.

Ovecka, M., Lang, I., Baluska, F., Ismail, A., Illes, P. and Lichtscheidl, I.K. (2005) Endocytosis and vesicle trafficking during tip growth of root hairs. *Protoplasma*, **226**, 39–54.

Paravicini, G., Horazdovsky, B.F. and Emr, S.D. (1992) Alternative pathways for the sorting of soluble vacuolar proteins in yeast: a vps35 null mutant missorts and secretes only a subset of vacuolar hydrolases. *Mol. Biol. Cell*, **3**, 415–427.

Park, S., Szumlanski, A. L., Gu, F., Guo, F., and Nielsen, E. (2011) A role for CSLD3 during cell-wall synthesis in apical plasma membranes of tip-growing root-hair cells. *Nature Cell Biology*, ***13*(8),** 973–980.

Parsons, H. T., and Lilley, K. S. (2018) Mass spectrometry approaches to study plant endomembrane trafficking. *Seminars in Cell & Developmental Biology*, ***80*,** 123–132.
Pattathil, S., Avci, U., Miller, J. S., and Hahn, M. G. (2012) Immunological approaches to plant cell wall and biomass characterization: Glycome Profiling. *Methods in Molecular Biology*, ***908***, 61–72.

Peterman, T. K., Ohol, Y. M., McReynolds, L. J., and Luna, E. J. (2004) Patellin1, a Novel Sec14-Like Protein, Localizes to the Cell Plate and Binds Phosphoinositides. *Plant Physiology*, ***136*(2),** 3080–3094.

Peyroche, A., Antonny, B., Robineau, S., Acker, J., Cherfils, J. and Jackson, C. L. (1999) Brefeldin A Acts to Stabilize an Abortive ARF–GDP–Sec7 Domain Protein Complex: Involvement of Specific Residues of the Sec7 Domain. *Mol. Cell*, **3**, 275–285.

Pourcher, M., Santambrogio, M., Thazar, N., Thierry, A.M., Fobis-Loisy, I., Miège, C., Jaillais, Y. and Gaude, T. (2010) Analyses of sorting nexins reveal distinct retromer-subcomplex functions in development and protein sorting in Arabidopsis thaliana. *Plant Cell*, **22**, 3980–3991.

Preuss, M.L., Schmitz, A.J., Thole, J.M., Bonner, H.K., Otegui, M.S. and Nielsen, E. (2006) A role for the RabA4b effector protein PI-4Kβ1 in polarized expansion of root hair cells in *Arabidopsis thaliana*. *J. Cell Biol.* **172**, 991–998.

Rambaut, A. and Drummond, A.J. (2007) *Tracer*. Version 1.5. http://beast.bio.ed.ac.uk/Tracer

Rensing, S. A. (2016) Plant Evo-Devo: How Tip Growth Evolved. *Current Biology, **26*(23),** R1228–R1230.

Richter, S., Geldner, N., Schrader, J., Wolters, H., Stierhof, Y.D., Rios, G., Koncz, C., Robinson, D.G. and Jürgens, G. (2007). Functional diversification of closely related ARF-GEFs in protein secretion and recycling. *Nature*, **448**, 488-92.

Richter, S., Müller, L.M., Stierhof , Y.D., Mayer, U., Takada, N., Kost, B., Vieten, A., Geldner, N., Koncz, C. and Jürgens, G. (2011) Polarized cell growth in Arabidopsis requires endosomal recycling mediated by GBF1-related ARF exchange factors. *Nat. Cell Biol.* **14**, 80-6.

Robinson, D.G. and Neuhaus, J.M. (2016) Receptor-mediated sorting of soluble vacuolar proteins: myths, facts, and a new model. *J. Exp. Bot.* **67**, 4435-4449.

Ronquist, F., Teslenko, M., van der Mark, P., Ayres, D.L., Darling, A., Höhna, S., Larget, B., Liu, L., Suchard, M.A. and Huelsenbeck, J.P. (2012) MrBayes 3.2: efficient Bayesian phylogenetic inference and model choice across a large model space. *Syst. Biol.* **61**, 539–542.

Sanderfoot, A.A., Kovaleva, V., Bassham, D.C. and Raikhel, N.V. (2001) Interactions between syntaxins identify at least five SNARE complexes within the golgi/prevacuolar system of the Arabidopsis cell. *Mol. Biol. Cell,* **12**, 3733-3743.

Sanderfoot, A. (2007) Increases in the Number of SNARE Genes Parallels the Rise of Multicellularity among the Green Plants. *Plant Physiology*, ***144*(1),** 6–17.

Sanmartín, M., Ordóñez, A., Sohn, E.J., Robert, S., Sánchez-Serrano, J.J., Surpin, M.A., Raikhel, N.V. and Rojo, E. (2007) Divergent functions of VTI12 and VTI11 in trafficking to storage and lytic vacuoles in Arabidopsis. *Proc. Natl. Acad. Sci.USA*. **104**, 3645–3650.

Sawa, S., Koizumi, K., Naramoto, S., Demura, T., Ueda, T., Nakano, A., and Fukuda, H. (2005) DRP1A is responsible for vascular continuity synergistically working with VAN3 in Arabidopsis. *Plant Physiology*, ***138*(2),** 819–826.

Seaman, M.N., Marcusson, E.G., Cereghino, J.L., and Emr, S.D. (1997) Endosome to Golgi retrieval of the vacuolar protein sorting receptor, Vps10p, requires the function of the VPS29, VPS30, and VPS35 gene products. *J. Cell Biol.* **137**, 79–92.

Seaman, M. N., McCaffery, J. M., and Emr, S. D. (1998) A membrane coat complex essential for endosome-to-Golgi retrograde transport in yeast. *The Journal of Cell Biology*. **142**, 665–681.

Seaman, M. N. J. (2004) Cargo-selective endosomal sorting for retrieval to the Golgi requires retromer. *The Journal of Cell Biology*, ***165*(1),** 111–122.

Seaman, M. N. J., Gautreau, A., and Billadeau, D. D. (2013) Retromer-mediated endosomal protein sorting: all WASHed up! *Trends in Cell Biology*, ***23*(11),** 522–528.

Shirakawa, M., Ueda, H., Shimada, T., Nishiyama, C., and Hara-Nishimura, I. (2009) Vacuolar SNAREs Function in the Formation of the Leaf Vascular Network by Regulating Auxin Distribution. *Plant and Cell Physiology*. **50,** 1319–1328.

Siegenthaler, B. M., & Rajendran, L. (2012) Retromers in Alzheimer's disease. *Neuro-Degenerative Diseases*. **10,** 116–121.

Simonetti, B., Danson, C.M., Heesom, K.J. and Cullen, P.J. (2017) Sequence-dependent cargo recognition by SNX-BARs mediates retromer-independent transport of CI-MPR. *J. Cell Biol.* **216**, 3695-3712.

Singh, M.K., Kruger, F., Beckmann, H., Brumm, S., Vermeer, J.E.M., Munnik, T., Mayer, U., Stierhof, Y-D., Grefen, C., and Schumacher, K. (2014) Protein Delivery to Vacuole Requires SAND Protein- Dependent Rab GTPase Conversion for MVB-Vacuole Fusion. *Curr. Biol.* **24**, 1383-1389.

Smith, J. M., Leslie, M. E., Robinson, S. J., Korasick, D. A., Zhang, T., Backues, S. K., and Heese, A. (2014) Loss of Arabidopsis thaliana Dynamin-Related Protein 2B reveals separation of innate immune signaling pathways. *PLoS Pathogens*, ***10*(12),** e1004578.

Steinmann, T., Geldner, N., Grebe, M., Mangold, S., Jackson, C. L., Paris, S., and Jürgens, G. (1999) Coordinated Polar Localization of Auxin Efflux Carrier PIN1 by GNOM ARF GEF. *Science*, ***286*(5438),** 316–318.

Stevens, P. F. (2001 onwards) Angiosperm Phylogeny Website. Version 12, July 2012. http://www.mobot.org/MOBOT/research/APweb/

Surpin, M., Zheng, H., Morita, M.T., Saito, C., Avila, E., Blakeslee, J.J., Bandyopadhyay, A., Kovaleva, V., Carter, D., Murphy, A., Tasaka, M. and Raikhel, N. (2003) The VTI family of SNARE proteins is necessary for plant viability and mediates different protein transport pathways. *Plant Cell,* **15**, 2885–2899.

Surpin, M., and Raikhel, N. (2004) Traffic jams affect plant development and signal transduction. *Nature Reviews Molecular Cell Biology*, ***5*(2),** 100–109.

Swarbrick, J. D., Shaw, D. J., Chhabra, S., Ghai, R., Valkov, E., Norwood, S. J., and Collins, B. M. (2011) VPS29 Is Not an Active Metallo-Phosphatase but Is a Rigid Scaffold Required for Retromer Interaction with Accessory Proteins. *PLoS ONE*, ***6*(5).**

Takac, T., Pechan, T., Samajova, O., Ovecka, M., Richter, H., Eck, C., Niehaus, K., and Samaj, J. (2012) Wortmannin Treatment induces changes in Arabidopsis root proteome and post-Golgi compartments. *J. Proteome Res.* **11**, 3127-3142.

Tammineni, P., Jeong, Y. Y., Feng, T., Aikal, D., and Cai, Q. (2017) Impaired axonal retrograde trafficking of the retromer complex augments lysosomal deficits in Alzheimer's disease neurons. *Human Molecular Genetics*, ***26*(22),** 4352–4366.

Taylor, N. G. (2011) A role for Arabidopsis dynamin related proteins DRP2A/B in endocytosis; DRP2 function is essential for plant growth. *Plant Molecular Biology*, ***76*,** 117–129.

Thazar-Poulot, N., Miquel, M., Fobis-Loisy, I. and Gaude, T. (2015) Peroxisome extensions deliver the Arabidopsis SDP1 lipase to oil bodies. *Proc. Natl. Acad. Sci. USA,* **112**, 4158–4163.

Velasquez, S. M., Ricardi, M. M., Dorosz, J. G., Fernandez, P. V., Nadra, A. D., Pol-Fachin, L., and Estevez, J. M. (2011) O-glycosylated cell wall proteins are essential in root hair growth. *Science, **332*(6036),** 1401–1403.

Vidali, L., Augustine, R. C., Kleinman, K. P., and Bezanilla, M. (2007) Profilin is essential for tip growth in the moss Physcomitrella patens. *The Plant Cell*, ***19*(11),** 3705–3722.

Voigt, B., Timmers, A.C., Šamaj, J., Hlavacka, A., Ueda, T., Preuss, M., Nielsen, E., Mathur, J., Emans, N., Stenmark, H., Nakano, A., Baluska, F. and Menzel D. (2005) Actin-based motility of endosomes is linked to the polar tip growth of root hairs. *Euro. J. Cell Biol.* **84**: 609–621.

Wang, Y., Zhang, W., Li, K., Sun, F., Han, C., Wang, Y. and Li, X. (2008) Salt-induced plasticity of root hair development is caused by ion disequilibrium in *Arabidopsis thaliana*. *J. Plant Res.* **121:** 87–96.

Wang, H., Toh, J., Ho, P., Tio, M., Zhao, Y., and Tan, E.-K. (2014) In vivo evidence of pathogenicity of VPS35 mutations in the Drosophila. *Molecular Brain*, ***7*,** 73.

Wang, P., Richardson, C., Hawes, C., and Hussey, P. J. (2016) Arabidopsis NAP1 Regulates the Formation of Autophagosomes. *Current Biology, **26*(15),** 2060–2069.

Wang, J., Fedoseienko, A., Chen, B., Burstein, E., Jia, D., and Billadeau, D. D. (2018) Endosomal receptor trafficking: Retromer and beyond. *Traffic*.

Williams, E. T., Glauser, L., Tsika, E., Jiang, H., Islam, S., and Moore, D. J. (2018) Parkin mediates the ubiquitination of VPS35 and modulates retromer-dependent endosomal sorting. *Human Molecular Genetics*.

Yamada, K., Hara-Nishimura, I., and Nishimura, M. (2011) Unique Defense Strategy by

the Endoplasmic Reticulum Body in Plants. *Plant and Cell Physiology*, ***52*(12),** 2039–2049.

Yamazaki, M., Shimada, T., Takahashi, H., Tamura, K., Kondo, M., Nishimura, M. and Hara-Nishimura, I. (2008) Arabidopsis VPS35, a Retromer Component, is Required for Vacuolar Protein Sorting and Involved in Plant Growth and Leaf Senescence. *Plant Cell Physiol.* **49:** 142–156.

Yanagisawa, M., Zhang, C., and Szymanski, D. B. (2013) ARP2/3-dependent growth in the plant kingdom: SCARs for life. *Frontiers in Plant Science*, ***4*,** 166.

Yano, D., Sato, M., Saito, C., Sato, M. H., Morita, M. T., and Tasaka, M. (2003) A SNARE complex containing SGR3/AtVAM3 and ZIG/VTI11 in gravity-sensing cells is important for Arabidopsis shoot gravitropism. *Proceedings of the National Academy of Sciences of the United States of America*, ***100*(14),** 8589–8594.

Yao, H.-Y., and Xue, H.-W. (2011) Signals and mechanisms affecting vesicular trafficking during root growth. *Current Opinion in Plant Biology*, ***14*(5),** 571–579.

Yoshinari, A., Fujimoto, M., Ueda, T., Inada, N., Naito, S., and Takano, J. (2016) DRP1-Dependent Endocytosis is Essential for Polar Localization and Boron-Induced Degradation of the Borate Transporter BOR1 in Arabidopsis thaliana. *Plant & Cell Physiology*, ***57*(9).**

Zelazny, E., Santambrogio, M., Pourcher, M., Chambrier, P., Berne-Dedieu, A., Fobis-Loisy, I., Miege, C., Jallais, Y. and Gaude, T. (2013) Mechanisms governing the endosomal membrane recruitment of the core retromer in Arabidopsis. *J Biol. Chem.* **288,** 8815–8825.

Zeng, M.-H., Liu, S.-H., Yang, M.-X., Zhang, Y.-J., Liang, J.-Y., Wan, X.-R., and Liang, H. (2013) Characterization of a Gene Encoding Clathrin Heavy Chain in Maize Up-Regulated by Salicylic Acid, Abscisic Acid and High Boron Supply. *International Journal of Molecular Sciences*, ***14*(7),** 15179–15198.

Zhang, D., Isack, N. R., Glodowski, D. R., Liu, J., Chen, C. C.-H., Xu, X. Z. S., and Rongo, C. (2012) RAB-6.2 and the retromer regulate glutamate receptor recycling through a retrograde pathway. *The Journal of Cell Biology*, ***196*(1),** 85–101.

Zheng, H., von Mollard, G. F., Kovaleva, V., Stevens, T. H., Raikhel, N. V., and Kaiser, C. (1999) The Plant Vesicle-associated SNARE AtVTI1a Likely Mediates Vesicle Transport from the Trans-Golgi Network to the Prevacuolar Compartment. *Molecular Biology of the Cell*. ***10***, 2251–2264.

APPENDIX A: Preliminary characterization of the role of putative VPS26C-interacting proteins, CCDC22 and CCDC93, in regulating root hair growth in Arabidopsis thaliana.

INTRODUCTION

Vacuolar Protein Sorting (VPS) 26C is a novel, evolutionarily conserved large retromer complex protein. VPS26C is essential for proper root hair growth under specific environmental conditions and localizes to endosomal membranes in root epidermal cells. The human VPS26C/DSCR3 ortholog can complement the root hair phenotype of the *vps26c* mutant in Arabidopsis (Jha et al., 2018). A recent work in human cell lines (McNally et al., 2017) has demonstrated the formation of the retromer-like 'Retriever' complex, involving the human VPS26C/DSCR3 ortholog. They have additionally shown that the WASH complex and CCC complexes interact sequentially to recruit the VPS26C-complex to the endosomal domain.

The mechanism of retromer recruitment in plants, unlike animals, is largely unknown as yet. We wanted to test whether in Arabidopsis, the VPS26C-retromer complex also follows CCC-complex mediated endosomal recruitment. We have data so far on a few of the preliminary studies that are done in understanding if CCDCs play a role in VPS26C-retromer function in Arabidopsis.

RESULTS

Human *CCDC22* and *CCDC93* have orthologs in *Arabidopsis thaliana*

The CCC complex proteins, or CCDCs, are largely uncharacterized in plant systems so far. In the BLAST searches we did for the human CCDCs, we found Arabidopsis orthologs of only two of the CCDCs, *CCDC22 (At1G55830)* and *CCDC93 (At4G32560*) (Figures 1 and 2). The amino acid sequence comparison between the human and Arabidopsis displays a shorter amino acid sequence for Arabidopsis. But the Arabidopsis sequences for both CCDC22 and CCDC93 have more than 65% similarity in the sequence that overlapped with that of human.

CCDC22 and *CCDC93* are essential for root hair growth

T-DNA insertion mutants of *CCDC22 (*SALK_047800) and *CCDC93* **(**SALK_039808C) were used for these studies. Seedlings were grown under continuous light for 5 days on 1X MS medium, pH6, and on 1X MS medium, pH6, supplemented with 200 mM mannitol, after which they were analyzed for defects in root hair growth. Both *ccdc22* and *ccdc93* seedlings grown on both media exhibited aberrant root hair growth when compared to wild type seedlings (Figure 3).

CCDC22 and *CCDC93* are down regulated in the *vps26c* mutant

To test whether the expression of *CCDC22* and *CCDC93* is dependent on *VPS26C,* we used qRT-PCR to determine the transcript of the two genes in wild type and *vps26c* seedlings. Both *CCDC22* and *CCDC93* were found to be significantly down regulated in the *vps26c* mutant (Figure 4).

This, along with the CCDC mutants showing a defective root hair growth indicates that CCDCs in *Arabidopsis thaliana* might be functioning in a VPS26C-dependent manner and have a role to play in controlling root hair growth.

METHODS

Plant material and growth conditions

Analysis of wild type and SALK mutant lines was performed using the Columbia-0 ecotype of Arabidopsis. The growth medium for Arabidopsis seedlings consisted of 1X Murashige-Skoog (MS) salts (Murashige and Skoog, 1962), 1% (w/v) sucrose, 5 mM 4-morpholineethanesulfonic acid sodium salt (MES), pH 6, 1X Gamborg's vitamin solution, and 1.3% (w/v) agarose (Invitrogen). For plants grown to maturity, seeds were sown on soil (Transplanting mix, Gardener's Supply, Intervale Rd, Burlington, VT) and placed in Conviron MTR30 growth chambers (Conviron, Winnipeg, CA, USA), using cool-white lights (80 μmol/m^2/sec; Licor photometer LI-189) under continuous light at 19° C.

Characterization of root hair phenotypes

Seeds were sterilized using 20% (v/v) bleach, followed by 5-6 washes in sterile distilled water. The sterilized seeds were stored in sterile water overnight in the dark at 4° C before plating them on solid media. Seedlings were grown on MS medium using petri plates placed vertically under continuous white light at 20°C for five days. Where indicated, 200 mM mannitol was included in the growth medium. To characterize root hair shape and growth, seedlings were mounted in sterile water on glass slides. Images were taken using a Nikon Eclipse TE200 inverted microscope with SPOT imaging software (Diagnostic

Instruments). The length of 10-15 root hairs/seedling for at least 10 seedlings per genotype were measured, using Image J and the calibrating tool in the SPOT software, and a Student's *t*-test was used for statistical analysis.

RNA isolation and transcript analysis using qRT-PCR

For transcript expression analysis 7-day-old whole seedlings were collected for three biological replicates. Approximately 200 seedlings were pooled for each genotype and treatment and three biological replicates were generated. For null mutant analysis, young leaves from each genotype and three biological replicates were generated for RNA extraction. All isolated tissues were frozen, ground in liquid nitrogen, and stored at -80°C. Total RNA was extracted using a Qiagen RNeasy Plant Mini Kit, quantified using a nanodrop (ThermoScientific) followed by generation of first strand cDNA using Superscript II Reverse Transcriptase (Invitrogen), according to the manufacturer's instructions. For quantitative RT-PCR, the first-strand cDNA was diluted 1:10 and then used as a template with iTaq Universal SYBR green Supermix (Bio-Rad). An Applied Biosystems Step-one Plus instrument was used to run the qRT-PCR. Three technical and three biological replicates were used for each qRT-PCR cycle. The differential expression values of transcripts were standardized against the transcript expression of *EF1α* and *ACT2* housekeeping genes.

Statistical Analysis

Statistical analyses were done using a Student's *t*-Test, where pairwise comparison was performed between genotypes, or treatments. For example, root hair growth measurements

were compared in a pair-wise fashion between wild type and each of the mutants individually, and significance was accepted at the $P<0.05$ level.

Accession numbers

CCDC22: At1G55830 (*ccdc22:* SALK_047800) and CCDC93: At4G32560 (*ccdc93:* SALK_039808C)

Primers used for qRT-PCR

CCDC22_qRT-PCR_F: 5' AGCAATGGGACGATGTAAGG 3'

CCDC22_qRT-PCR_R: 5' TTTTGGCTGCCTCTCAAGTT 3'

CCDC93_qRT-PCR_F: 5' AGATTGACGATGTGCCATGC 3'

CCDC93_qRT-PCR_R: 5' CAATAAGCTTCACACGGCCA 3'

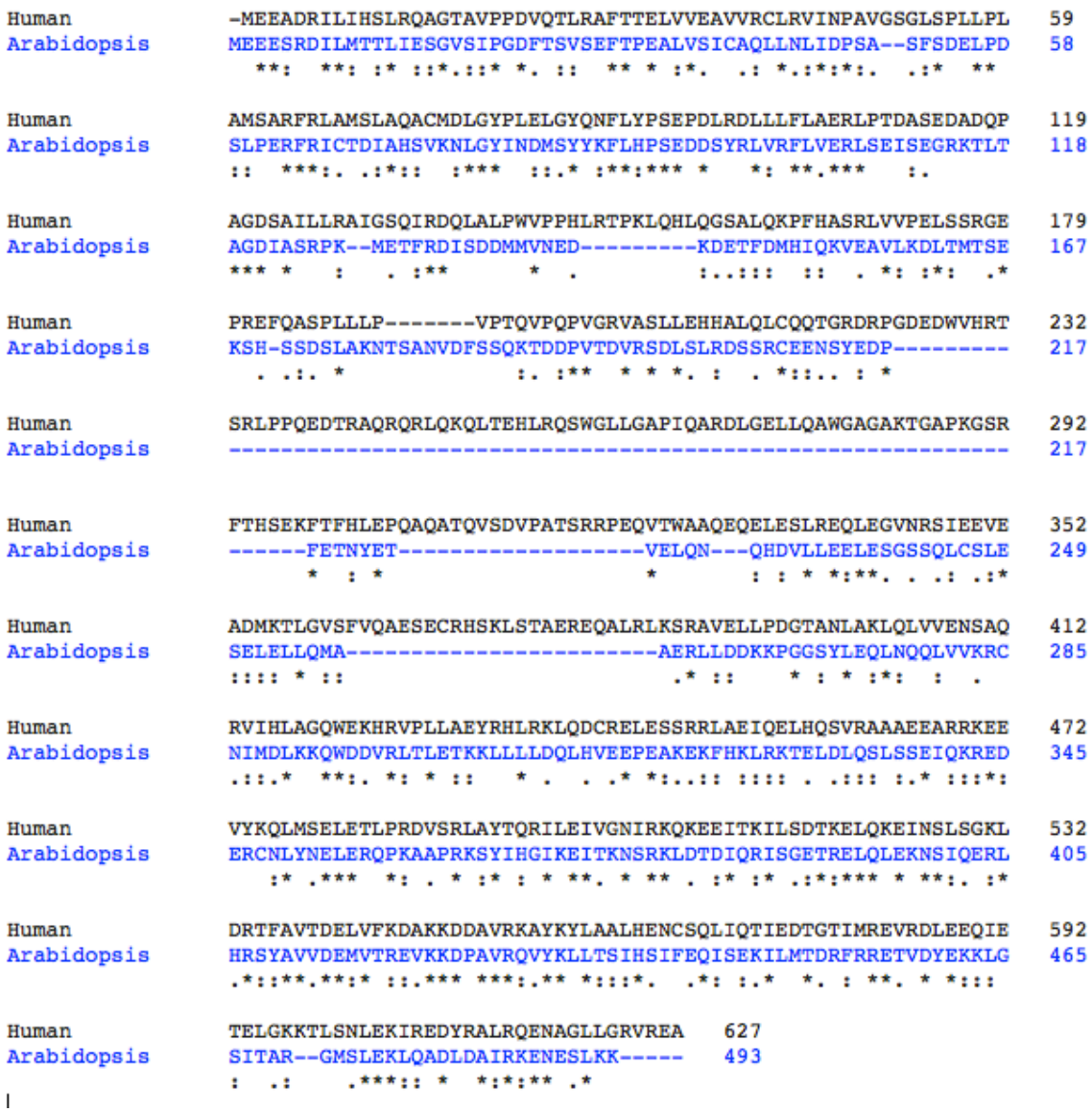

Figure 16: Alignment of the amino acid sequence of CCDC22 between Homo sapiens and Arabidopsis thaliana

Alignment of CCDC22 amino acid sequences of Arabidopsis and human illustrates that these orthologs share 64% amino acid sequence similarity. Legend: (*): fully conserved residues; (:) conserved residues with strongly similar properties; (.) conserved residues having less similar properties.

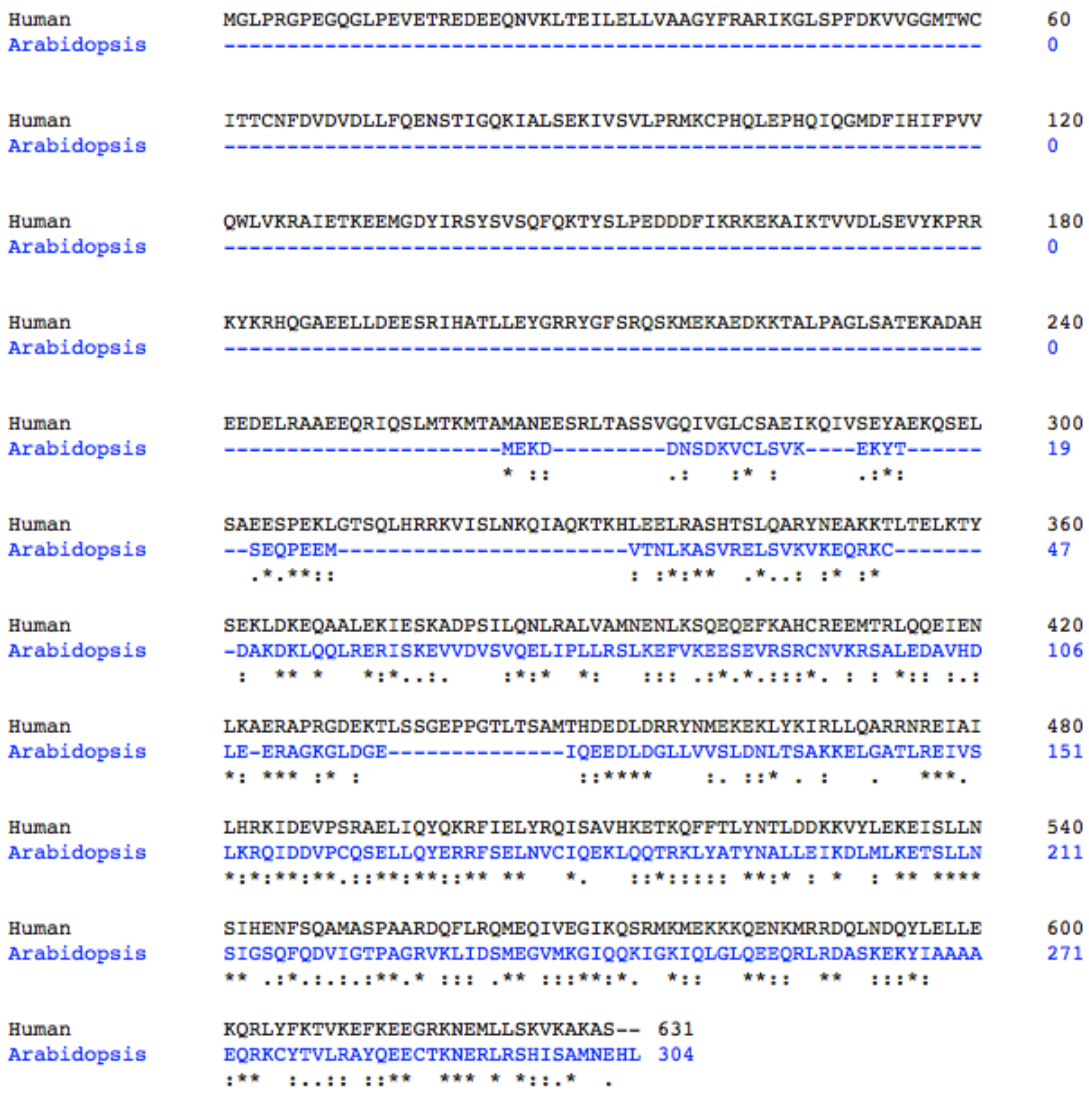

Figure 17: Alignment of the amino acid sequence of CCDC93 between Homo sapiens and Arabidopsis thaliana

Alignment of CCDC93 amino acid sequences of Arabidopsis and human demonstrates that these orthologs share 69% amino acid sequence similarity. Legend: (*): fully conserved residues; (:) conserved residues with strongly similar properties; (.) conserved residues having less similar properties.

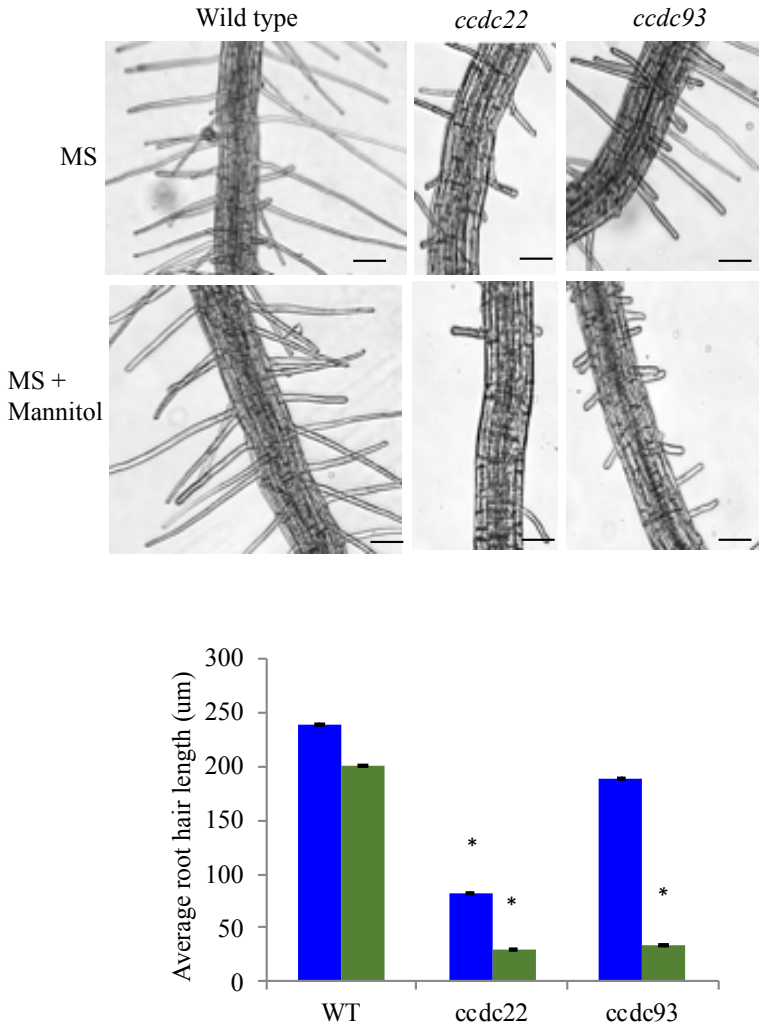

Figure 18: *ccdc22* and *ccdc93* are defective in root hair growth

Wild type seedlings and T-DNA insertion mutants of *ccdc22* and *ccdc93* were grown on 1X MS medium, pH6 (upper panel) and 1X MS medium, pH6 supplemented with 200 mM mannitol (lower panel) for five days after which root hair growth was imaged using bright field microscopy. *ccdc22* and *ccdc93* display shorter root hairs compared to wild type. Bars=100 µm

Comparison of root hair lengths. Root hairs of 15 seedlings per treatment per genotype were scored for length measurements, and 10-15 root hairs per seedling were measured for each biological replicate. The graph represents the average of three biological replicates. Asterisks denote statistical significance ($P<0.05$) based on the Student's *t*-test, where wild type was compared in a pair-wise manner with each of the genotypes. Error bars represent the standard error of mean of three biological replicates.

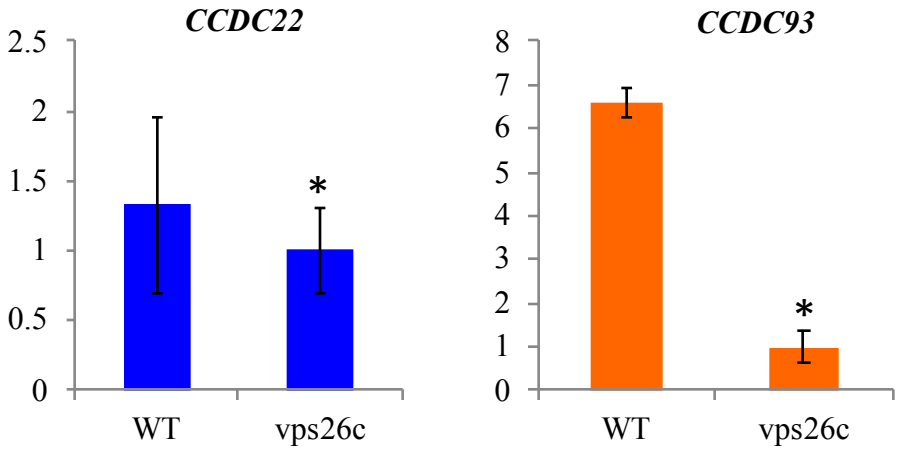

Figure 19: *CCDC22* and *CCDC93* transcripts are downregulated in *vps26c*

qRT-PCR analysis of *CCDC22* and *CCDC93* transcript levels in roots of wild type and *vps26c* seedlings grown on 1X MS medium, pH 6. Transcript levels of both *CCDC22* and *CCDC93* down regulated in *vps26c* mutant compared to wild type. Asterisks indicate statistical significance according to the Student's *t*-test ($P < 0.05$). Error bars represent the standard error of the mean of three biological replicates, run in triplicate.